Drug Monitoring of Kinase Inhibitors in the Context of Precision Medicine – Focus on Minimally Invasive Microsampling

Dissertation zur Erlangung des naturwissenschaftlichen
Doktorgrades der Julius-Maximilians-Universität Würzburg

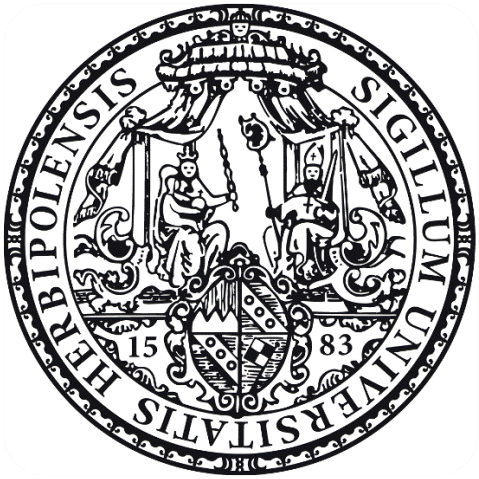

vorgelegt von
Sebastian Andres Zimmermann
aus
La Asunción

Würzburg 2024

Drug Monitoring of Kinase Inhibitors in the Context of Precision Medicine – Focus on Minimally Invasive Microsampling

Dissertation zur Erlangung des naturwissenschaftlichen
Doktorgrades der Julius-Maximilians-Universität Würzburg

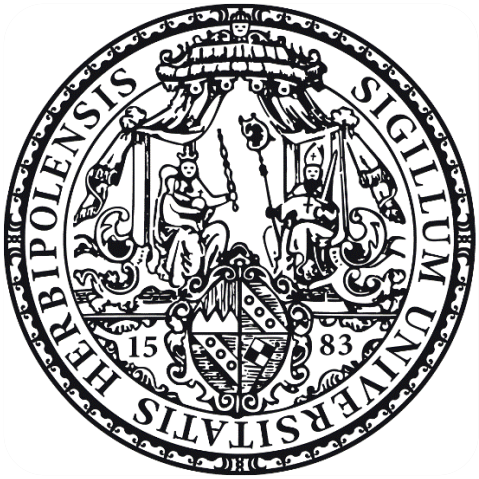

vorgelegt von
Sebastian Andres Zimmermann
aus
La Asunción

Würzburg 2024

Eingereicht bei der Fakultät für Chemie und Pharmazie am

_____

Gutachter der schriftlichen Arbeit

1. Gutachter: _____

2. Gutachter: _____

Prüfer des öffentlichen Promotionskolloquiums

1. Prüfer: _____

2. Prüfer: _____

3. Prüfer: _____

Datum des öffentlichen Promotionskolloquiums

_____

Doktorurkunde ausgehändigt am

_____

“Only if we understand, will we care. Only if we care, will we help. Only if we help shall all be saved.”

Dr. Jane Goodall

Für meine Eltern

Die vorliegende Arbeit

entstand auf Anregung und unter der Anleitung von

Herrn Prof. Dr. Oliver Scherf-Clavel.

Sie wurde am Institut für Pharmazie und Lebensmittelchemie

der Bayerischen Julius-Maximilians-Universität Würzburg angefertigt.

Danksagung

In erster Linie möchte ich Prof. Dr. Oliver Scherf-Clavel aufrichtig dafür danken, dass er mir die Gelegenheit und das Vertrauen gegeben hat, seinem jungen Arbeitskreis als einer der ersten Doktoranden beizutreten und meine Promotion auf diesem bedeutsamen Fachgebiet durchzuführen. Ich bin ihm für seine ständige Unterstützung, seine hilfreichen Ratschläge, seine Offenheit gegenüber neuen Ideen und Projekten und für die Möglichkeit, mich während dieser ereignisreichen Jahre auf diversen fachlichen und persönlichen Gebieten weiterzuentwickeln, sehr dankbar.

Vielen Dank an Prof. Dr. Dr. Matthias Kroiss, Prof. Dr. Martin Fassnacht, Dr. Max Kurlbaum und Sabine Kendl für die spannende und patientennahe Zusammenarbeit am Universitätsklinikum Würzburg und die Möglichkeit, im Rahmen der CaboACC-Studie in der Zentraleinheit für klinische Massenspektrometrie eigenständig mitzuarbeiten.

Die Durchführung der vorliegenden Arbeit wäre ohne die tatkräftige Unterstützung von Prof. Dr. Hartwig Klinker und Dr. Nora Isberner nicht möglich gewesen. Bei ihnen möchte ich mich besonders bedanken. Darüber hinaus danke ich der Hector-Stiftung für die finanzielle Förderung, sowie allen Studienbeteiligen und Mitarbeitern der Infektiologie des Universitätsklinikums Würzburg für deren engagierten Beitrag zur Patientenrekrutierung, Probenabnahme und Logistik. Ganz herzlichen Dank an Fatemeh Aghai-Trommeschläger – danke Mahssa für deine vielfache Unterstützung während unserer Promotionszeit.

Die überregionale Zusammenarbeit im Rahmen der ON-TARGET-Studie hat das Bewusstsein für die Bedeutung meiner Arbeit noch einmal verstärkt. Mein Dank gebührt dem gesamten Konsortium, allen voran Prof. Dr. Charlotte Kloft und Prof. Dr. Ulrich Jaehde.

Ich möchte mich auch bei allen Patienten bedanken, die zum Zweck der Forschung an einer der zahlenreichen klinischen Studien teilgenommen haben!

Vielen Dank an Prof. Dr. Ulrike Holzgrabe für die Betreuung im Rahmen meiner Weiterbildung zum Fachapotheker für Pharmazeutische Analytik. Ein großes Dankeschön an Jonas U., Jonas W., Adrian und Sebastian S. für die unterhaltsamen Stunden bei der Betreuung des 8. Semesters und an Jens, Lu, Frau Möhler und Frau Weidinger für die organisatorische Unterstützung.

Auch möchte ich Prof. Dr. Petra Högger für die freundliche Aufnahme am Institut und Einbindung in die Klinische Pharmazie danken.

Alex, Andi, Bettina, Charlotte, Flo, Jasmin, Linda, Max, Simon, Stoyan und Theresa, euch möchte ich nicht nur für eure Hilfsbereitschaft und kreativen Anregungen danken, viel mehr noch möchte ich die unvergesslichen Momente abseits der Uni hervorheben. Ich weiß die schönen Erlebnisse sehr zu schätzen. Ein besonderer Dank gilt Bettina, für den unbeschwerten Start, die gegenseitige Motivation und den vielfältigen Austausch. Danke für den gemeinsamen Abschnitt und die gewonnene Freundschaft!

Vielen Dank, Krissy und Marcus, für die aufschlussreichen Ratschläge und willkommene Ablenkung während dieser Zeit.

Zu guter Letzt möchte ich besonders meiner Familie danken – meinen Eltern, meinem Bruder, und meiner Frau. Vor allem dir, Sandra, möchte ich von ganzem Herzen danke sagen, für deinen bedingungslosen Rückhalt, deine Geduld und Motivation. Zu wissen, dass ich immer auf dich zählen kann, ist von unschätzbarem Wert.

Table of contents

1. Introduction

1.1. Kinase inhibitors

1.1.1. Protein kinases

Protein kinases entitle a class of enzymes that catalyze the transfer of a phosphate group onto a hydroxyl moiety of certain protein residues using ATP as their source of phosphate [1]. This biochemical modification, representing a mechanism of cell regulation, triggers a cascade of signal transductions that are responsible for several cellular processes, such as cell differentiation, cell growth, proliferation, and even apoptosis [1-4].

To date, the human kinome, which accounts for 2% of the human genome [3], comprises more than 500 different protein kinases [2, 3, 5, 6]. These are classified according to the amino acid residues that are phosphorylated. Since serine, threonine, and tyrosine are involved, with a relative abundance of 86.4%, 11.8%, and 1.8% respectively, they are also referred to by the same name as serine, threonine, and tyrosine kinases [2, 7]. The first two are often collectively referred to as serine/threonine kinases due to their ability to phosphorylate both amino acids [2]. In addition, tyrosine kinase-like enzymes are protein kinases that resemble tyrosine and serine/threonine kinases [2, 3]. Phosphorylation at other protein constituents, e.g., on the residues of histidine or aspartate, rarely occurs and plays only a minor role in eukaryotes [1, 2]. In contrast, within the so-called atypical protein kinase family other structures than proteins are phosphorylated, such as phospholipids [8, 9].

Protein kinase-mediated phosphorylation leads to an altered activity of the target protein. The covalent binding of the ATP-transmitted y-phosphate group changes the protein conformation to its activated state [2]. This post-translational modification is reversible through the activity of phosphatases, enzymes that act as counterparts to kinases transferring a phosphate group back to ADP [2, 10]. Thus, cell homeostasis is achieved through an interplay between phosphorylation and dephosphorylation [2, 11]. An imbalance however, either caused by overexpression, hyperactivity or malfunction causes a variety of diseases [2, 4, 10, 12]. Not only in metabolic disorders [13], autoimmunity [14], neurodegenerative [15], or infectious diseases [16] the phospho-signaling pathways are decisively involved. Especially in the development and progression of cancer, it plays an important role [4, 10]. Almost

all types of neoplastic malignancies have been linked to increased phosphotransferase activity of kinase signaling networks [2]. Hence, protein kinases are important targets for the selective treatment of many different diseases, both malignant and non-malignant [17].

1.1.2. Evolution of kinase inhibitors

Kinase inhibitors (KI) are small molecule drugs capable of blocking the kinase-mediated phosphorylation process [4, 17, 18]. In 2001, imatinib was approved by the United States Food and Drug Administration (FDA) as the first synthetic drug of this class [17, 19, 20]. The development of the drug was preceded by the discovery of a specific aberration in the chromosomes of leukemia patients by Peter Nowell and David Hungerford at their research institutes in Pennsylvania [21]. The genetic material of both chromosomes is exchanged by reciprocal translocation of chromosomes 9 and 22 which results in a shortened chromosome 22, known as the Philadelphia chromosome (Ph), with a chimeric *BCR-ABL* gene that carries the genetic information of the *ABL* gene from chromosome 9 in addition to the existing *BCR* gene [19, 22]. Following DNA transcription and ribosomal translation, this genetic defect leads to the synthesis of the BCR-ABL fusion protein, a tyrosine kinase whose constitutive activity drives resilient cellular proliferation leading to the development of chronic myeloid leukemia (CML) [22]. Imatinib occupies the ATP-binding site of the target enzyme in its inactive state, thereby competitively inhibiting the hyperactive phosphorylation reaction [23-25]. The catalytic center, the DFG (Asp-Phe-Gly) motif of the ATP-binding site, is highly conserved in protein kinases [25-27]. Imatinib is therefore not selective for the chimeric oncoprotein and inhibits other kinases as well, like the tyrosine kinase receptors c-Kit and the platelet-derived growth factor receptor (PDGFR) [19]. Thus, the approval also covers among others the treatment of c-kit-positive malignant gastrointestinal stromal tumors (GIST) and myelodysplastic/myeloproliferative disease (MDS/MPD) associated with *PDGFR* gene re-arrangements [28].

Although imatinib was the first synthetic approved KI by the FDA, sirolimus was found previously to inhibit an atypical serine/threonine kinase called mammalian target of rapamycin (mTOR) [29, 30]. Isolated from the bacterial species *streptomyces hygroscopicus*, the macrolide immunosuppressant, which is also called rapamycin, was approved by the FDA in 1999, two years earlier than imatinib [29-32]. It should also be mentioned that, prior to imatinib and sirolimus, in 1995, fasudil, an inhibitor of

Rho-kinase (ROCK), was licensed in Japan for the treatment of cerebral vasospasm but was not approved by the FDA [17, 32].

Over the past years, many molecular mechanisms have been identified that are responsible for the onset and progression of diseases based on the malfunction of kinases and the findings have driven the approval of a variety of new drugs, which are now complementing the armamentarium of treatment options (Figure 1) [18, 20, 32-34].

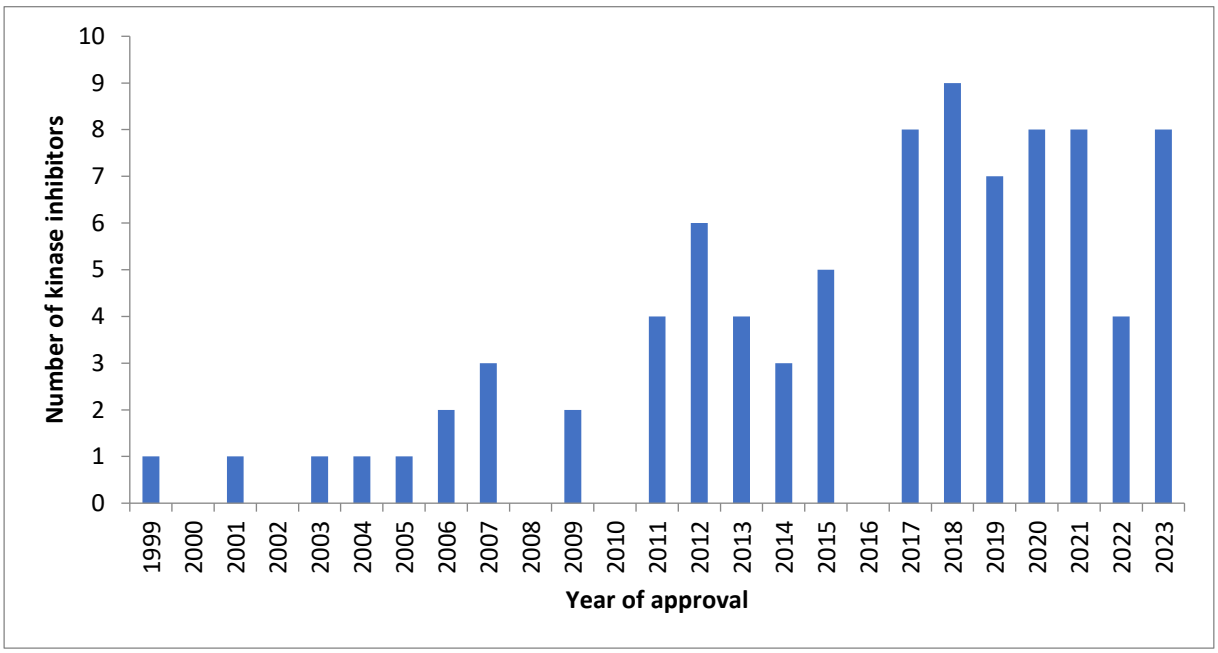

Figure 1: Annual number of small molecule KI approved by the FDA since 1999 [34, 35].

As of today, 86 different KI have been approved by the FDA (see Section 7.2. List of kinase inhibitors, according to [34, 35]). The rapid evolution of KI approval encompasses not only research and development of new drugs, but also indication extensions of already approved ones. As an example, in 2011, ruxolitinib, a selective inhibitor of the Janus kinases JAK1 and JAK2, was approved for the treatment of myelofibrosis [36, 37]. This was shortly followed by approval for the treatment of polycythemia vera in 2014, steroid refractory acute graft versus host disease (GvHD) in 2019, and chronic GvHD in 2021 [36]. In 2021, it was also approved for the local treatment of atopic dermatitis, which was extended to the treatment of nonsegmental vitiligo in 2022 [38-40]. In addition, several clinical trials on ruxolitinib are ongoing [41-43].

1.1.3. Classification of kinase inhibitors

KI can be classified according to their pharmacological target. For example, the BCR-ABL kinase is the primary pharmacological target of imatinib. The further research of this substance class led to the development of dasatinib, nilotinib, and bosutinib, which are considered as second-generation inhibitors, and ponatinib, a third-generation BCR-ABL inhibitor [4, 32, 44]. With asciminib, a further BCR-ABL inhibitor has been developed [45].

The pharmacological target is an important, but not the only characteristic for classifying KI. A further distinction can be made between selective antagonists and multikinase inhibitors. While the latter are targeting a broad spectrum of enzymes simultaneously, selective KI have functional moieties specifically adapted to potently antagonize only a few kinases, decreasing the risk of off-target adverse events [18]. Because of the highly conserved ATP-binding pocket among kinases, selective orthostatic inhibitors may be difficult to find [26]. From this concern and because of the mutation-induced resistance mechanism at the orthostatic binding site, attempts have been made to develop non-competitive inhibitors [46].

Accordingly, KI can also be classified by their mechanism or site of action. With approximately 80%, most of the currently approved KI are competing with ATP as an orthostatic antagonist, which is also true for the above mentioned BCR-ABL inhibitors except for asciminib [47, 48]. Depending on the binding affinity to the active or inactive conformation, this can be categorized as type I (bosutinib, dasatinib) or type II (imatinib, nilotinib, ponatinib), respectively [48-53]. In contrast, allosteric mechanisms altering the protein conformation may lead to suppression of the signaling cascade as well. Non-competitive allosteric inhibition near the catalytic site is the characteristic of type III ligands and, for example, the mechanism of action of trametinib, an inhibitor of the MEK1/2 kinases [48, 53]. Sirolimus prevents the catalytic conversion of the enzyme by allosteric protein-protein interaction between an FK-binding protein 12 (FKBP12) bound by sirolimus and the mTOR protein kinase [54]. Asciminib allosterically inhibits the fusion protein of the *bcr-abl* gene by binding to the myristoyl pocket of the enzyme [45, 55]. As these inhibitions take place outside the catalytic site, sirolimus and asciminib are considered as type IV inhibitors [48, 56]. Further types are distinguished according to bivalent binding, binding at a pseudokinase domain, or extracellular binding, but the literature is contradictory in this respect [48, 51, 53, 56, 57]. Covalent binding is also mentioned as a type of inhibition, a mechanism that has been reported

for drugs such as afatinib and osimertinib, second- and third-generation epidermal growth factor receptor (EGFR) inhibitors, respectively [51, 53, 56, 58].

Finally, not only small molecules are able to inhibit protein kinases. Large molecules are also used. Those can be antibodies, capable of either binding the kinase ligand such as bevacizumab, an antibody against the vascular endothelial growth factor (VEGF), or blocking the receptor itself, e.g., trastuzumab, an antagonist against the human epidermal growth factor receptor 2 (HER2) [4, 51, 59, 60]. Those antibodies may also be covalently linked to certain conjugates (antibody-drug conjugate (ADC)) for example with the combination of trastuzumab and the topoisomerase inhibitor I deruxtecan [4, 60]. Other macromolecules to inhibit protein kinases are nucleic acids (aptamers) [4, 60].

1.2. Precision medicine

1.2.1. The principle of precision medicine

The use of modern diagnostic methods, such as DNA sequencing, biomarker monitoring, or nuclear medical imaging procedures, has uncovered significant differences among individuals regarding disease development and progression [61-63]. Based on regulatory approval, it is common practice in disease management to rely on rigid therapy regimens that have proven to be effective for certain populations (i.e., based on phase III clinical trials). However, these rigid regimens can only capture the heterogeneity among patients to a limited extent. Medication in elderly is potentially inappropriate, as side effects occur more frequently than in other patient groups [64]. Children and pregnant women are usually not included in clinical trials, and therefore rarely treated with drugs. If treatment is nevertheless considered for these patient groups, safety must be ensured, despite their underrepresentation in clinical trials. The heterogeneity among patients extends beyond factors such as age, sex, and specific life circumstances (pregnancy, breastfeeding). It also encompasses variations in genetics, physical conditions, and the presence of comorbidities. Patients for example with organ dysfunction like chronic kidney failure requiring hemodialysis may have an altered xenobiotic elimination, which may result in an altered drug exposure [65]. Body weight (e.g., obesity) as well as the quality of nutrition (e.g., malnourishment) can both impact safety and efficacy and increase the uncertainty of treatment success [66-70]. Even habits, such as cigarette smoking during medication may lead to different therapeutic outcomes [71, 72].

This limitation has prompted inquiries into the extent to which individual differences should be considered in making treatment decisions [61]. Therefore, precision medicine addresses an opposed strategy to classic rigid regimens and describes the individual selection of preventive or therapeutic measures as a tailored and targeted approach for certain patients or patient collectives on the basis of individual genetic, molecular and clinical information, as well as their environment and lifestyle [61-63, 73]. Advanced monitoring methods, especially the so-called “omics” analyses, which comprise genomics, proteomics, and metabolomics, among others, have generated substantial data with the potential to precisely predict the course of diseases [73, 74]. Consequently, this individualized approach can maximize the quality of healthcare by enhancing disease prevention, as well as the safety and efficacy of drugs. Besides the patient’s individual information, decision-making is also based on general patterns that have been identified by means of modern diagnostics [61, 73]. As these data-based patterns may also be applied population-wide without personalizing the therapy of each patient anew, the term personalized medicine, which is often used synonymously for precision medicine, could be misinterpreted [61].

Preventive measures can be improved by enhanced risk prediction models, which include additional (individual) information like the presence of specific gene variants that are associated with an increased risk for the occurrence of certain diseases [61]. With this approach, for example, the need of a colonoscopy for early detection of colorectal cancer can be significantly better predicted compared to models relying solely on traditional factors like age and family history [61, 75].

Furthermore, genetic polymorphisms may impact drug safety and efficacy if these allelic variants affect pharmacokinetics (PK) or pharmacodynamics (PD) (Figure 2). An example illustrating the significance is the use of warfarin, a drug prescribed for the prophylaxis and treatment of thromboembolic diseases. The pharmacological target of warfarin is the protein complex VKORC1, while CYP2C9 is the major metabolic enzyme [62, 76, 77]. Polymorphisms exist for both genes, *VKORC1* and *CYP2C9* [62, 76, 77]. With altered enzyme activity among individuals, neither PK nor PD can be estimated without individual monitoring [61]. As a result, the dose that is required to achieve a target effect varies significantly among patients, differing by up to 20-fold [76, 78]. Given the narrow therapeutic index of warfarin, i.e., a low ratio of the median lethal dose (LD_{50}) to the median effective dose (ED_{50}) [79], genotyping is recommended before starting the therapy in order to reduce the risk of

adverse drug reactions such as major bleeding [61, 62, 80]. In addition, the therapy should be continuously monitored on the basis of the thromboplastin time [76].

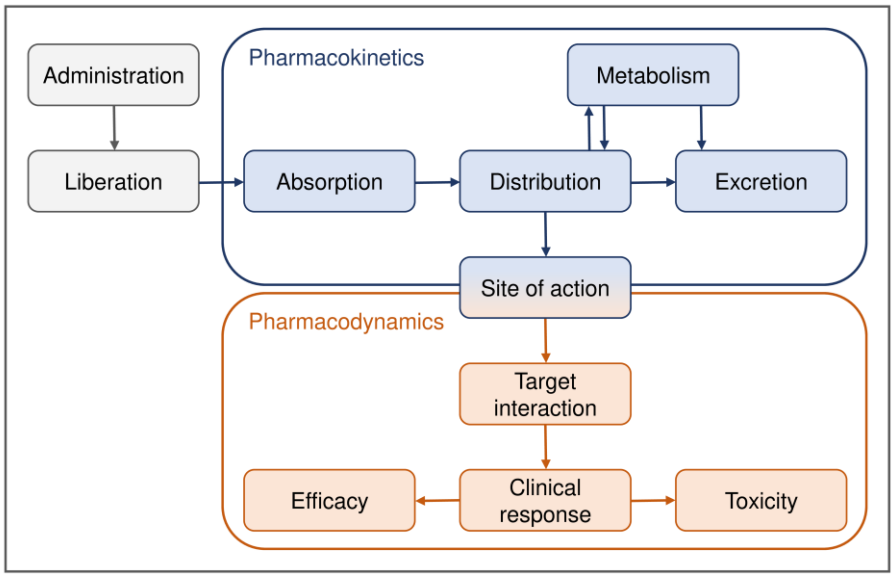

Figure 2 Schematic description of PK and PD. PK describe the body's response to a drug after administration (and liberation if necessary). The PK processes can be elucidated using the ADME model. This model represents key phases of the drug within the body, starting with absorption (A), such as after oral administration, followed by distribution (D) throughout the body, metabolism (M) involving the enzymatic transformation of the drug, and ultimately elimination (E) via the kidneys or liver. On the other hand, PD describes the affinity-related molecular interaction (activation, inhibition, or modulation) of the drug with the pharmacological target(s), e.g., a receptor, transporter, or enzyme.

Precision medicine also plays an important role in cancer therapy, as only a modest, but non-inferior overall efficacy was observed for the first-generation EGFR inhibitors in chemotherapy-pretreated patients with non-small-cell lung cancer (NSCLC) [18, 81, 82]. However, objective response and overall survival was superior in a certain patient collective with activating EGFR mutations, which subsequently represented a predictive biomarker for treatment response of EGFR inhibitors [18, 83, 84]. This targeted approach has also been taken with other KI, such as dabrafenib, whose use is dependent on the presence of a BRAFV600 mutation [85]. Consequently, individual factors determine the choice of the best therapy, shifting the focus towards treatment personalization.

1.2.2. Therapeutic drug monitoring

Since the first recommendations of blood concentration-based dosing, the use of an average dose was often critically discussed [86-90]. The one-size-fits-all approach may not be appropriate for all drugs, especially for those with narrow therapeutic index and high interindividual PK variability [91, 92]. Even if the dosage

remains the same, drug concentrations can vary significantly from one person to another [93]. This has led to the implementation of therapeutic drug monitoring (TDM), which is applied to improve patient care through individualized dose adjustment. Thereby, the therapy is continuously assessed during medication by measuring the blood concentration of the drug itself, representative metabolites, or biomarkers [94, 95]. Depending on whether the measured analyte concentration is below or above the therapeutic range, an exposure correction is indicated for optimized efficacy or reduced toxicity (Figure 3) and can be achieved in clinical routine by either adjusting the dosing interval or by modifying the maintenance dose [96].

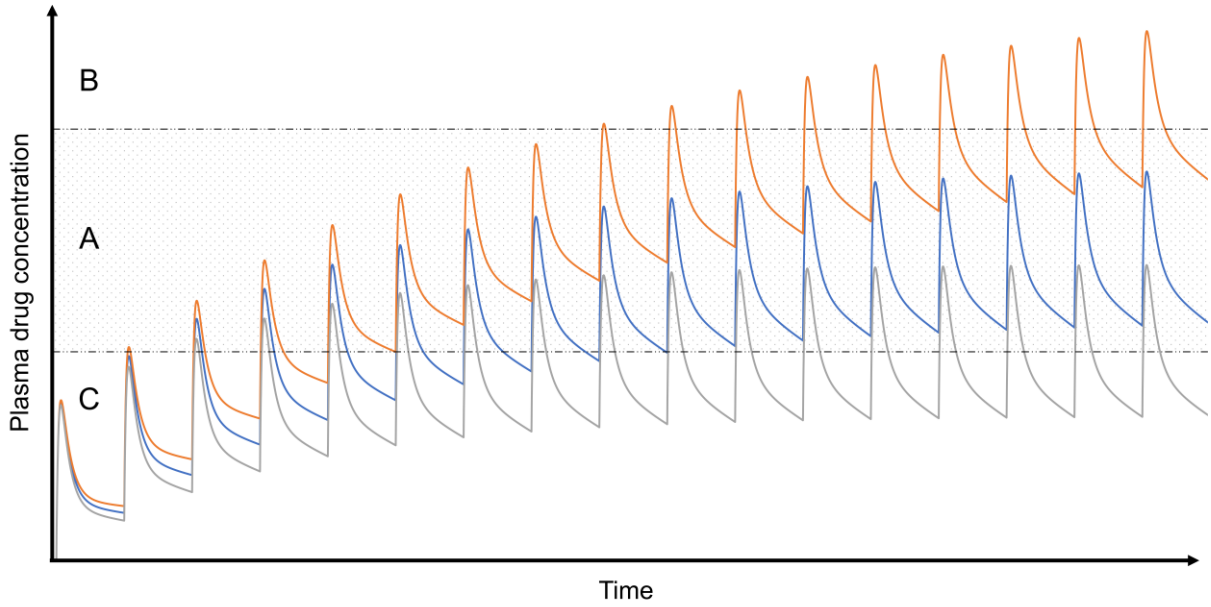

Figure 3 Schematic visualization of drug exposure over time. The highlighted area (A) shows the therapeutic range in which the therapy is considered safe and effective. The range above the highlighted area represents supratherapeutic level (B), the range below is defined as subtherapeutic (C). The dot-dashed line between the two areas A and B marks the maximum safe concentration, whereas the line between areas A and C represents the minimum effective concentration. Three scenarios are shown with only the blue line within the target window (in steady state). Drug exposure exceeding the maximum safe concentration may cause toxic side effects (orange line), while exposure below the minimum effective concentration increases the risk of treatment failure (grey line).

As an interdisciplinary clinical specialty, TDM requires close collaboration between physicians, clinical pharmacists, and pharmacologists to coordinate several steps that are pivotal for TDM, including the medical evaluation of therapy, biological sample collection and analysis, interpretation of results, and medical re-evaluation of the therapy [90, 91, 97]. The requirements that must be met in order to use the measured drug concentration to individually adjust the therapy and thus improve patient care are listed in Table 1. In some cases, long-term use of the drug is also indicated in the literature as a necessity for TDM to justify dose adjustment efforts [97,

98]. However, drug concentration is also monitored during antibiosis of severe bacterial infectious diseases, for example to control exposure of aminoglycosides or vancomycin [91]. Considering that antibiotics are mostly used for a short period of time, this contradicts the previous statement.

Table 1 Summary of the requirements that must be met for the use of TDM [91, 97, 98]

Requirements for therapeutic drug monitoring
• *Narrow therapeutic index of the drug*
• *High interindividual PK variability*
• *Absence of an easily measurable surrogate parameter for drug effect*
• *Existence of a correlation between the pharmacological effect and the analyte* concentration*
• *Availability of validated sensitive bioanalytical methods to monitor the analyte* exposure*
• *Validated target concentration or concentration range of the measured analyte**
• *Clinical evidence that the application of TDM results in patients benefiting from it*

* Depending on the area of application, the analyte may be the drug itself, a representative metabolite, or a biomarker

In general, the classes of pharmaceutical substances in which routine TDM is performed are diverse. Besides previously named antibiotics, these compounds include anticonvulsants such as phenytoin or valproic acid, immunosuppressants, e.g., tacrolimus and sirolimus, some antiretroviral drugs, antidepressants, the cardiac glycoside digoxin, and methylxanthines for the treatment of respiratory diseases [91]. Classic cytotoxic agents are less frequently monitored because dose individualization is rather performed on the basis of body surface area or body weight than on drug exposure [99, 100]. Methotrexate and busulfan are two examples of common candidates for TDM of this drug class [91, 100].

Considering high PK variability for KI, individual dose optimization might be beneficial in improving the therapy as exposure-response and -safety relationships have been reported for many KI [97, 98, 101-116]. Until now, this could only be demonstrated for some KI, e.g., imatinib or sunitinib, where prospective clinical trials have shown that PK-guided dosing is feasible to improve clinical outcome [98, 103, 107, 117-123].

1.2.3. Model-informed precision dosing

Model-informed precision dosing (MIPD) improves the personalized dosing of drugs by integrating mathematical models into the dosing process [124, 125]. In most cases, population data on PK provide the basis for the mathematical description [96, 125, 126]. Therefore, population pharmacokinetic (popPK) studies are conducted focusing on the investigation and modeling of PK processes within a population with the aim of understanding and quantifying inter- and intraindividual variability in drug response [126-131]. Nonlinear mixed effects (NLME) modeling provides one strategy for building a popPK model. It can be described by the combination of a structural model that includes the PK key phases of the drug within the body, a covariate model, and a statistical model [131-133]. The covariate model, which is used to explain the PK variability within the population (fixed effects), allows the determination of influencing variables (covariates) on certain PK parameters, whereas the statistical model characterizes the unexplained variability (random effects) [128, 131, 132]. Common examples for covariates are age, sex, body weight, organ function, and genetic variations.

The popPK model can be used in the framework of MIPD to simulate the course of the plasma concentration over time for each patient individually based on their covariates and to estimate the individual PK variability [134, 135]. With this approach, the most likely best initial dose can be selected *a priori* [96, 103]. With the approach of MIPD, the therapy can also be evaluated continuously based on bioanalytical data. Once a patient sample has been collected, the information from the analyzed sample, i.e., the plasma drug concentration, can be integrated into the mathematical model to further individualize and refine the prediction. Plasma samples are usually taken, but drug concentrations from other matrices are also conceivable to be integrated, such as capillary blood [136]. Using Bayesian statistics, individual PK parameters that are necessary to describe the concentration-time profile can be derived, such as apparent clearance and apparent distribution volume [96, 103]. Thereby, the maximum *a posteriori* (MAP) approach allows to make estimates for these PK parameters by combining initial (prior) knowledge based on the popPK model with the observed data, i.e., measured plasma concentrations [134, 137]. The aim of the MAP estimation is to find the parameter values (mode of the PK parameter distribution) that maximize the *a posteriori* probability (probability distribution of the unknown parameters) [137], which in this case ultimately provides the most probable individual PK parameters. By means

of those posterior values, more precise PK simulations can be performed, including dose-dependent simulations that provide prospective information on the extent to which a certain dosage or treatment regimen leads to the target concentration range being reached. Considering the complex probability distribution and the fact that the MAP estimation is only a one-point summary [137], it may be helpful to quantify the associated uncertainty. This can be done by stochastic simulations, in which representative (approximate) random samples are generated, for example using Markov-Chain-Monte-Carlo algorithms [137]. The more samples are collected, and the more concentration results are available from one patient, the more precise the estimate of the individual PK parameters becomes [96, 103, 138].

The advantage of MIPD is that it is not time dependent. PK simulations can be performed at any time and regardless of when a sample is taken (e.g., during absorption phase, C_{max}, or at trough levels), while in TDM trough levels are usually determined for therapy assessment [95, 96, 103, 134]. In addition, there is no need to wait until the steady state is reached [96, 103, 134]. This, however, is required in conventional TDM, as the target ranges correspond to these equilibrium concentrations [96]. Complete PK profiles can be generated, providing information on total drug exposure expressed as area under the concentration-time curve (AUC), which would otherwise require time-consuming sampling with many sampling time points, which is difficult to realize in routine clinical practice [103].

However, MIPD also comes with some limitations. The underlying PK models are rarely intended for the purpose of MIPD [96, 139, 140]. It must be verified first whether the selected model is suitable for the intended use [96, 125, 134, 140]. Another downside is that, due to the dynamic behavior of the human body, PK parameters may change over the course of treatment, e.g., in critically ill patients [65], which may result in an increased interoccasional variability, limiting the predictive performance [96, 139-142].

1.2.4. Therapeutic considerations for kinase inhibitors

KI are designed for selective prevention of specific intracellular signaling pathways. This approach of targeted therapy plays a pivotal role in the treatment of malignant diseases as most KI (> 80%) are used in oncology [32]. Most of the approvals were based on improved overall survival in advanced stage tumors that failed to respond to first-line therapy but in fact, many KI also proved superior to

conventional chemotherapy [18]. CML patients are now approaching normal life expectancy as prognosis has improved significantly over the last two decades with appropriate treatment with KI [143, 144]. The small molecule antagonists are also approved for therapies other than cancer, such as rheumatoid arthritis (RA) or glaucoma depending on their mode of action. JAK inhibitors for example (e.g., tofacitinib) proved to be effective as an oral immunosuppressant for the treatment of RA similar to commonly used disease-modifying anti-rheumatic drugs or biologicals [145, 146].

Although KI are considered targeted agents, their use is associated with severe side effects. Inhibition of proinflammatory cytokines, as it is the case with JAK inhibitors, results in more frequent infections, transaminitis, or cytopenia [146]. The use of antineoplastic KI targeting cancer cells is not inevitably associated with fewer and less severe side effects than it is with classic cytostatics [59, 106]. For BCR-ABL inhibitors it was reported that toxicity-induced, clinically relevant complications may occur for all those KI [147, 148]. The probability for the occurrence of mild to severe side effects is 50% [143]. Severe side effects can include hematotoxicity, hepatotoxicity, or cardiovascular events and some of them may even be irreversible [148-150]. Other KI may cause secondary tumors, e.g., vemurafenib [151]. On top of that, resistance mechanisms jeopardize the therapeutic outcome. The ability of cancer cells to evade certain signaling pathways is a crucial step in (acquired) tumor resistance [152, 153].

Oral KI are licensed and prescribed in standardized doses, but the dose is not inevitable suitable as a predictor for the therapeutic or toxic effect. There are many factors that affect the systemic drug exposure resulting in high interindividual pharmacokinetic variability (Figure 4).

The solubility of the drug and thus its liberation is influenced by the pH of the stomach, which can lead to altered or even incomplete absorption at low acidity [151, 154-157]. Between pH 1 and pH 7, the solubility of gefitinib for example is decreased by a factor greater than 10^4 [156]. In case of constantly reduced gastric oxonium ion concentration (pH > 5), e.g., due to H2 receptor antagonists, the exposure is decreased by 47% [158]. For bosutinib, the AUC may even be reduced by 74% [159]. Drug absorption may also be influenced by food effects, either positively or negatively. Although pazopanib is likely to be insoluble above pH 4, the systemic exposure (AUC

and C_{max}) is nearly doubled when taken together with a high- or low-fat meal (positive food effect) [156, 160]. Another example for positive food effects is the KI cabozantinib [157]. An increased release of bile acid is assumed to be the reason for the higher exposure, which leads to an increased formation of absorption-promoting micelles [161]. Negative food effects, on the other hand, i.e., an exposure reduction if taken at the same time as food, occur for example with afatinib and dabrafenib with an approximately 50% decrease in C_{max} for both KI and an exposure reduction (AUC) of 39% (afatinib) and 31% (dabrafenib) [157, 162, 163].

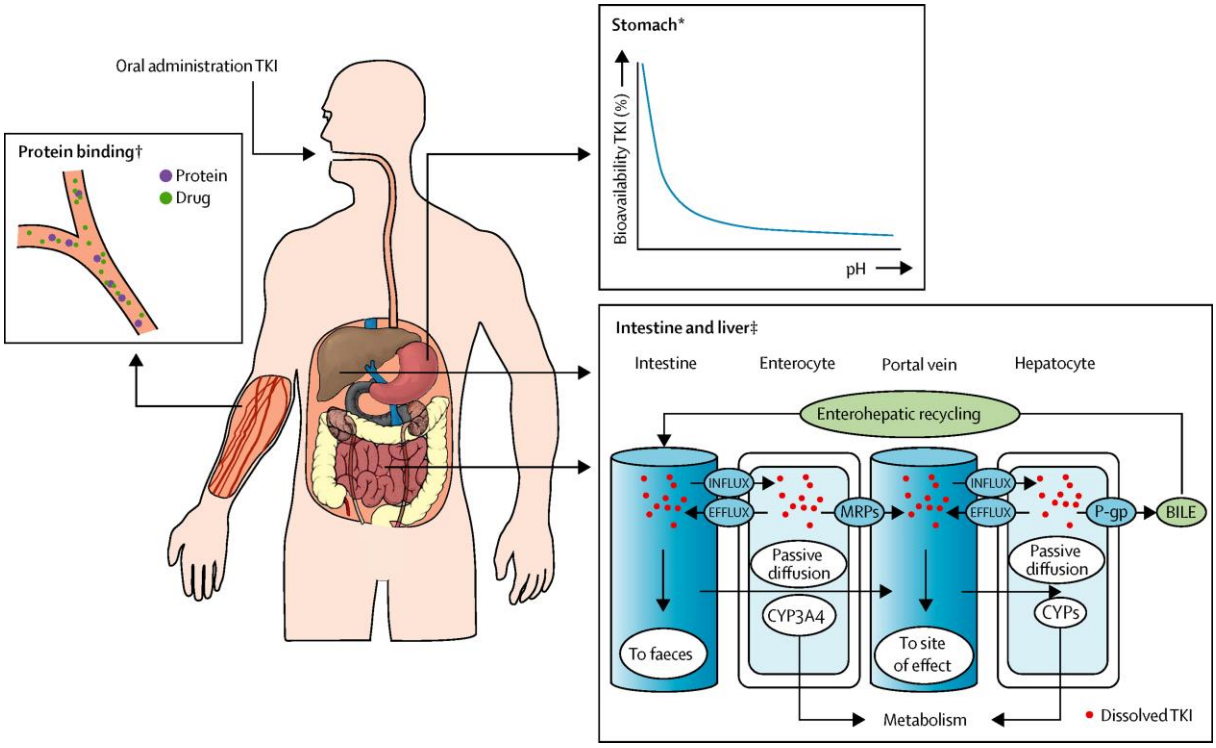

Figure 4 Overview of the major factors that affect the pharmacokinetics of KI after oral drug administration. Reprinted with permission from [151].

The distribution of oral anticancer drugs is mainly characterized by high (> 90%) plasma protein binding to albumin or α1 acid glycoprotein [106, 111, 151]. Competition with other drugs for plasma protein binding sites, e.g., warfarin or phenytoin, may increase the unbound fraction of those drugs causing toxic side effects, as has been observed in patients with concomitant administration of erlotinib [164, 165].

Almost all approved KI are substrates (victim drugs) to metabolizing cytochrome P450 isoenzymes (CYP), with CYP3A4 being the most important [166, 167]. Substances that interfere with the metabolic pathway (perpetrators) offer a significant potential for interactions. A large number of drugs, including KI themselves, as well as specific dietary components like furanocoumarins found in grapefruit and other citrus

fruits, or the polycyclic aromatic hydrocarbons present in smoke, are able to modulate the activity of CYP enzymes [166, 167]. Combining KI with CYP-inducing agents, drug-drug interactions (DDI) occur with a significant effect on drug exposure. The AUC of ruxolitinib was 70% lower when given rifampicin prior to the JAK inhibitor [168]. The same was observed for cabozantinib and axitinib with a decreased single dose plasma exposure (AUC) of 77% and 79%, respectively [166]. On the other hand, the combination of the CYP3A4 inhibitor ketoconazole with the KI nilotinib or bosutinib, for example, leads to a 3.0-fold or even 8.6-fold increase in drug exposure (AUC), respectively [166, 169, 170]. Consequently, severe side effects may occur by inhibition of the metabolizing enzymes [166, 171].

Less dominant but not negligible, several KI are subject to active transmembrane transporting peptides like organic anion transporters (OAT) or efflux transporters like P-glycoprotein (P-gp) and breast cancer resistance protein (BCRP), and some of them are also inhibited by KI [151]. In addition, there is an increased variability due to genetic polymorphism or organ dysfunction such as hepatic or renal impairment [102, 111, 166, 172-175].

1.3. Minimally invasive microsampling

1.3.1. Dried matrix methods

Biological samples collection is necessary to monitor the patients' therapy. Usually, plasma or serum samples are collected by venipuncture to determine the drug concentration [91, 176-179]. However, there are certain situations where conventional blood drawing is difficult, such as in newborns [177, 179]. In any case, the invasive collection of a few milliliters of venous blood can be stressful for the patients. The plasma samples are collected in a medical laboratory or clinic. Consequently, the patient must visit the doctor’s office for each sample collection. The further the distance, the greater the obstacle for the patient, especially in rural areas where public transportation is less available. In addition, since the drug concentration cannot be reported immediately and must be analyzed first with highly sensitive analytical devices, there is no direct feedback for the patients [176]. Regarding TDM, the therapy can only be adjusted at the next visit or at least after a certain lag time. From the perspective of healthcare professionals, the conventional blood draw can also be disadvantageous, as the plasma samples can only be stored in frozen condition (e.g., in a deep freezer with target temperature of -20°C or -80°C), resulting in higher storage

costs [177, 179, 180]. The same applies to shipping, as the samples are only sent on (dry) ice [179, 180].

These limitations have led to the development of minimally invasive alternatives. One such approach is the utilization of dried matrix methods (DMM), where biological specimens are dried on a matrix before being processed for sample analysis [180-185]. Thereby, drug exposure is primarily assessed in capillary blood rather than plasma or serum [176]. To achieve this, a lancet is used to prick the skin in a minimally invasive procedure, causing a few drops of blood to reach the surface [176, 177, 179]. Only a few microliters of blood are collected for microsampling [178, 186].

DMM were developed in the early twentieth century for blood glucose monitoring [180] and have been used since the 1960s to screen newborns for metabolic disorders using dried blood spots (DBS) [176, 180, 187], where capillary blood drops were applied onto a filter paper (non-volumetric) and dried, thereby avoiding the collection of larger volumes of blood [176, 180, 182]. The filter paper can be shipped via mail to specific laboratories, where the analytes of interest can be subsequently extracted and analyzed in the same manner as for conventional plasma sampling [176, 177, 188]. Since this approach is characterized by the small volume required for analysis, it is not only favored in newborns and infants [177, 179], but is also used in preclinical studies, to comply with the principles of 3R (replace, reduce, refine) [180, 188, 189]. DBS cards are the best-known microsampling device but there are also other techniques available (see Section 7.3. List of dried matrix microsampling devices, according to [184, 185]). In addition to the small volume, DMM offer the advantage of an increased patient adherence, ease of use, and the ability for the patients to collect samples themselves from remote locations [177, 180]. Because of the less invasive procedure and the higher convenience, multiple samples can be collected in a short period of time, which may be beneficial for investigating PK profiles [177]. Finally, the samples can be shipped and stored at room temperature minimizing the logistic efforts [177, 179].

DMM are mostly used for diagnostic screening purposes, monitoring enzymes, hormones, vitamins, and trace elements [176, 188]. Also for “omics” analyses, the biological matrix can be collected via microsampling devices [186]. For the purpose of TDM, on the other hand, minimally invasive microsampling is less common [176]. Nevertheless, many different DMM have been developed in the past years to be used for TDM. Those methods cover a variety of different drugs, especially

immunosuppressants [190-192], antiepileptics [193], and anticancer drugs [194-197], but also some antibiotics [198-200], antiretroviral drugs [201], antihypertensive drugs [202], antidiabetics [203], and many others [176, 177, 179-181, 188, 204-206].

In most methods, samples are taken using non-volumetric DBS cards, where a defined sample size can be punched out of the filter paper. However, this has the disadvantage that the diameter is defined, but not the volume. Variations in hematocrit (Hct), i.e., the proportion of cellular components of the blood, may impact the overall accuracy and precision. As the Hct affects the viscosity of the blood, different Hct values lead to different blood spreading on the filter paper (Hct effect) [188, 207]. DBS samples with the same punch diameter but with a higher proportion of cellular components result in a larger volume, whereas a lower Hct leads to larger blood spreading and thus reduces the punched-out blood volume [207]. In addition, the spot size (volume effect) and homogeneity (volcano effect) may vary which must be considered when analyzing DBS samples [208].

This might explain the growing popularity of volumetric sampling techniques, such as volumetric absorptive microsampling (VAMS), which enables the precise collection of a predetermined sample volume. VAMS is a device which uses a hydrophilic, polymeric material with a high absorption capacity for liquids that is able to absorb a defined volume of 10 µL, 20 µL, or 30 µL blood, depending on the tip size [184, 189, 209]. The collection procedure of VAMS is schematically illustrated below (Figure 5).

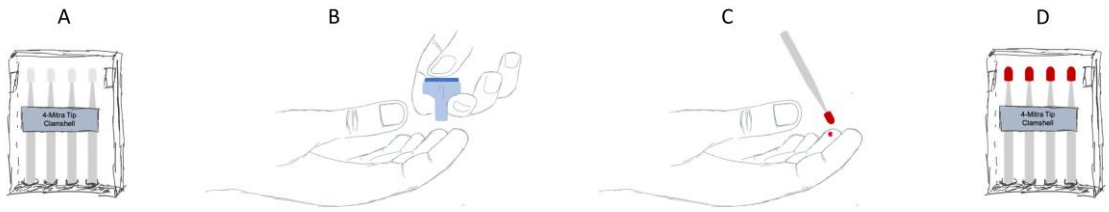

Figure 5 The VAMS collection procedure can roughly be described in four steps. A) Preparation of the materials which comprise VAMS device and clamshell, lancets, gauze, adhesive bandage, as well as documentation form and shipping envelope. B) The fingertip is cleaned and pricked with a lancet. C) The capillary blood is collected using the VAMS device. The device must be filled completely until the maximum sampling volume is reached. D) The puncture site is treated with gauze and bandage and VAMS is placed in the clamshell for drying. Collection date and time is documented and the packed envelop can be shipped per mail for sample analysis.

VAMS is characterized by a high volumetric precision, given as relative standard deviation of less than 5% [210] and fulfills the requirements under the In Vitro Diagnostic Medical Devices Regulation (IVDR), which has led to the attainment of

certified registration (CE-IVD) [211]. However, this also applies to other DMM devices. Besides sampling techniques to collect dried matrices, there are also devices available for the minimally invasive collection of liquid specimens. Examples are the TAB II device (Yourbio Health; Medford, MA, USA) or the MSW² Type Udck device (Shimadzu; Kyoto, Japan) [184, 185].

1.3.2. Clinical application

Due to their nature, DMM are suitable for use in the home environment. The question that arises is whether the samples can actually be taken by patients independently without the assistance of healthcare professionals. This must be demonstrated as part of feasibility studies [208]. In those studies, the sampling quality, i.e., whether the sampling was performed correctly and whether the samples can be used for analysis, should be investigated [208]. The quality of the samples can be assessed visually in the laboratory. Some DMM devices have an indicator control spot which gives direct feedback as to whether the procedure was successful, such as the Telimmune device [184, 185]. Regarding VAMS, sampling is performed correctly if the VAMS tip is completely red in color with no white residual areas. There is also little data on patient acceptance of the sampling method [212]. The extent to which the documented sampling time corresponds to the actual or scheduled sampling time should also be evaluated. Questionnaires and documentation forms can be used to assess patient acceptance and compliance [212].

In the context of TDM, capillary blood concentrations can only rarely be used in clinical routine [178, 181, 213]. As a result of conventional sampling, target concentrations are mostly determined in plasma or serum. The drug concentration in capillary blood is not necessarily equivalent to the concentrations determined in those matrices. Consequently, the pharmacokinetic distribution must be considered before interpreting the results.

1.3.3. Partitioning between blood cells and plasma

Only for a few drugs, such as gefitinib or busulfan, where the drug is evenly distributed between blood cells and plasma, the capillary blood concentration corresponds to the plasma concentration [213]. In those rare cases of direct correlation, no additional conversion of the capillary blood concentrations to plasma values is necessary [213]. In all other scenarios (if plasma or serum concentrations are to be assessed), the obtained concentrations must be converted into plasma or serum

concentrations first and the conversion procedure must be validated in order to generate reliable results [178, 181, 208, 213].

Various methods are available for the conversion of capillary blood concentrations into plasma or serum concentrations [178, 181, 208, 213]. One approach involves comparing the results of one method (DMM analysis) with those of a reference method (plasma or serum sample analysis), essentially constituting a form of cross validation [208]. The correlation between the measured dried capillary blood concentrations and plasma or serum concentrations can be statistically expressed using linear regression models [208, 213]. Passing-Bablok or weighted Deming regression should be used over standard linear regression [208, 213]. Based on the regression model, the analyzed capillary concentrations can be converted into calculated plasma/serum concentrations. However, the application of this conversion method requires the simultaneous collection of DMM and reference plasma/serum samples. It is recommended to collect at least 40 pairs of samples from at least 20 different patients [181, 208, 213].

With the availability of multiple paired samples, it is also possible to calculate a correction factor (CF) based on the measured plasma/serum ($C_{Pla/Ser}$) and capillary blood concentrations (C_{DMM}) (Eq. 1) [213].

$$CF = \frac{C_{Pla/Ser}}{C_{DMM}} \quad (1)$$

The CF can then be used for subsequent data sets to obtain the predicted plasma/serum concentrations (C_{pred}) from C_{DMM} without the need for regression analysis (Eq. 2).

$$C_{pred} = C_{DMM} \cdot CF \quad (2)$$

If no paired samples are available for either performing regression analysis or calculating a CF, the plasma concentration can also be predicted based on the partitioning of the drug between blood cells and plasma itself (Figure 6). The partitioning can be described by means of blood cells to plasma partitioning coefficient $K_{BC/Pla}$ as quotient between the total drug concentration in blood cells C_{BC} and the total drug concentration in plasma C_{Pla} (Eq. 3) [213].

$$K_{BC/Pla} = \frac{C_{BC}}{C_{Pla}} \quad (3)$$

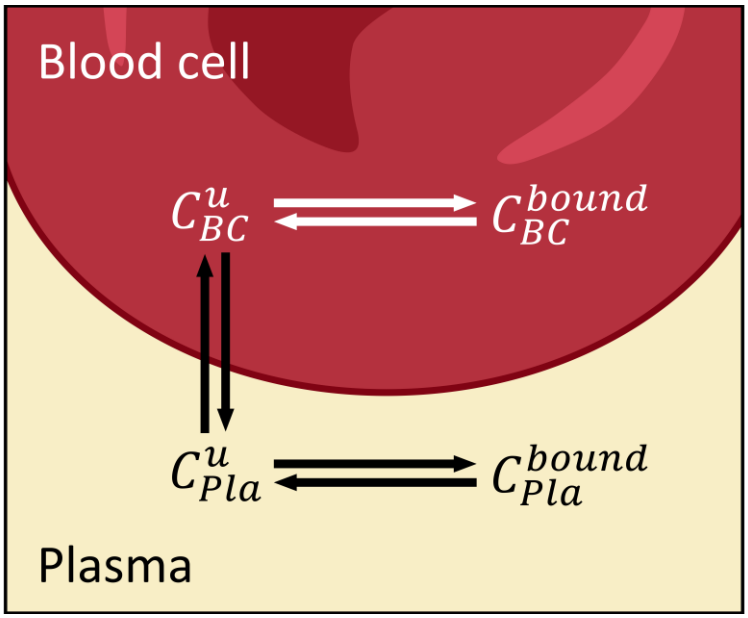

Figure 6 Schematic depiction of the partitioning of the drug between blood cell and plasma considering bound and unbound fractions.

As can be seen in Figure 6, the drug can be either bound or unbound in both compartments. Therefore, plasma protein binding must also be taken into account. The total plasma concentration can be calculated based on the unbound ("free") plasma concentration C_{Pla}^{u} and the fraction unbound f_u (Eq. 4) [213-215].

$$C_{Pla} = \frac{C_{Pla}^{u}}{f_u} \tag{4}$$

Both equations, Eq. 3 and Eq. 4, can be combined to Eq. 5. It must be noted that the quotient between the drug concentration in blood cells and the free plasma concentration represents ρ (rho), the drug affinity to blood cells (Eq. 6) [213]. Therefore, Eq. 5 can also be expressed as Eq. 7. Thus, the partitioning coefficient is dependent on the affinity to blood cells and the plasma protein binding.

$$K_{BC/Pla} = \frac{C_{BC}}{C_{Pla}^{u}} \cdot f_u \tag{5}$$

$$\frac{C_{BC}}{C_{Pla}^{u}} = \rho \tag{6}$$

$$K_{BC/Pla} = \rho \cdot f_u \tag{7}$$

The equations Eq. 3-7 enable the description of the partitioning of the drug between blood cells and plasma. The information can be used to be translated for calculation of whole blood concentrations (C_{WB}), combining blood cell and plasma

concentration, according to Eq. 8 [213-215]. However, one additional variable is necessary in this regard for calculation, the Hct.

$$C_{WB} = [\frac{1 - Hct}{f_u} + \mathrm{Hct} \times \rho\ ] \times C_{Pla}^{u} \quad (8)$$

In order to calculate the plasma concentration based on whole blood concentration, Eq. 8 must be converted according to Iacuzzi et al. (Eq. 9) [213].

$$C_{Pla} = \frac{C_{WB}}{(1 - Hct) + Hct \times \rho \times f_u} \quad (9)$$

Since no whole blood is collected by DMM, measured capillary blood concentrations are used for C_{WB}. However, capillary blood samples consist of both venous and arterial blood, as well as interstitial fluids, whereas whole blood samples are only obtained from venous blood [208]. Consequently, both matrices differ from each other, which must be taken into account. Further tests should be performed to assess the agreement between the predicted plasma concentrations and the measured plasma concentrations for all conversion methods (e.g., via Bland-Altman plots) [208].

1.4. Bioanalysis

1.4.1. Liquid chromatography – tandem mass spectrometry

Liquid chromatography in combination with mass-selective detectors (LC-MS) are primarily used for the quantitative determination of small molecules from biological matrices [179, 216-222]. The principle of HPLC (high performance liquid chromatography) is based on the interaction of the analytes between a mobile, liquid phase and a stationary phase. Due to different physicochemical properties of the molecules and thus different affinities between the two phases, the analytes are separated from one another [220]. The separation procedure comprises different techniques. Reversed phase (RP) chromatography, which uses (alkyl) modified (e.g., C18, C8) silica particles as stationary phase, is most preferred in clinical laboratory routine [218]. Other modifications may be selected for example to increase aromatic retention (π-π interaction) or to achieve chiral separation [220]. In addition, there are further separation modes by means of normal phase (NP), ion exchange (IE), hydrophilic interaction chromatography (HILIC), or dual retention mechanisms (mixed-mode chromatography) [220]. The mobile phase consists of a water-organic mixture

(e.g., methanol, acetonitrile), usually as a gradient elution [220]. Additives may be used to achieve constant pH or if necessary for ion pairing. However, care should be taken that the reagents are detector compatible.

For analyte detection, tandem mass spectrometry (MS/MS) is used. It is based on the construction of three separate quadrupoles that are combined for selective and sensitive analyte quantification [223]. This setup of tandem-in-space mass spectrometry consists of two single quadrupole mass analyzers connected in series and separated by a collision cell [223, 224]. Since the collision cell can also be built of four parallel arranged rod electrodes, the characteristic of a quadrupole, it is also known as triple-quad mass spectrometer (QqQ). However, the collision cell is not necessarily designed as a quadrupole but can also be a hexa- or octupole [224]. The first quadrupole (Q_1) serves as an ion filter based on the analyte mass and charge. With the combination of DC (direct current) and RF (radiofrequency) potential applied to the rod electrodes, ions can be stabilized in an alternating electrodynamic field on oscillating paths through the quadrupole [222, 224]. Thereby, specific mass-to-charge ratios (m/z) can be isolated. In a second step, the ion beam is directed into the collision cell, where a collision of the analyte ion with inert gas atoms (He, Ar) or molecules (N_2) is induced, leading to dissociation [224]. The collision-induced dissociation (CID) results in the fragmentation of the molecule [224]. The resulting fragments are then directed into another quadrupole (Q_3), where ions are isolated again according to their mass-to-charge ratios. Finally, the charged fragments are detected, e.g., through an electron multiplier. Other mass analyzers than the quadrupole may be used and combined depending on their area of use. Examples for these are time-of-flight (TOF), magnetic sector, (linear) quadrupole ion trap, Fourier transform ion cyclotron, or orbitrap [224].

A high vacuum of less than 10^{-5} Torr is necessary for the mass spectrometric application [224]. After chromatographic separation, however, the analytes are eluted under atmospheric pressure and must first be ionized and evaporated. Only then can the gas phase ions be transferred for MS/MS detection. Therefore, atmospheric pressure ionization (API) is required for online LC-MS application [220, 225]. Electrospray ionization (ESI) and atmospheric pressure chemical ionization (APCI) are the preferred ionization methods for quantitative drug analysis [217, 220].

1.4.2. Sample preparation

Biological matrices contain numerous small and large molecules, e.g., phospholipids, carbohydrates, endogenous ligands, and proteins, and may also contain high salt concentrations or intact cells, such as erythrocytes [226, 227]. Due to the complexity of the matrix, co-eluting endogenous compounds could cause interferences with the analyte(s) of interest, which may negatively affect chromatographic separation or drug ionization [226, 228]. Direct injection of the biological sample may damage the instruments by contamination [227, 229]. Plasma for example contains approx. 8% of proteins, which would, after direct injection, precipitate through the organic solvent in the mobile phase and clog the analytical system [226, 227]. On the other hand, analyte concentration may be very low and might not exceed the limit of quantification without additional analyte concentrating steps.

Different techniques are used for sample preparation. The simplest method is protein precipitation (PP), in which the contained proteins are precipitated by the addition of miscible organic solvents (acetonitrile, acetone, ethanol, methanol) and separated afterwards by centrifugation or filtration [227, 230]. The protein-free supernatant or filtrate is then analyzed. Instead of miscible organic solvents, acids, such as trichloroacetic acid, or salts can also be used as protein precipitants [227]. Through denaturation of the proteins, this sample preparation results in the determination of the total drug concentration. A high recovery is achieved by PP because small molecules remain present in the sample, but this also leads to high concentrations of phospholipids, which are a major cause of ion suppression or enhancement [227, 228, 231, 232].

To reduce the matrix effects, liquid-liquid extraction (LLE) is more suitable. For LLE, the sample, which must be in (aqueous) liquid form, is also extracted by an organic solvent, but other than PP, immiscible solvents are used. The extraction is based on the partitioning of the analyte between the two liquid phases [227]. Commonly used solvents are for example diethyl ether, dichloromethane, ethyl acetate, hexane, or methyl-tert-buthyl ether all of which have different physicochemical properties [226, 227]. Other extraction methods based on LLE are supported liquid extraction (SLE) and salting-out assisted liquid-liquid extraction (SALLE) [227, 230].

Besides PP and LLE, solid phase extraction (SPE) is also commonly used as an extraction method for biological samples. The dissolved analyte is absorbed on the

surface of a solid packed material [227]. Hence, the drug is retained on the stationary phase, while other compounds are washed out and thus separated from the drug. Afterwards, the retained analyte can be eluted with a suitable solvent and the extract can be further processed if necessary. This extraction method offers the advantage of less matrix effects compared to PP and higher recovery than LLE but comes with higher costs [226, 227]. It can also be coupled with the analytical instrument for online analysis (online SPE) [227, 233]. In addition, there are a variety of miniaturized SPE and LLE methods, as well as highly selective (immunological) extraction methods [226, 227, 230].

1.4.3. Bioanalytical method validation

The quality of a bioanalytical investigation depends largely on the quality of the underlying bioanalytical data [234]. Therefore, standardized guidelines are essential to ensure their reliability. Although the first efforts to find a common consensus on the requirements for bioanalytical methods were made as early as 1990, it took another decade for the FDA to publish their first guidance [234]. The final document in 2001 provided for the first time the framework conditions for bioanalytical method validation [235], which was followed by many authorities, such as the European Medicine Agency (EMA), to publish their own guideline [236]. To overcome the difficulties of combining all the requirements of different authorities, the International Council for Harmonisation of Technical Requirements for Pharmaceuticals for Human Use (ICH) has recently published a harmonized guideline (M10) to replace the existing, national guidelines [237]. The scope of the guideline refers to studies relevant to regulatory submissions and provides the international standards for bioanalytical methods. In addition, there are further guidelines whose scopes differ from the previous ones and which also specify validation parameters and acceptance criteria for method validation, such as the guideline of the Society of Toxicological and Forensic Chemistry (GTFCh) for quality assurance in forensic-toxicological analyses (appendix B) [238], the International Association for Therapeutic Drug Monitoring and Clinical Toxicology (IATDMCT) guideline for development and validation of dried blood spot-based methods for TDM [208], or the ICH guidelines Q2(R2) (validation of analytical procedures) [239] and Q14 (analytical procedure development) [240].

The following information refers solely to the current version of the ICH M10 guideline. A distinction is made between chromatographic methods, the requirements of which are presented in more detail below, and ligand binding assays. Depending on

the extent of validation it is also differentiated between partial validation, e.g., when method parameters are changed, cross validation to demonstrate the comparability of different laboratories, and full validation. The latter should be performed when a newly developed bioanalytical method is intended for its use in (regulatory) clinical and nonclinical studies. Before validation is started, it must be ensured that the method is suitable for this purpose. The design, procedures, operating conditions, as well as the limits and suitability should be previously defined during method development. The reference standard should be of high quality, well characterized, and identical to the analyte. For method validation as well as study sample analysis, preparation of calibrators (CR) and quality control (QC) samples is required by spiking blank matrix with (separate) reference standard stock or working solutions. The use of an isotope-labeled internal standard (IS) of the analyte is recommended for LC-MS/MS to compensate for example unequal ionization (matrix effect) and should be added during sample preparation to CR, QC, and study samples. Full validation does require the investigation of several elements, including selectivity, specificity, matrix effects, calibration curve and range, accuracy and precision (A&P), carry-over, dilution integrity, stability, and reinjection reproducibility (Table 2).

Table 2 Validation elements necessary for full validation according to ICH M10 [237].

Validation parameter	Rationale for validation
• *Selectivity*	Can an analyte be determined without interference?
• *Specificity*	Can an analyte be determined in the presence of other components?
• *Matrix effect*	Is there an alteration in response caused by the matrix?
• *Calibration Curve and Range*	Is there a relationship between the nominal analyte concentration and its instrument response within the interval of lower and upper limit of quantification?
• *Accuracy and Precision (A&P)*	How closely does the determined analyte concentration agree with the nominal value and how large is the scatter among multiple analyses?
• *Carry-over*	Does analyte from a preceding sample remain in the analytical instrument and to what extent can the analyte be determined in subsequent samples?

• *Dilution Integrity*	Does sample dilution procedure, e.g., for concentrations above the upper limit of quantification, impact the measured concentration of an analyte?
• *Stability*	To what extent do specific storage and use conditions affect the degradation of the analyte in a specific matrix?
• *Reinjection Reproducibility*	Can reproducible results be obtained when reinjecting samples?

Depending on the nature of the bioanalytical method, additional considerations may be required for validation. A surrogate matrix approach or the use of a standard addition approach may be necessary (among others) to overcome the challenges that arise when the analyte of interest is also an endogenous compound. For methods that employ sample extraction, the extraction efficiency (recovery) should be evaluated for the analyte and IS during method validation in addition to the above listed elements. In the case of new or alternative technologies, including sampling strategies like DMM, measures must be taken to ensure that these methods also provide reliable results. Measures for DMM-specific validation may include but are not limited to the examination of hematocrit effect, sample homogeneity, especially for punched samples from filter cards, extraction of the sample from the dried matrix, and sample collection for incurred sample reanalysis (ISR). These criteria for the evaluation of DMM-specific methods are also recommended by the IATDMCT [208].

1.5. References

[1] Cohen, P., The origins of protein phosphorylation. *Nature Cell Biology*, 2002. **4**(5): p. E127-30.

[2] Ardito, F., Giuliani, M., Perrone, D., Troiano, G., and Lo Muzio, L., The crucial role of protein phosphorylation in cell signaling and its use as targeted therapy (Review). *International Journal of Molecular Medicine*, 2017. **40**(2): p. 271-280.

[3] Manning, G., Whyte, D.B., Martinez, R., Hunter, T., and Sudarsanam, S., The protein kinase complement of the human genome. *Science*, 2002. **298**(5600): p. 1912-34.

[4] Zhong, L., Li, Y., Xiong, L., Wang, W., Wu, M., Yuan, T., et al., Small molecules in targeted cancer therapy: advances, challenges, and future perspectives. *Signal Transduction and Targeted Therapy*, 2021. **6**(1): p. 201.

[5] Deribe, Y.L., Pawson, T., and Dikic, I., Post-translational modifications in signal integration. *Nature Structural & Molecular Biology*, 2010. **17**(6): p. 666-72.

[6] Wilson, L.J., Linley, A., Hammond, D.E., Hood, F.E., Coulson, J.M., MacEwan, D.J., et al., New Perspectives, Opportunities, and Challenges in Exploring the Human Protein Kinome. *Cancer Research*, 2018. **78**(1): p. 15-29.

[7] Olsen, J.V., Blagoev, B., Gnad, F., Macek, B., Kumar, C., Mortensen, P., and Mann, M., Global, in vivo, and site-specific phosphorylation dynamics in signaling networks. *Cell*, 2006. **127**(3): p. 635-48.

[8] Heath, C.M., Stahl, P.D., and Barbieri, M.A., Lipid kinases play crucial and multiple roles in membrane trafficking and signaling. *Histology and Histopathology*, 2003. **18**: p. 989-998.

[9] Kanev, G.K., de Graaf, C., de Esch, I.J.P., Leurs, R., Wurdinger, T., Westerman, B.A., and Kooistra, A.J., The Landscape of Atypical and Eukaryotic Protein Kinases. *Trends in Pharmacological Sciences*, 2019. **40**(11): p. 818-832.

[10] Hunter, T., Signaling--2000 and beyond. *Cell*, 2000. **100**(1): p. 113-27.

[11] Tonks, N.K., Protein tyrosine phosphatases: from genes, to function, to disease. *Nature Reviews Molecular Cell Biology*, 2006. **7**(11): p. 833-46.

[12] Cohen, P., The role of protein phosphorylation in human health and disease. The Sir Hans Krebs Medal Lecture. *European Journal of Biochemistry*, 2001. **268**(19): p. 5001-10.

[13] Batista, T.M., Jayavelu, A.K., Wewer Albrechtsen, N.J., Iovino, S., Lebastchi, J., Pan, H., et al., A Cell-Autonomous Signature of Dysregulated Protein Phosphorylation Underlies Muscle Insulin Resistance in Type 2 Diabetes. *Cell Metabolism*, 2020. **32**(5): p. 844-859 e5.

[14] Zarrin, A.A., Bao, K., Lupardus, P., and Vucic, D., Kinase inhibition in autoimmunity and inflammation. *Nature Reviews Drug Discovery*, 2021. **20**(1): p. 39-63.

[15] Wesseling, H., Mair, W., Kumar, M., Schlaffner, C.N., Tang, S., Beerepoot, P., et al., Tau PTM Profiles Identify Patient Heterogeneity and Stages of Alzheimer's Disease. *Cell*, 2020. **183**(6): p. 1699-1713 e13.

[16] Bouhaddou, M., Memon, D., Meyer, B., White, K.M., Rezelj, V.V., Correa Marrero, M., et al., The Global Phosphorylation Landscape of SARS-CoV-2 Infection. *Cell*, 2020. **182**(3): p. 685-712 e19.

[17] Cohen, P., Protein kinases--the major drug targets of the twenty-first century? *Nature Reviews Drug Discovery*, 2002. **1**(4): p. 309-15.

[18] Bedard, P.L., Hyman, D.M., Davids, M.S., and Siu, L.L., Small molecules, big impact: 20 years of targeted therapy in oncology. *The Lancet*, 2020. **395**(10229): p. 1078-1088.

[19] Savage, D.G. and Antman, K.H., Imatinib mesylate--a new oral targeted therapy. *The New England Journal of Medicine*, 2002. **346**(9): p. 683-93.

[20] Cohen, P., Cross, D., and Janne, P.A., Kinase drug discovery 20 years after imatinib: progress and future directions. *Nature Reviews Drug Discovery*, 2021. **20**(7): p. 551-569.

[21] Nowell, P.C. and Hungerford, D.A., Chromosome studies on normal and leukemic human leukocytes. *Journal of the National Cancer Institute*, 1960. **25**: p. 85-109.

[22] Kurzrock, R., Gutterman, J.U., and Talpaz, M., The molecular genetics of Philadelphia chromosome-positive leukemias. *The New England Journal of Medicine*, 1988. **319**(15): p. 990-8.

[23] Zhang, J., Yang, P.L., and Gray, N.S., Targeting cancer with small molecule kinase inhibitors. *Nature Reviews Cancer*, 2009. **9**(1): p. 28-39.

[24] Fabbro, D., 25 years of small molecular weight kinase inhibitors: potentials and limitations. *Molecular Pharmacology*, 2015. **87**(5): p. 766-75.

[25] Liu, Y. and Gray, N.S., Rational design of inhibitors that bind to inactive kinase conformations. *Nature Chemical Biology*, 2006. **2**(7): p. 358-64.

[26] Huang, D., Zhou, T., Lafleur, K., Nevado, C., and Caflisch, A., Kinase selectivity potential for inhibitors targeting the ATP binding site: a network analysis. *Bioinformatics*, 2010. **26**(2): p. 198-204.

[27] Pargellis, C., Tong, L., Churchill, L., Cirillo, P.F., Gilmore, T., Graham, A.G., et al., Inhibition of p38 MAP kinase by utilizing a novel allosteric binding site. *Nature Structural & Molecular Biology*, 2002. **9**(4): p. 268-72.

[28] European Medicine Agency. Glivec: summary of product characteristics. https://www.ema.europa.eu/en/documents/product-information/glivec-epar-product-information_en.pdf Accessed March 04, 2023.

[29] Mao, B., Zhang, Q., Ma, L., Zhao, D.-S., Zhao, P., and Yan, P., Overview of Research into mTOR Inhibitors. *Molecules*, 2022. **27**(16): p. 5295.

[30] Laplante, M. and Sabatini, D.M., mTOR signaling in growth control and disease. *Cell*, 2012. **149**(2): p. 274-93.

[31] Li, J., Kim, S.G., and Blenis, J., Rapamycin: one drug, many effects. *Cell Metabolism*, 2014. **19**(3): p. 373-9.

[32] Ayala-Aguilera, C.C., Valero, T., Lorente-Macias, A., Baillache, D.J., Croke, S., and Unciti-Broceta, A., Small Molecule Kinase Inhibitor Drugs (1995-2021): Medical Indication, Pharmacology, and Synthesis. *Journal of Medicinal Chemistry*, 2022. **65**(2): p. 1047-1131.

[33] Roskoski, R., Jr., Properties of FDA-approved small molecule protein kinase inhibitors: A 2023 update. *Pharmacological Research*, 2023. **187**: p. 106552.

[34] Roskoski, R., Properties of FDA-approved small molecule protein kinase inhibitors: A 2024 update. *Pharmacological Research*, 2024. **200**: p. 107059.

[35] Food and Drug Administration Center for Drug Evaluation and Research. Novel Drug Approvals for 2023. https://www.fda.gov/drugs/new-drugs-fda-cders-new-molecular-entities-and-new-therapeutic-biological-products/novel-drug-approvals-2023 Accessed April 07, 2023.

[36] Le, R.Q., Wang, X., Zhang, H., Li, H., Przepiorka, D., Vallejo, J., et al., FDA Approval Summary: Ruxolitinib for Treatment of Chronic Graft-Versus-Host Disease after Failure of One or Two Lines of Systemic Therapy. *The Oncologist*, 2022. **27**(6): p. 493-500.

[37] Mascarenhas, J. and Hoffman, R., Ruxolitinib: the first FDA approved therapy for the treatment of myelofibrosis. *Clinical Cancer Research*, 2012. **18**(11): p. 3008-14.

[38] Sheikh, A., Rafique, W., Owais, R., Malik, F., and Ali, E., FDA approves Ruxolitinib (Opzelura) for Vitiligo Therapy: A breakthrough in the field of dermatology. *Annals of Medicine and Surgery*, 2022. **81**: p. 104499.

[39] Tavoletti, G., Avallone, G., Conforti, C., Roccuzzo, G., Maronese, C.A., Mattioli, M.A., et al., Topical ruxolitinib: A new treatment for vitiligo. *Journal of the European Academy of Dermatology and Venereology*, 2023. **37**(11): p. 2222 - 2230.

[40] Hoy, S.M., Ruxolitinib Cream 1.5%: A Review in Mild to Moderate Atopic Dermatitis. *American Journal of Clinical Dermatology*, 2023. **24**(1): p. 143-151.

[41] Abboud, R., Choi, J., Ruminski, P., Schroeder, M.A., Kim, S., Abboud, C.N., and DiPersio, J.F., Insights into the role of the JAK/STAT signaling pathway in graft-versus-host disease. *Therapeutic Advances in Hematology*, 2020. **11**: p. 1-13.

[42] European Medicine Agency. EU Clinical Trials Register. https://www.clinicaltrialsregister.eu Accessed March 04, 2023.

[43] U.S. National Library of Medicine. ClinicalTrials.gov. https://clinicaltrials.gov/ct2/home Accessed March 04, 2023.

[44] Rossari, F., Minutolo, F., and Orciuolo, E., Past, present, and future of Bcr-Abl inhibitors: from chemical development to clinical efficacy. *Journal of Hematology & Oncology*, 2018. **11**(1): p. 84.

[45] Deeks, E.D., Asciminib: First Approval. *Drugs*, 2022. **82**(2): p. 219-226.

[46] Gavrin, L.K. and Saiah, E., Approaches to discover non-ATP site kinase inhibitors. *MedChemComm*, 2013. **4**(1): p. 41-51.

[47] Bogoyevitch, M.A. and Fairlie, D.P., A new paradigm for protein kinase inhibition: blocking phosphorylation without directly targeting ATP binding. *Drug Discovery Today*, 2007. **12**(15-16): p. 622-33.

[48] Pan, Y. and Mader, M.M., Principles of Kinase Allosteric Inhibition and Pocket Validation. *Journal of Medicinal Chemistry*, 2022. **65**(7): p. 5288-5299.

[49] Dar, A.C. and Shokat, K.M., The evolution of protein kinase inhibitors from antagonists to agonists of cellular signaling. *Annual Review of Biochemistry*, 2011. **80**: p. 769-95.

[50] Lamba, V. and Ghosh, I., New directions in targeting protein kinases: focusing upon true allosteric and bivalent inhibitors. *Current Pharmaceutical Design*, 2012. **18**(20): p. 2936-45.

[51] Bhullar, K.S., Lagaron, N.O., McGowan, E.M., Parmar, I., Jha, A., Hubbard, B.P., and Rupasinghe, H.P.V., Kinase-targeted cancer therapies: progress, challenges and future directions. *Molecular Cancer*, 2018. **17**(1): p. 48.

[52] Levinson, N.M. and Boxer, S.G., A conserved water-mediated hydrogen bond network defines bosutinib's kinase selectivity. *Nature Chemical Biology*, 2014. **10**(2): p. 127-32.

[53] Shapiro, P. (2020) Next Generation Kinase Inhibitors: Moving Beyond the ATP Binding/Catalytic Sites. Springer International Publishing.

[54] Dumont, F.J. and Su, Q., Mechanism of action of the immunosuppressant rapamycin. *Life Sciences*, 1996. **58**(5): p. 373-95.

[55] Hughes, T.P., Mauro, M.J., Cortes, J.E., Minami, H., Rea, D., DeAngelo, D.J., et al., Asciminib in Chronic Myeloid Leukemia after ABL Kinase Inhibitor Failure. *The New England Journal of Medicine*, 2019. **381**(24): p. 2315-2326.

[56] Roskoski, R., Jr., Classification of small molecule protein kinase inhibitors based upon the structures of their drug-enzyme complexes. *Pharmacological Research*, 2016. **103**: p. 26-48.

[57] Lu, X., Smaill, J.B., and Ding, K., New Promise and Opportunities for Allosteric Kinase Inhibitors. *Angewandte Chemie International Edition*, 2020. **59**(33): p. 13764-13776.

[58] Zhang, H., Three generations of epidermal growth factor receptor tyrosine kinase inhibitors developed to revolutionize the therapy of lung cancer. *Drug Design, Development and Therapy*, 2016. **10**: p. 3867-3872.

[59] Gharwan, H. and Groninger, H., Kinase inhibitors and monoclonal antibodies in oncology: clinical implications. *Nature Reviews Clinical Oncology*, 2016. **13**(4): p. 209-27.

[60] Lee, Y.T., Tan, Y.J., and Oon, C.E., Molecular targeted therapy: Treating cancer with specificity. *European Journal of Pharmacology*, 2018. **834**: p. 188-196.

[61] Goetz, L.H. and Schork, N.J., Personalized medicine: motivation, challenges, and progress. *Fertility and Sterility*, 2018. **109**(6): p. 952-963.

[62] Ashley, E.A., Towards precision medicine. *Nature Reviews Genetics*, 2016. **17**(9): p. 507-522.

[63] Hamburg, M.A. and Collins, F.S., The Path to Personalized Medicine. *The New England Journal of Medicine*, 2010. **363**(4): p. 301-304.

[64] The American Geriatrics Society Beers Criteria Update Expert, P., American Geriatrics Society Updated Beers Criteria for Potentially Inappropriate Medication Use in Older Adults. *Journal of the American Geriatrics Society*, 2012. **60**(4): p. 616-631.

[65] Roberts, D.J. and Hall, R.I., Drug absorption, distribution, metabolism and excretion considerations in critically ill adults. *Expert Opinion on Drug Metabolism & Toxicology*, 2013. **9**(9): p. 1067-1084.

[66] Hirai, T., Funaki, A., Murakami, K., Hanada, K., and Itoh, T., Effects of overweight and underweight on the treatment outcomes of rheumatoid arthritis patients treated with biological drugs: A retrospective observational descriptive study. *Journal of Clinical Pharmacy and Therapeutics*, 2020. **45**(4): p. 666-673.

[67] Verrest, L., Wilthagen, E.A., Beijnen, J.H., Huitema, A.D.R., and Dorlo, T.P.C., Influence of Malnutrition on the Pharmacokinetics of Drugs Used in the Treatment of Poverty-Related Diseases: A Systematic Review. *Clinical Pharmacokinetics*, 2021. **60**(9): p. 1149-1169.

[68] McQuade, J.L., Daniel, C.R., Hess, K.R., Mak, C., Wang, D.Y., Rai, R.R., et al., Association of body-mass index and outcomes in patients with metastatic melanoma treated with targeted therapy, immunotherapy, or chemotherapy: a retrospective, multicohort analysis. *The Lancet Oncology*, 2018. **19**(3): p. 310-322.

[69] Seneadza, N.A.H., Antwi, S., Yang, H., Enimil, A., Dompreh, A., Wiesner, L., et al., Effect of malnutrition on the pharmacokinetics of anti-TB drugs in Ghanaian children. *Int J Tuberc Lung Dis*, 2021. **25**(1): p. 36-42.

[70] Hanley, M.J., Abernethy, D.R., and Greenblatt, D.J., Effect of Obesity on the Pharmacokinetics of Drugs in Humans. *Clinical Pharmacokinetics*, 2010. **49**(2): p. 71-87.

[71] Valodia, P.N., The role of heat-not-burn, snus and other nicotine-containing products as interventions for epileptic patients who take phenytoin and smoke cigarettes. *Toxicology Reports*, 2022. **9**: p. 1114-1119.

[72] Kroon, L.A., Drug interactions with smoking. *American Journal of Health-System Pharmacy*, 2007. **64**(18): p. 1917-1921.

[73] Konig, I.R., Fuchs, O., Hansen, G., von Mutius, E., and Kopp, M.V., What is precision medicine? *European Respiratory Journal*, 2017. **50**(4).

[74] Hulsen, T., Jamuar, S.S., Moody, A.R., Karnes, J.H., Varga, O., Hedensted, S., et al., From Big Data to Precision Medicine. *Frontiers in Medicine*, 2019. **6**: p. 34.

[75] Jeon, J., Du, M., Schoen, R.E., Hoffmeister, M., Newcomb, P.A., Berndt, S.I., et al., Determining Risk of Colorectal Cancer and Starting Age of Screening Based on Lifestyle, Environmental, and Genetic Factors. *Gastroenterology*, 2018. **154**(8): p. 2152-2164.e19.

[76] Ma, Z., Cheng, G., Wang, P., Khalighi, B., and Khalighi, K., Clinical Model for Predicting Warfarin Sensitivity. *Scientific Reports*, 2019. **9**(1): p. 12856.

[77] D'Andrea, G., D'Ambrosio, R.L., Di Perna, P., Chetta, M., Santacroce, R., Brancaccio, V., et al., A polymorphism in the VKORC1 gene is associated with an interindividual variability in the dose-anticoagulant effect of warfarin. *Blood*, 2005. **105**(2): p. 645-649.

[78] Zhao, C., Han, S.Y., and Li, P.P., Pharmacokinetics of Gefitinib: Roles of Drug Metabolizing Enzymes and Transporters. *Current Drug Delivery*, 2017: p. 282-288.

[79] Habet, S., Narrow Therapeutic Index drugs: clinical pharmacology perspective. *Journal of Pharmacy and Pharmacology*, 2021. **73**(10): p. 1285-1291.

[80] Shaw, K., Amstutz, U., Kim, R.B., Lesko, L.J., Turgeon, J., Michaud, V., et al., Clinical Practice Recommendations on Genetic Testing of CYP2C9 and VKORC1 Variants in Warfarin Therapy. *Therapeutic Drug Monitoring*, 2015. **37**(4).

[81] Shepherd, F.A., Rodrigues Pereira, J., Ciuleanu, T., Tan, E.H., Hirsh, V., Thongprasert, S., et al., Erlotinib in previously treated non-small-cell lung cancer. *The New England Journal of Medicine*, 2005. **353**(2): p. 123-32.

[82] Kim, E.S., Hirsh, V., Mok, T., Socinski, M.A., Gervais, R., Wu, Y.L., et al., Gefitinib versus docetaxel in previously treated non-small-cell lung cancer (INTEREST): a randomised phase III trial. *The Lancet*, 2008. **372**(9652): p. 1809-18.

[83] Paez, J.G., Janne, P.A., Lee, J.C., Tracy, S., Greulich, H., Gabriel, S., et al., EGFR mutations in lung cancer: correlation with clinical response to gefitinib therapy. *Science*, 2004. **304**(5676): p. 1497-500.

[84] Lynch, T.J., Bell, D.W., Sordella, R., Gurubhagavatula, S., Okimoto, R.A., Brannigan, B.W., et al., Activating mutations in the epidermal growth factor receptor underlying responsiveness of non-small-cell lung cancer to gefitinib. *The New England Journal of Medicine*, 2004. **350**(21): p. 2129-39.

[85] European Medicine Agency. Tafinlar: summary of product characteristics. https://www.ema.europa.eu/en/documents/product-information/tafinlar-epar-product-information_en.pdf Accessed July 19, 2021.

[86] Wuth, O., Rational bromide treatment: new methods for its control. *Journal of the American Medical Association*, 1927. **88**(26): p. 2013-2017.

[87] Cattell, M. and Gold, H., The dose of a drug. *The American Journal of Medicine*, 1947. **2**(3): p. 296-308.

[88] Koch-Weser, J., Serum Drug Concentrations as Therapeutic Guides. *The New England Journal of Medicine*, 1972. **287**(5): p. 227-231.

[89] Atkinson, A.J., Jr., Individualization of drug therapy: an historical perspective. *Translational and Clinical Pharmacology*, 2014. **22**(2): p. 52-54.

[90] Ates, H.C., Roberts, J.A., Lipman, J., Cass, A.E.G., Urban, G.A., and Dincer, C., On-Site Therapeutic Drug Monitoring. *Trends in Biotechnology*, 2020. **38**(11): p. 1262-1277.

[91] Dasgupta, A. (2012) Therapeutic Drug Monitoring: Newer Drugs and Biomarkers. Academic Press.

[92] Clark, W. and Dasgupta, A. (2016) Clinical Challenges in Therapeutic Drug Monitoring: Special Populations, Physiological Conditions and Pharmacogenomics. Elsevier.

[93] Food and Drug Administration. Population Pharmacokinetics Guidance for Industry. https://www.fda.gov/regulatory-information/search-fda-guidance-documents/population-pharmacokinetics Accessed July 18, 2023.

[94] Bardin, C., Veal, G., Paci, A., Chatelut, E., Astier, A., Leveque, D., et al., Therapeutic drug monitoring in cancer--are we missing a trick? *European Journal of Cancer*, 2014. **50**(12): p. 2005-9.

[95] Holford, N., Ma, G., and Metz, D., TDM is dead. Long live TCI! *British Journal of Clinical Pharmacology*, 2022. **88**(4): p. 1406-1413.

[96] Wicha, S.G., Märtson, A.-G., Nielsen, E.I., Koch, B.C.P., Friberg, L.E., Alffenaar, J.-W., et al., From Therapeutic Drug Monitoring to Model-Informed Precision Dosing for Antibiotics. *Clinical Pharmacology & Therapeutics*, 2021. **109**(4): p. 928-941.

[97] Buclin, T., Thoma, Y., Widmer, N., Andre, P., Guidi, M., Csajka, C., and Decosterd, L.A., The Steps to Therapeutic Drug Monitoring: A Structured Approach Illustrated With Imatinib. *Frontiers in Pharmacology*, 2020. **11**: p. 177.

[98] Groenland, S.L., Mathijssen, R.H.J., Beijnen, J.H., Huitema, A.D.R., and Steeghs, N., Individualized dosing of oral targeted therapies in oncology is crucial in the era of precision medicine. *European Journal of Clinical Pharmacology*, 2019. **75**(9): p. 1309-1318.

[99] Stojanova, J., Carland, J.E., Murnion, B., Seah, V., Siderov, J., and Lemaitre, F., Therapeutic drug monitoring in oncology - What's out there: A bibliometric evaluation on the topic. *Frontiers in Oncology*, 2022. **12**: p. 959741.

[100] de Jonge, M.E., Huitema, A.D.R., Schellens, J.H.M., Rodenhuis, S., and Beijnen, J.H., Individualised Cancer Chemotherapy: Strategies and Performance of Prospective Studies on Therapeutic Drug Monitoring with Dose Adaptation. *Clinical Pharmacokinetics*, 2005. **44**(2): p. 147-173.

[101] Buclin, T., Widmer, N., Biollaz, J., and Decosterd, L.A., Who is in charge of assessing therapeutic drug monitoring? The case of imatinib. *The Lancet Oncology*, 2011. **12**(1): p. 9-11.

[102] Klümpen, H.J., Samer, C.F., Mathijssen, R.H., Schellens, J.H., and Gurney, H., Moving towards dose individualization of tyrosine kinase inhibitors. *Cancer Treatment Reviews*, 2011. **37**(4): p. 251-60.

[103] Mueller-Schoell, A., Groenland, S.L., Scherf-Clavel, O., van Dyk, M., Huisinga, W., Michelet, R., et al., Therapeutic drug monitoring of oral targeted antineoplastic drugs. *European Journal of Clinical Pharmacology*, 2021. **77**(4): p. 441-464.

[104] Gao, B., Yeap, S., Clements, A., Balakrishnar, B., Wong, M., and Gurney, H., Evidence for therapeutic drug monitoring of targeted anticancer therapies. *Journal of Clinical Oncology*, 2012. **30**(32): p. 4017-25.

[105] Widmer, N., Bardin, C., Chatelut, E., Paci, A., Beijnen, J., Leveque, D., et al., Review of therapeutic drug monitoring of anticancer drugs part two--targeted therapies. *European Journal of Cancer*, 2014. **50**(12): p. 2020-36.

[106] Cardoso, E., Guidi, M., Blanchet, B., Schneider, M.P., Decosterd, L.A., Buclin, T., et al., Therapeutic Drug Monitoring of Targeted Anticancer Protein Kinase Inhibitors in Routine Clinical Use: A Critical Review. *Therapeutic Drug Monitoring*, 2020. **42**(1): p. 33-44.

[107] Groenland, S.L., van Eerden, R.A.G., Westerdijk, K., Meertens, M., Koolen, S.L.W., Moes, D., et al., Therapeutic drug monitoring-based precision dosing of oral targeted therapies in oncology: a prospective multicenter study. *Annals of Oncology*, 2022.

[108] Verheijen, R.B., Yu, H., Schellens, J.H.M., Beijnen, J.H., Steeghs, N., and Huitema, A.D.R., Practical Recommendations for Therapeutic Drug Monitoring of Kinase Inhibitors in Oncology. *Clinical Pharmacology & Therapeutics*, 2017. **102**(5): p. 765-776.

[109] Janssen, J.M., Dorlo, T.P.C., Steeghs, N., Beijnen, J.H., Hanff, L.M., van Eijkelenburg, N.K.A., et al., Pharmacokinetic Targets for Therapeutic Drug Monitoring of Small Molecule Kinase Inhibitors in Pediatric Oncology. *Clinical Pharmacology & Therapeutics*, 2020. **108**(3): p. 494-505.

[110] Groenland, S.L., van Eerden, R.A.G., Verheijen, R.B., Koolen, S.L.W., Moes, D., Desar, I.M.E., et al., Therapeutic Drug Monitoring of Oral Anticancer Drugs: The Dutch Pharmacology Oncology Group-Therapeutic Drug Monitoring Protocol for a Prospective Study. *Therapeutic Drug Monitoring*, 2019. **41**(5): p. 561-567.

[111] Josephs, D.H., Fisher, D.S., Spicer, J., and Flanagan, R.J., Clinical pharmacokinetics of tyrosine kinase inhibitors: implications for therapeutic drug monitoring. *Therapeutic Drug Monitoring*, 2013. **35**(5): p. 562-87.

[112] Decosterd, L.A., Widmer, N., Zaman, K., Cardoso, E., Buclin, T., and Csajka, C., Therapeutic drug monitoring of targeted anticancer therapy. *Biomarkers in Medicine*, 2015. **9**(9): p. 887-93.

[113] Cheng, F., Li, Q., Cui, Z., Hong, M., Li, W., and Zhang, Y., Dose optimization strategy of the tyrosine kinase inhibitors imatinib, dasatinib, and nilotinib for chronic myeloid leukemia: From clinical trials to real-life settings. *Frontiers in Oncology*, 2023. **13**: p. 1146108.

[114] Puisset, F., Mseddi, M., Mourey, L., Pouessel, D., Blanchet, B., Chatelut, E., and Chevreau, C., Therapeutic Drug Monitoring of Tyrosine Kinase Inhibitors in the Treatment of Advanced Renal Cancer. *Cancers*, 2023. **15**(1): p. 313.

[115] Meertens, M., Muntinghe-Wagenaar, M.B., Sikkema, B.J., Lopez-Yurda, M., Retel, V.P., Paats, M.S., et al., Therapeutic drug monitoring guided dosing versus standard dosing of alectinib in advanced ALK positive non-small cell lung cancer patients: Study protocol for an international, multicenter phase IV randomized controlled trial (ADAPT ALEC). *Frontiers in Oncology*, 2023. **13**: p. 1136221.

[116] Escudero-Ortiz, V., Domínguez-Leñero, V., Catalán-Latorre, A., Rebollo-Liceaga, J., and Sureda, M., Relevance of Therapeutic Drug Monitoring of Tyrosine Kinase Inhibitors in Routine Clinical Practice: A Pilot Study. *Pharmaceutics*, 2022. **14**(6): p. 1216.

[117] Gotta, V., Widmer, N., Decosterd, L.A., Chalandon, Y., Heim, D., Gregor, M., et al., Clinical usefulness of therapeutic concentration monitoring for imatinib dosage individualization: results from a randomized controlled trial. *Cancer Chemotherapy and Pharmacology*, 2014. **74**(6): p. 1307-19.

[118] Lankheet, N.A., Kloth, J.S., Gadellaa-van Hooijdonk, C.G., Cirkel, G.A., Mathijssen, R.H., Lolkema, M.P., et al., Pharmacokinetically guided sunitinib dosing: a feasibility study in patients with advanced solid tumours. *British Journal of Cancer*, 2014. **110**(10): p. 2441-9.

[119] Verheijen, R.B., Bins, S., Mathijssen, R.H.J., Lolkema, M.P., van Doorn, L., Schellens, J.H.M., et al., Individualized Pazopanib Dosing: A Prospective Feasibility Study in Cancer Patients. *Clinical Cancer Research*, 2016. **22**(23): p. 5738-5746.

[120] de Wit, D., van Erp, N.P., den Hartigh, J., Wolterbeek, R., den Hollander-van Deursen, M., Labots, M., et al., Therapeutic drug monitoring to individualize the dosing of pazopanib: a pharmacokinetic feasibility study. *Therapeutic Drug Monitoring*, 2015. **37**(3): p. 331-8.

[121] Lankheet, N.A.G., Desar, I.M.E., Mulder, S.F., Burger, D.M., Kweekel, D.M., van Herpen, C.M.L., et al., Optimizing the dose in cancer patients treated with imatinib, sunitinib and pazopanib. *British Journal of Clinical Pharmacology*, 2017. **83**(10): p. 2195-2204.

[122] Guchelaar, N.A.D., van Eerden, R.A.G., Groenland, S.L., Doorn, L.v., Desar, I.M.E., Eskens, F.A.L.M., et al., Feasibility of therapeutic drug monitoring of sorafenib in patients with liver or thyroid cancer. *Biomedicine & Pharmacotherapy*, 2022. **153**: p. 113393.

[123] Fahmy, A., Hopkins, A.M., Sorich, M.J., and Rowland, A., Evaluating the utility of therapeutic drug monitoring in the clinical use of small molecule kinase inhibitors: a review of the literature. *Expert Opinion on Drug Metabolism & Toxicology*, 2021. **17**(7): p. 803-821.

[124] Kluwe, F., Michelet, R., Mueller-Schoell, A., Maier, C., Klopp-Schulze, L., van Dyk, M., et al., Perspectives on Model-Informed Precision Dosing in the Digital Health Era: Challenges, Opportunities, and Recommendations. *Clinical Pharmacology & Therapeutics*, 2021. **109**(1): p. 29-36.

[125] Darwich, A.S., Ogungbenro, K., Vinks, A.A., Powell, J.R., Reny, J.L., Marsousi, N., et al., Why Has Model-Informed Precision Dosing Not Yet Become Common Clinical Reality? Lessons From the Past and a Roadmap for the Future. *Clinical Pharmacology & Therapeutics*, 2017. **101**(5): p. 646-656.

[126] Sheiner, L.B., Rosenberg, B., and Melmon, K.L., Modelling of individual pharmacokinetics for computer-aided drug dosage. *Computers and Biomedical Research*, 1972. **5**(5): p. 441-459.

[127] Sheiner, L.B., Rosenberg, B., and Marathe, V.V., Estimation of population characteristics of pharmacokinetic parameters from routine clinical data. *Journal of Pharmacokinetics and Pharmacodynamics*, 1977. **5**(5): p. 445-79.

[128] Sheiner, L.B., The Population Approach to Pharmacokinetic Data Analysis: Rationale and Standard Data Analysis Methods. *Drug Metabolism Reviews*, 1984. **15**(1-2): p. 153-171.

[129] Ette, E.I. and Williams, P.J., Population Pharmacokinetics I: Background, Concepts, and Models. *Annals of Pharmacotherapy*, 2004. **38**(10): p. 1702-1706.

[130] Duffull, S.B., Wright, D.F.B., and Winter, H.R., Interpreting population pharmacokinetic-pharmacodynamic analyses – a clinical viewpoint. *British Journal of Clinical Pharmacology*, 2011. **71**(6): p. 807-814.

[131] Mould, D.R. and Upton, R.N., Basic Concepts in Population Modeling, Simulation, and Model-Based Drug Development. *CPT: Pharmacometrics & Systems Pharmacology*, 2012. **1**(9): p. 6.

[132] Pillai, G., Mentré, F., and Steimer, J.-L., Non-Linear Mixed Effects Modeling – From Methodology and Software Development to Driving Implementation in Drug Development Science. *Journal of Pharmacokinetics and Pharmacodynamics*, 2005. **32**(2): p. 161-183.

[133] Ette, E.I. and Williams, P.J., Population pharmacokinetics II: estimation methods. *Annals of Pharmacotherapy*, 2004. **38**(11): p. 1907-15.

[134] Rousseau, A. and Marquet, P., Application of pharmacokinetic modelling to the routine therapeutic drug monitoring of anticancer drugs. *Fundamental & Clinical Pharmacology*, 2002. **16**(4): p. 253-262.

[135] Mc Laughlin, A.M., Schmulenson, E., Teplytska, O., Zimmermann, S., Opitz, P., Groenland, S.L., et al., Developing a Nationwide Infrastructure for Therapeutic Drug Monitoring of Targeted Oral Anticancer Drugs: The ON-TARGET Study Protocol. *Cancers (Basel)*, 2021. **13**(24): p. 6281.

[136] Isberner, N., Gesierich, A., Balakirouchenane, D., Schilling, B., Aghai-Trommeschlaeger, F., Zimmermann, S., et al., Monitoring of Dabrafenib and Trametinib in Serum and Self-Sampled Capillary Blood in Patients with BRAFV600-Mutant Melanoma. *Cancers (Basel)*, 2022. **14**(19): p. 4566.

[137] Maier, C., Hartung, N., de Wiljes, J., Kloft, C., and Huisinga, W., Bayesian Data Assimilation to Support Informed Decision Making in Individualized Chemotherapy. *CPT: Pharmacometrics & Systems Pharmacology*, 2020. **9**(3): p. 153-164.

[138] Sheiner, L.B., Beal, S., Rosenberg, B., and Marathe, V.V., Forecasting individual pharmacokinetics. *Clinical Pharmacology & Therapeutics*, 1979. **26**(3): p. 294-305.

[139] Broeker, A., Nardecchia, M., Klinker, K.P., Derendorf, H., Day, R.O., Marriott, D.J., et al., Towards precision dosing of vancomycin: a systematic evaluation of pharmacometric models for Bayesian forecasting. *Clinical Microbiology and Infection*, 2019. **25**(10): p. 1286.e1-1286.e7.

[140] Keizer, R.J., ter Heine, R., Frymoyer, A., Lesko, L.J., Mangat, R., and Goswami, S., Model-Informed Precision Dosing at the Bedside: Scientific Challenges and Opportunities. *CPT: Pharmacometrics & Systems Pharmacology*, 2018. **7**(12): p. 785-787.

[141] Karlsson, M.O. and Sheiner, L.B., The importance of modeling interoccasion variability in population pharmacokinetic analyses. *Journal of Pharmacokinetics and Biopharmaceutics*, 1993. **21**(6): p. 735-750.

[142] Abrantes, J.A., Jönsson, S., Karlsson, M.O., and Nielsen, E.I., Handling interoccasion variability in model-based dose individualization using therapeutic drug monitoring data. *British Journal of Clinical Pharmacology*, 2019. **85**(6): p. 1326-1336.

[143] Djodikromo, M.F., Hermens, R.P., Bemt, B., Smit, Y., Govers, T.M., Bekker, C.L., and Blijlevens, N.M., Patient-guided dose reduction of tyrosine kinase inhibitors in chronic myeloid leukaemia (RODEO study): study protocol for a prospective, multicentre, single-arm trial. *BMC Cancer*, 2023. **23**(1): p. 231.

[144] Bower, H., Bjorkholm, M., Dickman, P.W., Hoglund, M., Lambert, P.C., and Andersson, T.M., Life Expectancy of Patients With Chronic Myeloid Leukemia Approaches the Life Expectancy of the General Population. *Journal of Clinical Oncology*, 2016. **34**(24): p. 2851-7.

[145] Rivellese, F., Lobasso, A., Barbieri, L., Liccardo, B., de Paulis, A., and Rossi, F.W., Novel Therapeutic Approaches in Rheumatoid Arthritis: Role of Janus Kinases Inhibitors. *Current Medicinal Chemistry*, 2019. **26**(16): p. 2823-2843.

[146] Jegatheeswaran, J., Turk, M., and Pope, J.E., Comparison of Janus kinase inhibitors in the treatment of rheumatoid arthritis: a systemic literature review. *Immunotherapy*, 2019. **11**(8): p. 737-754.

[147] Hochhaus, A., Baccarani, M., Silver, R.T., Schiffer, C., Apperley, J.F., Cervantes, F., et al., European LeukemiaNet 2020 recommendations for treating chronic myeloid leukemia. *Leukemia*, 2020. **34**(4): p. 966-984.

[148] Steegmann, J.L., Baccarani, M., Breccia, M., Casado, L.F., Garcia-Gutierrez, V., Hochhaus, A., et al., European LeukemiaNet recommendations for the management and avoidance of adverse events of treatment in chronic myeloid leukaemia. *Leukemia*, 2016. **30**(8): p. 1648-71.

[149] Valent, P., Hadzijusufovic, E., Schernthaner, G.H., Wolf, D., Rea, D., and le Coutre, P., Vascular safety issues in CML patients treated with BCR/ABL1 kinase inhibitors. *Blood*, 2015. **125**(6): p. 901-6.

[150] Pinilla-Ibarz, J., Cortes, J., and Mauro, M.J., Intolerance to tyrosine kinase inhibitors in chronic myeloid leukemia: Definitions and clinical implications. *Cancer*, 2011. **117**(4): p. 688-97.

[151] van Leeuwen, R.W., van Gelder, T., Mathijssen, R.H., and Jansman, F.G., Drug-drug interactions with tyrosine-kinase inhibitors: a clinical perspective. *The Lancet Oncology*, 2014. **15**(8): p. e315-26.

[152] Fabro, F., Lamfers, M.L.M., and Leenstra, S., Advancements, Challenges, and Future Directions in Tackling Glioblastoma Resistance to Small Kinase Inhibitors. *Cancers (Basel)*, 2022. **14**(3).

[153] Lovly, C.M. and Shaw, A.T., Molecular pathways: resistance to kinase inhibitors and implications for therapeutic strategies. *Clinical Cancer Research*, 2014. **20**(9): p. 2249-56.

[154] Smidova, V., Michalek, P., Goliasova, Z., Eckschlager, T., Hodek, P., Adam, V., and Heger, Z., Nanomedicine of tyrosine kinase inhibitors. *Theranostics*, 2021. **11**(4): p. 1546-1567.

[155] Augustijns, P., Wuyts, B., Hens, B., Annaert, P., Butler, J., and Brouwers, J., A review of drug solubility in human intestinal fluids: implications for the prediction of oral absorption. *European Journal of Pharmaceutical Sciences*, 2014. **57**: p. 322-32.

[156] Budha, N.R., Frymoyer, A., Smelick, G.S., Jin, J.Y., Yago, M.R., Dresser, M.J., et al., Drug absorption interactions between oral targeted anticancer agents and PPIs: is pH-dependent solubility the Achilles heel of targeted therapy? *Clinical Pharmacology & Therapeutics*, 2012. **92**(2): p. 203-13.

[157] Willemsen, A.E., Lubberman, F.J., Tol, J., Gerritsen, W.R., van Herpen, C.M., and van Erp, N.P., Effect of food and acid-reducing agents on the absorption of oral targeted therapies in solid tumors. *Drug Discovery Today*, 2016. **21**(6): p. 962-76.

[158] European Medicine Agency. Iressa: summary of product characteristics. https://www.ema.europa.eu/en/documents/product-information/iressa-epar-product-information_en.pdf Accessed April 20, 2023.

[159] European Medicine Agency. Bosulif: summary of product characteristics. https://www.ema.europa.eu/en/documents/product-information/bosulif-epar-product-information_en.pdf Accessed February 09, 2024.

[160] European Medicine Agency. Votrient: summary of product characteristics. https://www.ema.europa.eu/en/documents/product-information/votrient-epar-product-information_en.pdf Accessed April 20, 2023.

[161] McCaleb, R.V., Gandhi, A.S., Clark, S.M., and Clemmons, A.B., Clinical Outcomes of Acid Suppressive Therapy Use in Hematology/Oncology Patients at an Academic Medical Center. *Annals of Pharmacotherapy*, 2016. **50**(7): p. 541-547.

[162] Ouellet, D., Grossmann, K.F., Limentani, G., Nebot, N., Lan, K., Knowles, L., et al., Effects of particle size, food, and capsule shell composition on the oral bioavailability of dabrafenib, a BRAF inhibitor, in patients with BRAF mutation-positive tumors. *Journal of Pharmaceutical Sciences*, 2013. **102**(9): p. 3100-3109.

[163] Wind, S., Schnell, D., Ebner, T., Freiwald, M., and Stopfer, P., Clinical Pharmacokinetics and Pharmacodynamics of Afatinib. *Clinical Pharmacokinetics*, 2017. **56**(3): p. 235-250.

[164] Thomas, K.S., Billingsley, A., Amarshi, N., and Nair, B.A., Elevated international normalized ratio associated with concomitant warfarin and erlotinib. *American Journal of Health-System Pharmacy*, 2010. **67**(17): p. 1426-9.

[165] Grenader, T., Gipps, M., Shavit, L., and Gabizon, A., Significant drug interaction: phenytoin toxicity due to erlotinib. *Lung Cancer*, 2007. **57**(3): p. 404-6.

[166] Teo, Y.L., Ho, H.K., and Chan, A., Metabolism-related pharmacokinetic drug-drug interactions with tyrosine kinase inhibitors: current understanding, challenges and recommendations. *British Journal of Clinical Pharmacology*, 2015. **79**(2): p. 241-53.

[167] Hakkola, J., Hukkanen, J., Turpeinen, M., and Pelkonen, O., Inhibition and induction of CYP enzymes in humans: an update. *Archives of Toxicology*, 2020. **94**(11): p. 3671-3722.

[168] European Medicine Agency. Jakavi: summary of product characteristics. https://www.ema.europa.eu/en/documents/product-information/jakavi-epar-product-information_en.pdf Accessed September 18, 2020.

[169] Abbas, R., Hug, B.A., Leister, C., Burns, J., and Sonnichsen, D., Effect of Ketoconazole on the Pharmacokinetics of Oral Bosutinib in Healthy Subjects. *The Journal of Clinical Pharmacology*, 2011. **51**(12): p. 1721-1727.

[170] Tanaka, C., Yin, O.Q.P., Smith, T., Sethuraman, V., Grouss, K., Galitz, L., et al., Effects of Rifampin and Ketoconazole on the Pharmacokinetics of Nilotinib in Healthy Participants. *The Journal of Clinical Pharmacology*, 2011. **51**(1): p. 75-83.

[171] Gambillara, E., Laffitte, E., Widmer, N., Decosterd, L.A., Duchosal, M.A., Kovacsovics, T., and Panizzon, R.G., Severe pustular eruption associated with imatinib and voriconazole in a patient with chronic myeloid leukemia. *Dermatology*, 2005. **211**(4): p. 363-5.

[172] Pajares, B., Torres, E., Trigo, J.M., Saez, M.I., Ribelles, N., Jimenez, B., and Alba, E., Tyrosine kinase inhibitors and drug interactions: a review with practical recommendations. *Clinical and Translational Oncology*, 2012. **14**(2): p. 94-101.

[173] van Erp, N.P., Gelderblom, H., and Guchelaar, H.J., Clinical pharmacokinetics of tyrosine kinase inhibitors. *Cancer Treatment Reviews*, 2009. **35**(8): p. 692-706.

[174] Atkinson, A.J., Huang, S.-M., Lertora, J.J.L., and Vicini, P. (2021) Atkinson's Principles of Clinical Pharmacology. 4 ed.: Academic Press.

[175] van Eerden, R.A.G., Ijzerman, N.S., van Meekeren, M., Oomen-de Hoop, E., Guchelaar, N.A.D., Visser, A.M.W., et al., CYP3A4*22 Genotype-Guided Dosing of Kinase Inhibitors in Cancer Patients. *Clinical Pharmacokinetics*, 2023.

[176] Edelbroek, P.M., van der Heijden, J., and Stolk, L.M., Dried blood spot methods in therapeutic drug monitoring: methods, assays, and pitfalls. *Therapeutic Drug Monitoring*, 2009. **31**(3): p. 327-36.

[177] Wilhelm, A.J., den Burger, J.C., and Swart, E.L., Therapeutic drug monitoring by dried blood spot: progress to date and future directions. *Clinical Pharmacokinetics*, 2014. **53**(11): p. 961-73.

[178] Antunes, M.V., Charao, M.F., and Linden, R., Dried blood spots analysis with mass spectrometry: Potentials and pitfalls in therapeutic drug monitoring. *Clinical Biochemistry*, 2016. **49**(13-14): p. 1035-46.

[179] Avataneo, V., D'Avolio, A., Cusato, J., Cantu, M., and De Nicolo, A., LC-MS application for therapeutic drug monitoring in alternative matrices. *Journal of Pharmaceutical and Biomedical Analysis*, 2019. **166**: p. 40-51.

[180] Londhe, V. and Rajadhyaksha, M., Opportunities and obstacles for microsampling techniques in bioanalysis: special focus on DBS and VAMS. *Journal of Pharmaceutical and Biomedical Analysis*, 2020. **182**: p. 113102.

[181] Enderle, Y., Foerster, K., and Burhenne, J., Clinical feasibility of dried blood spots: Analytics, validation, and applications. *Journal of Pharmaceutical and Biomedical Analysis*, 2016. **130**: p. 231-243.

[182] Francke, M.I., Peeters, L.E.J., Hesselink, D.A., Kloosterboer, S.M., Koch, B.C.P., Veenhof, H., and de Winter, B.C.M., Best Practices to Implement Dried Blood Spot Sampling for Therapeutic Drug Monitoring in Clinical Practice. *Therapeutic Drug Monitoring*, 2022. **44**(5): p. 696-700.

[183] Morgan, P.E., Microsampling Devices for Routine Therapeutic Drug Monitoring-Are We There Yet? *Therapeutic Drug Monitoring*, 2021. **43**(3): p. 322-334.

[184] Delahaye, L., Veenhof, H., Koch, B.C.P., Alffenaar, J.C., Linden, R., and Stove, C., Alternative Sampling Devices to Collect Dried Blood Microsamples: State-of-the-Art. *Therapeutic Drug Monitoring*, 2021. **43**(3): p. 310-321.

[185] Roberts, J.L., Whiley, L., Gray, N., Gay, M., and Lawler, N.G. *Advanced Microsamples: Current Applications and Considerations for Mass Spectrometry-Based Metabolic Phenotyping Pipelines*. Separations, 2022. **9**, DOI: 10.3390/separations9070175.

[186] Nys, G., Kok, M.G.M., Servais, A.-C., and Fillet, M., Beyond dried blood spot: Current microsampling techniques in the context of biomedical applications. *TrAC Trends in Analytical Chemistry*, 2017. **97**: p. 326-332.

[187] Guthrie, R. and Susi, A., A Simple Phenylalanine Method for Detecting Phenylketonuria in Large Populations of Newborn Infants. *Pediatrics*, 1963. **32**: p. 338-43.

[188] Freeman, J.D., Rosman, L.M., Ratcliff, J.D., Strickland, P.T., Graham, D.R., and Silbergeld, E.K., State of the science in dried blood spots. *Clinical Chemistry*, 2018. **64**(4): p. 656-679.

[189] Kok, M.G.M. and Fillet, M., Volumetric absorptive microsampling: Current advances and applications. *Journal of Pharmaceutical and Biomedical Analysis*, 2018. **147**: p. 288-296.

[190] Deprez, S. and Stove, C.P., Dried blood microsampling-assisted therapeutic drug monitoring of immunosuppressants: An overview. *Journal of Chromatography A*, 2023. **1689**: p. 463724.

[191] Kocur, A. and Pawiński, T., Volumetric Absorptive Microsampling in Therapeutic Drug Monitoring of Immunosuppressive Drugs - From Sampling and Analytical Issues to Clinical Application. *International Journal of Molecular Sciences*, 2023. **24**(1): p. 681.

[192] Brunet, M., van Gelder, T., Asberg, A., Haufroid, V., Hesselink, D.A., Langman, L., et al., Therapeutic Drug Monitoring of Tacrolimus-Personalized Therapy: Second Consensus Report. *Therapeutic Drug Monitoring*, 2019. **41**(3): p. 261-307.

[193] D'Urso, A., Locatelli, M., Tartaglia, A., Molteni, L., D'Ovidio, C., Savini, F., et al., Therapeutic Drug Monitoring of Antiseizure Medications Using Volumetric Absorptive Microsampling: Where Are We? *Pharmaceuticals*, 2021. **14**(7).

[194] Rood, J.J.M., Schellens, J.H.M., Beijnen, J.H., and Sparidans, R.W., Recent developments in the chromatographic bioanalysis of approved kinase inhibitor drugs in oncology. *Journal of Pharmaceutical and Biomedical Analysis*, 2016. **130**: p. 244-263.

[195] Shafiei, M., Mahmood, A., Beale, P., Galettis, P., Martin, J., McLachlan, A.J., and Blinman, P., Dried Blood Spot Sampling in the Monitoring of Anticancer Therapy for Solid Tumors: A Systematic Review. *Therapeutic Drug Monitoring*, 2023.

[196] Sulochana, S.P., Daram, P., Srinivas, N.R., and Mullangi, R., Review of DBS methods as a quantitative tool for anticancer drugs. *Biomedical Chromatography*, 2019. **33**(1): p. e4445.

[197] Verougstraete, N., Stove, V., Verstraete, A.G., and Stove, C.P., Therapeutic Drug Monitoring of Tyrosine Kinase Inhibitors Using Dried Blood Microsamples. *Frontiers in Oncology*, 2022. **12**: p. 821807.

[198] la Marca, G., Villanelli, F., Malvagia, S., Ombrone, D., Funghini, S., De Gaudio, M., et al., Rapid and sensitive LC-MS/MS method for the analysis of antibiotic linezolid on dried blood spot. *Journal of Pharmaceutical and Biomedical Analysis*, 2012. **67-68**: p. 86-91.

[199] Beechinor, R.J., Cohen-Wolkowiez, M., Jasion, T., Hornik, C.P., Lang, J.E., Hernandez, R., and Gonzalez, D., A Dried Blood Spot Analysis for Solithromycin in Adolescents, Children, and Infants: A Short Communication. *Therapeutic Drug Monitoring*, 2019. **41**(6): p. 761-765.

[200] Ramadan, O., Schatz, L.M., van den Heuvel, I., Masjosthusmann, K., Groll, A.H., and Hempel, G., Developing a Method for Quantifying Meropenem in Children—Volumetric Adsorptive Microsampling Versus Plasma Sampling. *Therapeutic Drug Monitoring*, 2023. **45**(5).

[201] Kromdijk, W., Mulder, J.W., Smit, P.M., Ter Heine, R., Beijnen, J.H., and Huitema, A.D., Therapeutic drug monitoring of antiretroviral drugs at home using dried blood spots: a proof-of-concept study. *Antiviral Therapy*, 2013. **18**(6): p. 821-5.

[202] Peeters, L.E.J., Feyz, L., Hameli, E., Zwart, T., Bahmany, S., Daemen, J., et al., Clinical Validation of a Dried Blood Spot Assay for 8 Antihypertensive Drugs and 4 Active Metabolites. *Therapeutic Drug Monitoring*, 2020. **42**(3): p. 460-467.

[203] Scherf-Clavel, M. and Hogger, P., Analysis of metformin, sitagliptin and creatinine in human dried blood spots. *Journal of Chromatography B*, 2015. **997**: p. 218-28.

[204] Protti, M., Marasca, C., Cirrincione, M., Cavalli, A., Mandrioli, R., and Mercolini, L., Assessment of capillary volumetric blood microsampling for the analysis of central nervous system drugs and metabolites. *Analyst*, 2020. **145**(17): p. 5744-5753.

[205] Tey, H.Y. and See, H.H., A review of recent advances in microsampling techniques of biological fluids for therapeutic drug monitoring. *Journal of Chromatography A*, 2021. **1635**: p. 461731.

[206] Zakaria, R., Allen, K.J., Koplin, J.J., Roche, P., and Greaves, R.F., Advantages and Challenges of Dried Blood Spot Analysis by Mass Spectrometry Across the Total Testing Process. *The Journal of the International Federation of Clinical Chemistry and Laboratory Medicine*, 2016. **27**(4): p. 288-317.

[207] Velghe, S., Delahaye, L., and Stove, C.P., Is the hematocrit still an issue in quantitative dried blood spot analysis? *Journal of Pharmaceutical and Biomedical Analysis*, 2019. **163**: p. 188-196.

[208] Capiau, S., Veenhof, H., Koster, R.A., Bergqvist, Y., Boettcher, M., Halmingh, O., et al., Official International Association for Therapeutic Drug Monitoring and Clinical Toxicology Guideline: Development and Validation of Dried Blood Spot-Based Methods for Therapeutic Drug Monitoring. *Therapeutic Drug Monitoring*, 2019. **41**(4): p. 409-430.

[209] Harahap, Y., Diptasaadya, R., and Purwanto, D.J., Volumetric Absorptive Microsampling as a Sampling Alternative in Clinical Trials and Therapeutic Drug Monitoring During the COVID-19 Pandemic: A Review. *Drug Design, Development and Therapy*, 2020. **14**: p. 5757-5771.

[210] Neoteryx. Mitra Specification Sheet. https://www.neoteryx.com/hubfs/2022%20Mitra%20Collateral/Mitra%20Specification%20Sheet%20(3).pdf?hsCtaTracking=9ad4e3e3-5f23-4249-ba49-f2a731c0ad9e%7C66fe06ef-6741-4114-b04e-af2083a5d43d Accessed April 30, 2023.

[211] Neoteryx. Press Release: Trajan's Microsampling Devices Earn CE-IVD Registration in Europe, UK. https://www.neoteryx.com/microsampling-news/trajans-microsampling-devices-earn-ce-ivd-registration-in-europe-uk Accessed July 22, 2023.

[212] Van Uytfanghe, K., Heughebaert, L., and Stove, C.P., Self-sampling at home using volumetric absorptive microsampling: coupling analytical evaluation to volunteers' perception in the context of a large scale study. *Clinical Chemistry and Laboratory Medicine*, 2021. **59**(5): p. e185-e187.

[213] Iacuzzi, V., Posocco, B., Zanchetta, M., Gagno, S., Poetto, A.S., Guardascione, M., and Toffoli, G., Dried Blood Spot Technique Applied in Therapeutic Drug Monitoring of Anticancer Drugs: a Review on Conversion Methods to Correlate Plasma and Dried Blood Spot Concentrations. *Pharmaceutical Research*, 2021. **38**(5): p. 759-778.

[214] Emmons, G. and Rowland, M., Pharmacokinetic considerations as to when to use dried blood spot sampling. *Bioanalysis*, 2010. **2**(11): p. 1791-6.

[215] Rowland, M. and Emmons, G.T., Use of dried blood spots in drug development: pharmacokinetic considerations. *The AAPS Journal*, 2010. **12**(3): p. 290-3.

[216] Berna, M.J., Ackermann, B.L., and Murphy, A.T., High-throughput chromatographic approaches to liquid chromatographic/tandem mass spectrometric bioanalysis to support drug discovery and development. *Analytica Chimica Acta*, 2004. **509**(1): p. 1-9.

[217] Pandey, S., Pandey, P., Tiwari, G., and Tiwari, R., Bioanalysis in drug discovery and development. *Pharmaceutical Methods*, 2010. **1**(1): p. 14-24.

[218] Kocova Vlckova, H., Pilarova, V., Svobodova, P., Plisek, J., Svec, F., and Novakova, L., Current state of bioanalytical chromatography in clinical analysis. *Analyst*, 2018. **143**(6): p. 1305-1325.

[219] Unger, S., Li, W., Flarakos, J., and Tse, F.L.S., *Roles of LC-MS Bioanalysis in Drug Discovery, Development, and Therapeutic Drug Monitoring*, in *Handbook of LC-MS Bioanalysis: Best Practices, Experimental Protocols, and Regulations*. 2013. p. 3-13.

[220] Gey, M.H. (2015) Instrumentelle Analytik und Bioanalytik: Biosubstanzen, Trennmethoden, Strukturanalytik, Applikationen. 3rd ed.: Springer Spektrum, .

[221] Adaway, J.E. and Keevil, B.G., Therapeutic drug monitoring and LC–MS/MS. *Journal of Chromatography B*, 2012. **883-884**: p. 33-49.

[222] Wanner, K.T. and Höfner, G. (2007) Mass Spectrometry in Medicinal Chemistry. Wiley-VCH Verlag.

[223] McLafferty, F.W., Tandem mass spectrometry. *Science*, 1981. **214**(4518): p. 280-287.

[224] Gross, J.H. (2013) Massenspektrometrie: Ein Lehrbuch. 1st ed.: Springer Spektrum.

[225] Horning, E.C., Carroll, D.I., Dzidic, I., Haegele, K.D., Horning, M.G., and Stillwell, R.N., Atmospheric pressure ionization (API) mass spectrometry. Solvent-mediated ionization of samples introduced in solution and in a liquid chromatograph effluent stream. *Journal of Chromatographic Science*, 1974. **12**(11): p. 725-9.

[226] Nováková, L., Challenges in the development of bioanalytical liquid chromatography–mass spectrometry method with emphasis on fast analysis. *Journal of Chromatography A*, 2013. **1292**: p. 25-37.

[227] Li, W., Jian, W., and Fu, Y. (2019) Sample Preparation in LC-MS Bioanalysis. John Wiley & Sons.

[228] Ismaiel, O.A., Zhang, T., Jenkins, R.G., and Karnes, H.T., Investigation of endogenous blood plasma phospholipids, cholesterol and glycerides that contribute to matrix effects in bioanalysis by liquid chromatography/mass spectrometry. *Journal of Chromatography B*, 2010. **878**(31): p. 3303-3316.

[229] Soltani, S. and Jouyban, A., Biological sample preparation: attempts on productivity increasing in bioanalysis. *Bioanalysis*, 2014. **6**(12): p. 1691-710.

[230] Singleton, C., Recent advances in bioanalytical sample preparation for LC–MS analysis. *Bioanalysis*, 2012. **4**(9): p. 1123-1140.

[231] Xia, Y.Q. and Jemal, M., Phospholipids in liquid chromatography/mass spectrometry bioanalysis: comparison of three tandem mass spectrometric techniques for monitoring plasma phospholipids, the effect of mobile phase composition on phospholipids elution and the association of phospholipids with matrix effects. *Rapid Communications in Mass Spectrometry*, 2009. **23**(14): p. 2125-38.

[232] Jemal, M., Ouyang, Z., and Xia, Y.-Q., Systematic LC-MS/MS bioanalytical method development that incorporates plasma phospholipids risk avoidance, usage of incurred sample and well thought-out chromatography. *Biomedical Chromatography*, 2010. **24**(1): p. 2-19.

[233] Núñez, O., Gallart-Ayala, H., Martins, C.P.B., Lucci, P., and Busquets, R., State-of-the-art in fast liquid chromatography–mass spectrometry for bio-analytical applications. *Journal of Chromatography B*, 2013. **927**: p. 3-21.

[234] Shah, V.P., The history of bioanalytical method validation and regulation: Evolution of a guidance document on bioanalytical methods validation. *The AAPS Journal*, 2007. **9**(1): p. 43-47.

[235] Food and Drug Administration. Bioanalytical Method Validation Guidance for Industry. https://www.moh.gov.bw/Publications/drug_regulation/Bioanalytical%20Method%20Validation%20FDA%202001.pdf Accessed May 21, 2023.

[236] European Medicine Agency. Guideline on bionalatyical method validation. https://www.ema.europa.eu/en/documents/scientific-guideline/guideline-bioanalytical-method-validation_en.pdf Accessed May 30, 2020.

[237] International Council for Harmonisation of Technical Requirements for Pharmaceuticals for Human Use. Bioanalytical method validation and study sample analysis M10 https://database.ich.org/sites/default/files/M10_Guideline_Step4_2022_0524.pdf Accessed July 03, 2023.

[238] Gesellschaft für Toxikologische und Forensische Chemie. Guidelines for quality assurance in forensic-toxicological analyses; Appendix B - Requirements for the validation of analytical methods. https://www.gtfch.org/cms/images/stories/files/Appendix%20B%20GTFCh%2020090601.pdf Accessed March 06, 2024.

[239] International Council for Harmonisation of Technical Requirements for Pharmaceuticals for Human Use. Validation of analytical procedures Q2(R2). https://database.ich.org/sites/default/files/ICH_Q2%28R2%29_Guideline_2023_1130.pdf Accessed March 06, 2024.

[240] International Council for Harmonisation of Technical Requirements for Pharmaceuticals for Human Use. Analytical procedure development Q14. https://database.ich.org/sites/default/files/ICH_Q14_Guideline_2023_1116.pdf Accessed March 06, 2024.

2. Aims of the thesis

The determination of the underlying drug concentration is a key component of TDM and thus a central element of precision medicine. It is the focus of this work to develop new mass spectrometric methods to determine the drug concentration of oral small molecule KI in biological samples. The present thesis covers three different aspects, each offering a different perspective on drug monitoring. First, an example for the importance of KI drug monitoring. Second, the development and validation of a new bioanalytical method to potentially overcome existing limitations. And finally, the clinical validation of this newly developed method to demonstrate its feasibility for clinical use. The respective topics are described below in more detail.

Drug monitoring of cabozantinib in advanced adrenocortical carcinoma

Within the framework of this project, a mass spectrometric method should be developed at the Core Unit Clinical Mass Spectrometry of the University Hospital of Würzburg and validated in compliance with applicable quality regulations. The developed method is intended for monitoring the cabozantinib drug exposure in patients with adrenocortical carcinoma (ACC). In view of the off-label use of cabozantinib in those patients, drug monitoring may help to ensure therapy safety and potentially also efficacy.

Minimally invasive microsampling for kinase inhibitor drug monitoring

The aim is to develop a mass spectrometric method for the simultaneous determination of different KI from dried capillary blood samples. Thereby, the implementation of TDM should be less dependent on the patient's visit to the clinic in terms of time and location. For this purpose, the minimally invasive technique of VAMS is to be used. In addition to the regulatory guidelines from FDA and EMA, the bioanalytical method should be validated to meet DMM-specific requirements.

Clinical feasibility of volumetric absorptive microsampling

Target thresholds for TDM rarely refer to blood concentrations, but rather to plasma or serum levels. VAMS results in a specimen collection whose concentrations need to be converted into plasma or serum levels first in order to evaluate the therapy. The conversion of capillary blood concentrations into serum concentrations should be

investigated in a non-interventional study. To a greater degree, this conversion method should be clinically validated. Since VAMS is also used in the patient's home environment, the aim is to investigate the feasibility of at-home VAMS under real world conditions.

3. Results

3.1. Simulation-based interpretation of therapeutically monitored cabozantinib plasma concentration in advanced adrenocortical carcinoma with hemodialysis

Sebastian Zimmermann[1], Max Kurlbaum[1], Stefanie Mayer, Martin Fassnacht, Matthias Kroiss, Oliver Scherf-Clavel

[1] These authors contributed equally to this work.

Copyright

https://doi.org/10.1097/FTD.0000000000000905

Abstract

Background: Adrenocortical carcinoma (ACC) is an orphan but aggressive malignancy with limited treatment options. The tyrosine kinase inhibitor (TKI) cabozantinib (CAB) emerged as new potential treatment. However, no data were available, if and how CAB can be administered in patients on hemodialysis.

Methods: An LC-MS/MS method was developed and validated according to the EMA and FDA guidelines on bioanalytical method validation. Sample preparation was performed by protein precipitation and online solid phase extraction (SPE). The method was applied to clinical samples of an ACC patient on CAB treatment receiving 80 mg daily. During the ten-day observation interval, the patient received periodic hemodialysis on seven days. Pharmacokinetic (PK) simulations were performed by Bayesian forecasting according to an existing population PK model for CAB.

Results: Based on PK simulation, a mean plasma trough concentration in steady state of 1375 ng/mL (90% prediction interval (PI) 601-2602 ng/mL) at a daily dose of 80 mg was expected for CAB. However, an individual simulation including measured plasma levels of the patient resulted in a mean trough concentration of 348 ng/mL (90% PI 278-430 ng/mL). The model based on individual PK parameters

estimated accessible plasma levels of 521 ng/mL, 625 ng/mL and 834 ng/mL by dose adjustment to 100 mg, 120 mg and 160 mg respectively.

Conclusion: After establishment of an LC-MS/MS method for TDM of CAB, our analyses in a single patient undergoing hemodialysis indicated that higher doses of CAB were required than expected to achieve reasonable plasma concentrations. Our study demonstrates the value of TDM for the management of 'new' drugs in patients with renal impairment.

INTRODUCTION

Adrenocortical carcinoma (ACC) is an orphan, malignant disease of the adrenal cortex with a reported incidence of up to two cases per million per year. Sixty percent of these malignant neoplasms secrete cortical steroids[1, 2], whereas forty percent are non-functional, poorly differentiated tumors. This hypersecretion of steroid hormones is often characterized by cortisol and sex-hormone excess resulting in Cushing's syndrome and virilization. In most cases, the surgical removal of the localized tumor is the only curative therapy. Nevertheless, the majority of patients already have metastases at the time of primary diagnosis or develop them during the course of their disease. Mitotane, an adrenostatic agent, is the only approved drug and is used in an adjuvant setting[3] and in advanced disease[1, 2, 4, 5]. Standard therapy in advanced stages is the combination of mitotane with etoposid, doxorubicin and cisplatin[6]. Still, the objective response (23%) and 5-year-survival rate (10-15%) are poor, demanding for new, more effective treatment options. Therefore, several novel targeted anticancer drugs such as tyrosine kinase inhibitors (TKI) came into the focus and have been investigated in case series and clinical trials[7-13]. Cabozantinib (CAB) is a multi-kinase receptor antagonist of vascular endothelial growth factor receptor (VEGFR), hepatocyte growth factor receptor kinase MET and other tyrosine kinases, like AXL and RET[14-16]. CAB is currently approved for the therapy of medullary thyroid carcinoma (MTC), advanced renal cell carcinoma (RCC) and hepatocellular carcinoma (HCC). As VEGFR and MET are often highly overexpressed in the tumor tissue, CAB might be effective as a treatment of ACC and clinical trials are ongoing[17-20].

Only very limited data on TKI plasma levels and pharmacokinetics (PK) are available. Unfortunately, even less information is available for patients with specific clinical conditions. Thus, there are virtually no data for patients under hemodialysis,

making TKI therapy nearly inaccessible. Recently, in the context of a study evaluating response of CAB for the treatment of advanced ACC, for a subset of five patients, plasma steady state levels were collected. Extensive interindividual variability in plasma concentrations was observed, possibly related to CYP3A4 metabolism altered by previous or concomitant medication[13]. The complexity of TKI pharmacology further increases as receptor activities of the main CAB metabolites (monohydroxy-CAB, CAB-N-oxide, 6-amide cleavage product) are greatly reduced, but still show inhibition of other enzymes and transporters, e.g. CYP2C8 and organic anion transporter (OAT)[21]. As a consequence of concomitant medication, the risk for drug-drug interaction (DDI) that may result in clinically relevant adverse effects (AE) or sub therapeutic exposure and development of receptor resistance, is highly increased[22]. Moreover, disorders such as renal or hepatic impairment further increase the PK variability of TKI. These mechanisms considerably endanger the therapeutic success and safety[23]. Therapeutic drug monitoring (TDM) offers an opportunity to minimize the risk for AE and treatment failure by individually optimizing drug exposure[24] as demonstrated for several TKI. Based on the metabolic pathway, PK variability or the relationship between PK and pharmacodynamics, TDM has been proposed to be potentially useful for most kinase inhibitors, although this needs further corroboration for CAB[25, 26].

In this study, we developed and validated an LC-MS/MS method to quantify CAB in human plasma and used this method to monitor the drug exposure in a patient with advanced ACC, end-stage renal disease, daily hemodialysis and extensive concomitant medication. These results were brought into context with simulated data obtained from a population pharmacokinetics (popPK) modeling approach.

MATERIALS AND METHODS

Chemicals

CAB-(S)-malate was purchased from Biozol (Eching, Germany). Isotope labeled internal standard (IS) CAB-d4 was purchased from Alsachim (Illkirch Graffenstaden, France). HPLC grade acetonitrile (ACN), LC-MS grade water and Methanol (MeOH) were obtained from VWR International (Darmstadt, Germany) and dimethyl sulfoxide (DMSO) and formic acid, purity > 98%, were purchased from Merck (Darmstadt,

Germany). Analyte-free plasma was obtained from the University Hospital of Würzburg (Würzburg, Germany).

Instrumentation and chromatographic condition

The LC-MS/MS system consisted of a Sciex QTRAP 4500 MD (Framingham, MA, USA) linked to an Agilent 1290 UHPLC system (Waldbronn, Germany). Mobile phase for HPLC analysis was composed of A: water, containing 2% ACN and 0.1% formic acid (v/v/v), and B: ACN, containing 2% water and 0.1% formic (v/v/v). Chromatography was performed with an XBridge® BEH C18 column (3.5 µm, 2.1 x 50 mm; Waters, Milford, MA, USA) as stationary phase in combination with an Oasis® HLB column (25 µm, 2.1 x 20 mm; Waters, Milford, MA, USA) for online solid phase extraction (SPE). Gradient flow was set at 400 µL/min and increased from 10% mobile phase B at the beginning of the acquisition to 75% B. The acquisition ended after 7.50 minutes at starting conditions (details are shown in supplementary data (SD) S1). CAB and CAB-d4 were detected in electrospray ionization positive mode using multiple reaction monitoring 502.2 → 391.4 m/z for CAB and 506.0 → 391.4 m/z for CAB-d4. Collision energy was set at 40 eV for both transitions. Analyst software (version 1.6.3 MD) was used for peak area related quantification.

Sample preparation

Ten calibrators (CR) within the calibration range of 6-1000 ng/mL and five quality control (QC) level were prepared in human plasma by serial dilution. Details on the preparation of stock solution, CR and QC are listed in SDC. Sample preparation was performed by protein precipitation using MeOH/ACN (1:1, v/v). 50 µL plasma and 100 µL precipitation agent, including CAB-d4 (0.2 µg/mL) were mixed in a 1.5 mL polypropylene tube. After five seconds of vortexing and subsequent centrifugation for five minutes at 14,000 g at 4°C, 50 µL of the supernatant and 150 µL water were mixed and transferred into glass vial with insert (polypropylene). Autosampler temperature was set at 4°C and injection volume was 20 µL.

Method validation

The method validation was performed according to the FDA and EMA guidelines on bioanalytical method validation[27, 28] including linearity, accuracy and precision, sensitivity, selectivity, dilution integrity, the extent of carry over and matrix effects as

well as recovery and stability. The analytical method was cross validated at the Radboud University, Nijmegen, Netherlands[29].

Patient characteristics and plasma sampling

Plasma samples were from a 34-year-old female patient (80 kg bodyweight) treated with 80 mg COMETRIQ® capsules daily. The patient was diagnosed with hormonally active ENSAT stage II ACC (T2N0M0). After adjuvant mitotane treatment, she subsequently developed advanced disease and received additional cytostatic treatment. During chemotherapy, the patient developed chronic kidney failure and required chronic hemodialysis. Prior to CAB treatment, mitotane was discontinued, mitotane plasma concentration was undetectable before initiation of CAB (for concomitant medication, see SD S2). The TKI exposure was monitored for ten days. Four plasma samples (different sampling times) were collected on days one to four during routine blood draw, two samples were taken on days five and six and one plasma sample each was taken from the seventh day on. Periodic hemodialysis was received on each day except days two, six and nine.

PK simulation

The software R and package mrgsolve were used to simulate CAB plasma levels according to a published popPK model for CAB in various cancer types[30]. The popPK model did not contain data on ACC, therefore, the disease covariate “other” was used for simulation. Individual PK parameters and random effects on apparent clearance (η1), apparent volume of distribution (η2), relative oral bioavailability (η3) and absorption rate (η4) were determined using maximum a posteriori (MAP) and Markov chain Monte Carlo (MCMC) estimation implemented in R. After determination of the patient’s PK parameters, the most likely steady state plasma levels for possible dose adjustments were calculated prospectively.

RESULTS

Method validation

The method was successfully validated according to the regulatory guidelines. Validation results are presented in the SD (S3-S5).

PK simulation

The CAB steady state trough concentration was simulated for a reference population of 1000 cases corresponding to the patient's background (covariates: sex, race, weight, drug formulation, malignancy, age, dose and liver function). For a daily dose of 80 mg CAB capsules, the resulting expected mean plasma concentration was 1375 ng/mL. The 90% prediction interval (PI) ranged from 601 to 2602 ng/mL. Measured CAB values of days one to five were included in the initial model to simulate the most likely individual plasma course. The CAB exposure for this patient was lower than the predicted concentration (Figure 1, A).

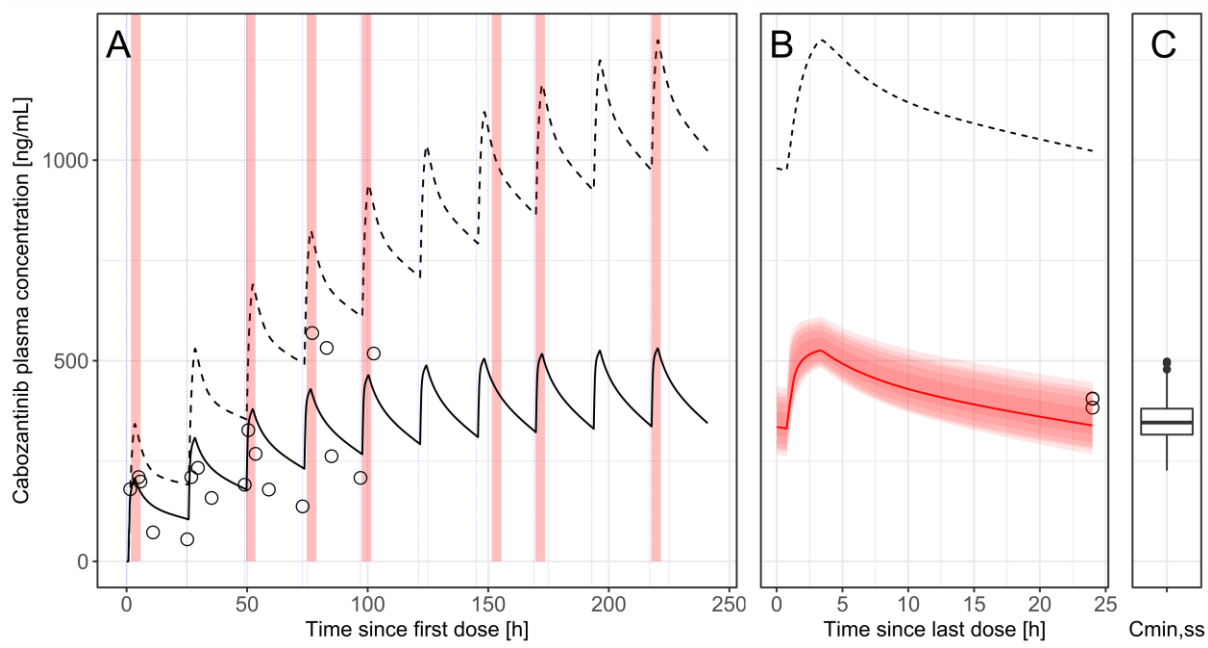

Figure 1: A: CAB popPK simulation of the typical patient (dashed line) and individual simulation using MAP Bayesian estimation (solid line), including measured plasma values (circle); time of dialysis are represented by vertical red bars. B: Simulation of the most likely individual concentration curve compared to the predicted value (dashed line) on the tenth day of CAB therapy. Individual simulation was performed by using MCMC estimation (mode = red line) with PI (95%, 90%, 85%, 75% and 50%). Circles indicate plasma concentrations on days eight, nine and ten. C: Box plot of the simulated steady state trough level based on plasma concentrations measured on days one to five. Data are visualized as median with interquartile range (two hinges). The whiskers extend from the hinges to the largest (upper whisker) or lowest (lower whisker) value with a maximum extension of 1.5 times the interquartile range. Outlying data are visualized separately (black dots).

Individual PK parameters were compared to the simulated population parameters according to the disease covariate "other". Apparent patient clearance (7.71 L/h) was higher than expected (typical value: 2.41 L/h), the apparent individual distribution volume was 316.06 L, twice as high as in the reference collective (161.20 L) (SD S6). Individual random effect distribution calculation revealed that random effects on apparent clearance (η1) and apparent volume of distribution (η2)

clearly deviated from the reference collective, whereas random effects on relative oral availability (η3) and absorption rate (η4) could not be estimated with a higher precision in the *in-silico* simulation. However, the measured concentrations provided information for reestimating individual clearance and volume of distribution. According to the initial simulation which included individual sample concentrations prior to the steady state, estimated mean trough plasma concentration for the individual steady state was 348 ng/mL (90% PI 278-430 ng/mL) (Figure 1, C). The measured plasma trough concentrations on days eight, nine and ten (383 ng/mL, 406 ng/mL and 405 ng/mL, respectively) were within the predicted range (Figure 1, B) and indeed at steady state. According to the individual PK parameters of this patient, simulated mean trough concentration for increased dosage of 100 mg daily, 120 mg daily and 160 mg daily would have been 521 ng/mL, 625 ng/mL and 834 ng/mL, respectively (Figure 2).

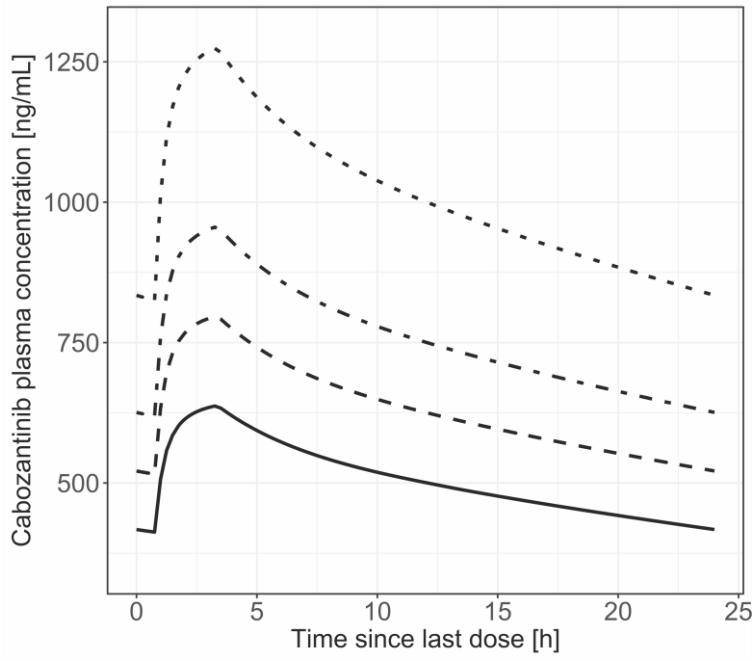

Figure 2: Prediction of the individual plasma concentration profile after virtual dose adjustment from 80 mg CAB daily (solid line) to A: 100 mg (dashed line), B: 120 mg (dot-dashed line) and C: 160 mg (dotted line).

A dosage adaptation was not performed. At the beginning and after four months of CAB therapy, tissue imaging via positron emission tomography (PET) scans were recorded to assess the tumor status and the therapeutic response, reduction in size and amount of tumor tissue was observed over the evaluated period.

DISCUSSION

TKI play an increasingly important role in the targeted therapy of a variety of malignant diseases. Data on PK are still limited especially in the context of DDI and renal impairment. In the absence of data on hemodialysis, responsible therapy with TKI requires individualized consideration of drug exposure. Prospective monitoring might contribute to optimizing therapy particularly for this patient subpopulation and enables safe access to novel treatment options.

The trough levels in this study determined as 383 ng/mL, 406 ng/mL and 405 ng/mL were significantly lower than the expected values (1054 ng/mL after ten days, 90% PI 509-1757 ng/mL) based on popPK simulation and published data. Renal failure, hemodialysis and the large number of co-administered drugs that hold the potential for DDI with regard to CYP3A4 (inhibition or induction) are plausible reasons for deviating plasma concentrations. In previous studies, none of the investigated TKI resulted in clinically meaningful response or significant improvement in therapy[7, 9-12, 31]. With the exception of linsitinib, all TKI that have been evaluated in ACC treatment are metabolized by CYP3A4, but plasma levels were not monitored during the therapy.

Therefore, rapid metabolism resulting in insufficient drug exposure may contribute to the limited effectiveness observed for these drugs. It has been shown that intake of rifampicin, a strong CYP3A4 inducer leads to a more than 4-fold increased CAB clearance and decreases the area under the curve (AUC) by 77%[32]. The intake of mitotane induces the expression of CYP3A4 as well[22], but was discontinued before initiation of therapy with CAB. Instead, therapy was given with metyrapone as an alternative treatment for Cushing's syndrome. Metyrapone acts as an inhibitor of CYP3A4[33] while inducing the expression of this metabolizing enzyme via pregnane X receptor activation[34]. Consequently, TKI clearance cannot be estimated without drug monitoring.

There is no information on the influence of hemodialysis on PK of CAB so far. Filtration by hemodialysis may have increased clearance, but due to the plasma protein binding of 99.7% enhanced elimination seems not to be the main reason for low plasma levels. For a patient undergoing hemodialysis and receiving dabrafenib, a TKI with a comparable plasma protein binding, Park et al. showed that elimination via dialysis only played a minor role[35]. In accordance with this observation, sunitinib and its active metabolite, according to the European public assessment report[36], is not eliminated by

hemodialysis, which is explained by the *in-vitro* binding to human plasma protein of 95% for sunitinib itself and of 90% for the primary metabolite. Consequently, dose adjustments of sunitinib are not recommended in patients with hemodialysis. In contrast, for ruxolitinib specific dose adaption is recommended for patients undergoing dialysis despite excessive protein binding (97%), even though hemodialysis is not expected to enhance the elimination of the drug[37]. Other physiological alterations might explain the recommendation for dose adjustment. Altered protein binding is frequently observed in patients with renal dysfunction arising from lower serum albumin concentrations or the accumulation of endogenous and exogenous substances, resulting in drug displacement from plasma proteins. The decreased protein binding could lead to an increased volume of distribution. On the other hand, adsorption processes on filter material during hemodialysis and altered body fluid composition (e.g., edema) may also increase the apparent volume of distribution. With an individual estimate of more than 300 L, far above the typical value of the PK parameter, these phenomena may explain the observations in our case. The increased individual apparent clearance suggests that potentially reduced bioavailability of the drug additionally may have played a role.

Low TKI exposure in patients with advanced ACC is not unusual and might explain the poor results in previous clinical trials[13]. In our case, 18-fluorodeoxyglucose positron emission tomography (FDG-PET) and computed tomography (CT) after 3 months of treatment showed decreased tracer uptake and tumor necrosis despite lower than predicted CAB concentrations. However, the patient deceased 6 months later from the disease. Thus, adapted plasma levels might contribute to a better clinical outcome perspectively. Dose adaptation was not performed in our case as dose-effect relationships are not established for CAB and are subject of current research. Nonetheless, definition of target values for MET/VEGFR inhibitors for tumor therapy is under discussion. For example, the correlation between CAB exposure and progression-free survival was investigated by the FDA for the approval of CAB in advanced RCC. After administration of 60 mg CAB daily, medium trough concentration was found to be 1125 ng/mL. Additional simulated dose change led to a smaller reduction in tumor size, from -11.9% for 60 mg daily to -9.1% for 40 mg and -4.5% for 20 mg, as well as a worse objective response rate. By changing the CAB exposure to 67% and 33% of the primary value, the hazard ratio increased to 1.1 and 1.39 respectively[16]. According to these data, lower plasma levels, as observed in our case,

would decrease changes of a successful therapy. The malignancy itself, renal impairment or the related supportive therapy could largely affect the PK of CAB. In MTC, apparent clearance was approximately doubled in comparison to other malignancies[30]. Due to potential of DDI, as holds true for many other TKI, monitoring of plasma levels is imperative in order to interpret results of clinical phase II studies correctly. Even if these results cannot be generalized, the importance of further systematic investigations on pathophysiological conditions, specific sub-populations, and DDI influencing PK of CAB has been identified.

CONCLUSION

ACC is an orphan but aggressive disease with limited chemotherapeutic options. TKI might be a promising approach but many questions, also on PK aspects, are still open. Nevertheless, new therapies should be made available to patients with severe courses on an individual basis. Therefore, an LC-MS/MS method for TDM of the TKI CAB with short acquisition- and preparation time fulfilling high throughput requirements for bioanalytical monitoring was developed. The method was applied to monitor CAB exposure in a patient undergoing hemodialysis. The measured plasma concentrations were lower than expected and higher doses of CAB would have been required to achieve expected plasma concentrations according to our simulations. As a result, PK modeling and simulations were performed showing pronounced individual variability in PK characteristics and significant deviation from population predicted values. These results encourage further investigations for subpopulation-specific CAB monitoring and underline the potential use of TDM in personalized management of ACC therapy.

Acknowledgments

We would like to acknowledge Nielka van Erp from the Radboud University in Nijmegen, Netherlands for cross validating the method. Furthermore, we would like to thank Sabine Kendl for technical assistance. The support from the German Research Foundation is also acknowledged.

Source of Support

This study was supported by the German Research Foundation (project 314061271 – TRR 205) and Hector Stiftung II gGmbH (Weinheim, Germany, Project MED 1807).

Disclosure

Oliver Scherf-Clavel reports endowed professorship grant (Horphag research Ltd) and received funding from the Hector Stiftung II gGmbH. Matthias Kroiss received institutional grant support and travel support from Ipsen Pharma GmbH. The remaining authors declare that the research was conducted in absence of any commercial or financial relationships that could be construed as a potential conflict of interest.

Ethics approval

This study was part of the European Network for the Study of Adrenal Tumors (ENSAT) registry, which has been approved by the ethics committee of the University of Würzburg (approval numbers 86/03 and 88/11). The study was performed in accordance with the ethical standards of the Declaration of Helsinki of 1964 and its later amendments.

All participants and their authorized representatives gave their written informed consent and assent before inclusion in this study.

REFERENCES

1. Fassnacht M, Assie G, Baudin E, et al. Adrenocortical carcinomas and malignant phaeochromocytomas: ESMO-EURACAN Clinical Practice Guidelines for diagnosis, treatment and follow-up. *Annals of Oncology*. Nov 2020;31(11):1476-1490. doi:10.1016/j.annonc.2020.08.2099

2. Else T, Kim AC, Sabolch A, et al. Adrenocortical carcinoma. *Endocrine Reviews*. Apr 2014;35(2):282-326. doi:10.1210/er.2013-1029

3. Terzolo M, Angeli A, Fassnacht M, et al. Adjuvant mitotane treatment for adrenocortical carcinoma. *N Engl J Med*. Jun 7 2007;356(23):2372-80. doi:10.1056/NEJMoa063360

4. Megerle F, Herrmann W, Schloetelburg W, et al. Mitotane Monotherapy in Patients With Advanced Adrenocortical Carcinoma. *The Journal of Clinical Endocrinology and Metabolism*. Apr 1 2018;103(4):1686-1695. doi:10.1210/jc.2017-02591

5. Fassnacht M, Dekkers OM, Else T, et al. European Society of Endocrinology Clinical Practice Guidelines on the management of adrenocortical carcinoma in adults, in collaboration with the European Network for the Study of Adrenal Tumors. *European Journal of Endocrinology*. Oct 1 2018;179(4):G1-G46. doi:10.1530/EJE-18-0608

6. Fassnacht M, Terzolo M, Allolio B, et al. Combination chemotherapy in advanced adrenocortical carcinoma. *The New England Journal of Medicine*. Jun 7 2012;366(23):2189-97. doi:10.1056/NEJMoa1200966

7. Berruti A, Sperone P, Ferrero A, et al. Phase II study of weekly paclitaxel and sorafenib as second/third-line therapy in patients with adrenocortical carcinoma. *European Journal of Endocrinology*. Mar 2012;166(3):451-8. doi:10.1530/EJE-11-0918

8. O'Sullivan C, Edgerly M, Velarde M, et al. The VEGF inhibitor axitinib has limited effectiveness as a therapy for adrenocortical cancer. *The Journal of Clinical Endocrinology and Metabolism*. Apr 2014;99(4):1291-7. doi:10.1210/jc.2013-2298

9. Quinkler M, Hahner S, Wortmann S, et al. Treatment of advanced adrenocortical carcinoma with erlotinib plus gemcitabine. *The Journal of Clinical Endocrinology and Metabolism*. Jun 2008;93(6):2057-62. doi:10.1210/jc.2007-2564

10. Kroiss M, Quinkler M, Johanssen S, et al. Sunitinib in refractory adrenocortical carcinoma: a phase II, single-arm, open-label trial. *The Journal of Clinical Endocrinology and Metabolism*. Oct 2012;97(10):3495-503. doi:10.1210/jc.2012-1419

11. Fassnacht M, Berruti A, Baudin E, et al. Linsitinib (OSI-906) versus placebo for patients with locally advanced or metastatic adrenocortical carcinoma: a double-blind, randomised, phase 3 study. *The Lancet Oncology*. Apr 2015;16(4):426-35. doi:10.1016/S1470-2045(15)70081-1

12. Samnotra V, Vassilopoulou-Sellin R, Fojo AT, et al. A phase II trial of gefitinib monotherapy in patients with unresectable adrenocortical carcinoma (ACC). *Journal of Clinical Oncology*. 2007;25(18_suppl):15527-15527. doi:10.1200/jco.2007.25.18_suppl.15527

13. Kroiss M, Megerle F, Kurlbaum M, et al. Objective Response and Prolonged Disease Control of Advanced Adrenocortical Carcinoma with Cabozantinib. *The Journal of Clinical Endocrinology and Metabolism*. May 1 2020;105(5):1461-1468. doi:10.1210/clinem/dgz318

14. Yakes FM, Chen J, Tan J, et al. Cabozantinib (XL184), a novel MET and VEGFR2 inhibitor, simultaneously suppresses metastasis, angiogenesis, and tumor growth. *Molecular Cancer Therapeutics*. Dec 2011;10(12):2298-308. doi:10.1158/1535-7163.Mct-11-0264

15. Kurzrock R, Sherman SI, Ball DW, et al. Activity of XL184 (Cabozantinib), an oral tyrosine kinase inhibitor, in patients with medullary thyroid cancer. *Journal of Clinical Oncology*. Jul 1 2011;29(19):2660-6. doi:10.1200/jco.2010.32.4145

16. Singh H, Brave M, Beaver JA, et al. U.S. Food and Drug Administration Approval: Cabozantinib for the Treatment of Advanced Renal Cell Carcinoma. *Clinical Cancer Research*. Jan 15 2017;23(2):330-335. doi:10.1158/1078-0432.CCR-16-1073

17. Phan LM, Fuentes-Mattei E, Wu W, et al. Hepatocyte Growth Factor/cMET Pathway Activation Enhances Cancer Hallmarks in Adrenocortical Carcinoma. *Cancer Research*. Oct 1 2015;75(19):4131-42. doi:10.1158/0008-5472.Can-14-3707

18. Ciamporcero E, Miles KM, Adelaiye R, et al. Combination Strategy Targeting VEGF and HGF/c-met in Human Renal Cell Carcinoma Models. *Molecular Cancer Therapeutics*. 2015;14(1):101-110. doi:10.1158/1535-7163.Mct-14-0094

19. Sennino B, Ishiguro-Oonuma T, Wei Y, et al. Suppression of tumor invasion and metastasis by concurrent inhibition of c-Met and VEGF signaling in pancreatic neuroendocrine tumors. *Cancer Discovery*. Mar 2012;2(3):270-87. doi:10.1158/2159-8290.Cd-11-0240

20. Qian F, Engst S, Yamaguchi K, et al. Inhibition of Tumor Cell Growth, Invasion, and Metastasis by EXEL-2880 (XL880, GSK1363089), a Novel Inhibitor of HGF and VEGF Receptor Tyrosine Kinases. *Cancer Research*. 2009;69(20):8009-8016. doi:10.1158/0008-5472.Can-08-4889

21. Lacy S, Hsu B, Miles D, Aftab D, Wang R, Nguyen L. Metabolism and Disposition of Cabozantinib in Healthy Male Volunteers and Pharmacologic Characterization of Its Major Metabolites. *Drug Metabolism and Disposition*. Aug 2015;43(8):1190-207. doi:10.1124/dmd.115.063610

22. Kroiss M, Quinkler M, Lutz WK, Allolio B, Fassnacht M. Drug interactions with mitotane by induction of CYP3A4 metabolism in the clinical management of adrenocortical carcinoma. *Clinical Endocrinology*. Nov 2011;75(5):585-91. doi:10.1111/j.1365-2265.2011.04214.x

23. Teo YL, Ho HK, Chan A. Metabolism-related pharmacokinetic drug-drug interactions with tyrosine kinase inhibitors: current understanding, challenges and recommendations. *British Journal of Clinical Pharmacology*. Feb 2015;79(2):241-53. doi:10.1111/bcp.12496

24. Kang JS, Lee MH. Overview of therapeutic drug monitoring. *The Korean Journal of Internal Medicine*. Mar 2009;24(1):1-10. doi:10.3904/kjim.2009.24.1.1

25. Widmer N, Bardin C, Chatelut E, et al. Review of therapeutic drug monitoring of anticancer drugs part two--targeted therapies. *European Journal of Cancer*. Aug 2014;50(12):2020-36. doi:https://doi.org/10.1016/j.ejca.2014.04.015

26. Mueller-Schoell A, Groenland SL, Scherf-Clavel O, et al. Therapeutic drug monitoring of oral targeted antineoplastic drugs. *European Journal of Clinical Pharmacology*. Nov 9 2020;doi:https://doi.org/10.1007/s00228-020-03014-8

27. European Medicine Agency. Guideline on bionalatyical method validation. Accessed May 30, 2020. https://www.ema.europa.eu/en/documents/scientific-guideline/guideline-bioanalytical-method-validation_en.pdf

28. Food and Drug Administration. Bioanalytical Method Validation Guidance for Industry. Accessed September 09, 2021. https://www.fda.gov/files/drugs/published/Bioanalytical-Method-Validation-Guidance-for-Industry.pdf

29. Krens SD, van der Meulen E, Jansman FGA, Burger DM, van Erp NP. Quantification of cobimetinib, cabozantinib, dabrafenib, niraparib, olaparib, vemurafenib, regorafenib and its metabolite regorafenib M2 in human plasma by UPLC-MS/MS. *Biomedical Chromatography*. Mar 2020;34(3):e4758. doi:10.1002/bmc.4758

30. Nguyen L, Chapel S, Tran BD, Lacy S. Updated Population Pharmacokinetic Model of Cabozantinib Integrating Various Cancer Types Including Hepatocellular Carcinoma. *The Journal of Clinical Pharmacology*. Nov 2019;59(11):1551-1561. doi:10.1002/jcph.1467

31. Zhang J, Wang C, Gao J, et al. Adrenal cortical neoplasms: a study of clinicopathological features related to epidermal growth factor receptor gene status. *Diagnostic Pathology*. Jan 23 2014;9:19. doi:10.1186/1746-1596-9-19

32. Nguyen L, Holland J, Miles D, et al. Pharmacokinetic (PK) drug interaction studies of cabozantinib: Effect of CYP3A inducer rifampin and inhibitor ketoconazole on cabozantinib plasma PK and effect of cabozantinib on CYP2C8 probe substrate rosiglitazone plasma PK. *The Journal of Clinical Pharmacology*. Sep 2015;55(9):1012-23. doi:10.1002/jcph.510

33. Williams PA, Cosme J, Vinkovic DM, et al. Crystal structures of human cytochrome P450 3A4 bound to metyrapone and progesterone. *Science*. Jul 30 2004;305(5684):683-6. doi:10.1126/science.1099736

34. Harvey JL, Paine AJ, Maurel P, Wright MC. Effect of the Adrenal 11-β-Hydroxylase Inhibitor Metyrapone on Human Hepatic Cytochrome P-450 Expression: Induction of Cytochrome P-450 3A4. *Drug Metabolism and Disposition*. 2000;28(1):96-101.

35. Park JJ, Boddy AV, Liu X, et al. Pharmacokinetics of dabrafenib in a patient with metastatic melanoma undergoing haemodialysis. *Pigment Cell & Melanoma Research*. Jan 2017;30(1):68-71. doi:10.1111/pcmr.12557

36. European Medicine Agency. Sutent: summary of product characteristics. Accessed September 18, 2020. https://www.ema.europa.eu/en/documents/product-information/sutent-epar-product-information_en.pdf

37. European Medicine Agency. Jakavi: summary of product characteristics. Accessed September 18, 2020. https://www.ema.europa.eu/en/documents/product-information/jakavi-epar-product-information_en.pdf

Supplemental Digital Content

SUPPLEMENTARY MATERIALS AND METHODS

Preparation of Stock Solutions, Calibrators and Quality Controls

Stock solutions were prepared by dissolving CAB malate in DMSO and CAB-d4 in ACN to final concentrations equivalent to 1 mg/mL free base. Working stock solution was prepared by dilution of stock solution in DMSO (1:5). The working stock solution was spiked to human plasma for the highest calibrator (CR) and quality control (QC) level. Ten CR with final concentrations 1000 ng/mL, 840 ng/mL, 600 ng/mL, 500 ng/mL, 340 ng/mL, 180 ng/mL, 90 ng/mL, 45 ng/mL, 18 ng/mL and 6 ng/mL and five QC levels with 740 ng/mL QC high (QC H), 440 ng/mL QC medium (QC M), 54 ng/mL QC intermediate (QC I), 18 ng/mL QC low (QC L) and 6 ng/mL QC LLOQ were prepared by serial dilution. CR and QC samples were prepared from independent stock solutions and stored until analysis at -80°C.

Method validation

The method validation was performed according to the FDA and EMA guidelines on bioanalytical method validation. Linearity was evaluated for the calibration range (6-1000 ng/mL) by the analysis of ten CR levels in three independent runs. The calibration curves were linearly fitted with weighting of 1/conc2 for quantification of CAB plasma levels. According to the guidelines, at least 75% of the CR should be within ± 15% of the nominal concentration (± 20% at LLOQ). Human blank plasma from six different individuals was analyzed for interferences. The extent of carryover was evaluated by injecting drug-free plasma after an ULOQ sample (upper limit of quantification, 1000 ng/mL). For both validation parameters, selectivity and carryover, the CAB response in blank samples should not exceed 20% of LLOQ and the IS response should not exceed 5% of the average IS signal. Sensitivity was evaluated by analyte response at the LLOQ, which should be at least the five-fold response of the zero CR. Intra-day and inter-day accuracy and precision (A&P) were assessed on three consecutive days by analyzing a set of ten CR and QC samples (QC H, QC M, QC I, QC L, QC LLOQ) with five replicates each. Acceptance criteria for measured concentrations were ± 15% of the nominal concentration for QC H, QC M, QC I and QC L and ± 20% for QC LLOQ. The coefficient of variance (CV) should be ≤ 15% for all QC levels (≤ 20% at LLOQ). Analysis of variance (ANOVA) was performed to

compare the individual validation runs. The matrix effect of hemolytic, icteric and lipemic (H/I/L) plasma samples on accuracy and precision was evaluated for QC H and QC L on five individual replicates each (no further specification of hemolytic, icteric or lipemic condition). Six individual sources of human blank plasma were used to determine recovery and matrix effects. Plasma was spiked with CAB and CAB-d4 before and after extraction (QC H, QC M and QC L). The same amount of analyte and IS were prepared in precipitation solvent (MeOH/ACN, 1:1, v/v) and spiked to water as neat solvent. The recovery was calculated as the ratio of IS-corrected analyte area in the extracted plasma samples versus the IS-corrected analyte area in the blank samples spiked after extraction. For matrix effects, the IS-normalized Matrix Factor (MF) was calculated for the analyte and the IS by the ratio of peak area in the plasma samples spiked after extraction compared to the peak area in the neat solution. Dilution integrity was evaluated to demonstrate the suitability of the method for amounts above the ULOQ. Plasma was spiked with CAB working stock solution to achieve a final concentration of 1500 ng/mL (QC D). Before extraction, the QC D samples were diluted with blank matrix (1:1, v/v). As acceptance criteria, the accuracy and precision should range within ± 15% of the nominal concentration. CAB stock solution stability was determined after six-month storage in DMSO at -80°C. Spiked plasma samples were prepared and stored at two levels – QC H (740 ng/mL) and QC L (18 ng/mL) and evaluated for bench-top, autosampler (2-8°C), freeze-thaw and long-term stability. QC samples for bench-top stability were extracted and analyzed after 24 hours storage at room temperature and light exposure, whereas QC samples for autosampler stability were extracted and stored for 24 hours at 4°C without light exposure before analysis. Freeze-thaw samples were frozen at -20°C for a minimum of twelve hours followed by thawing at room temperature. After four freeze-thaw cycles the samples were extracted and analyzed. QC H and QC L samples were stored at -80°C for three months to determine long-term stability. On every stability run, samples were compared to freshly prepared QC samples. Inter laboratory accuracy was evaluated by cross validation of three different plasma samples obtained from patients under CAB treatment as well as four QC samples (Radboud University, Nijmegen, Netherlands).

SUPPLEMENTARY RESULTS

Method validation

Correlation coefficients for calibration curves were > 0.995 (n=5) and back-calculated concentrations were within ± 15% of the nominal concentration for all CR. Analyte free plasma showed no relevant interferences as the analyte area in blank samples was found to be 4.9% of the LLOQ and IS area 0.4%, based on the average IS response. Carryover signal did not exceed 20% of the LLOQ response. The mean IS response in the carryover samples was 0.8% of the average IS response in corresponding analytical runs. The mean CAB signal in the LLOQ was the 16-fold response (n=5) compared to the zero CR and at least > 6 times the response on every run. Accuracy and precision results for all five QC levels are shown in Table S3. The intra-day accuracy ranged from 95.2% to 106.7% (CV ≤ 9.1%). Inter-day CV ranged from 4.4% to 9.7% with no significant impact throughout the inter-day accuracy, calculated via ANOVA. Accuracy and Precision of H/I/L plasma samples ranged within ± 15%. The recovery and IS-normalized MF were consistent and reproducible (Table S4). Dilution integrity was demonstrated for the dilution factor of 1.5-fold ULOQ (1500 ng/mL) by mean accuracy value of the QC D samples of 105.3% (CV 6.6%). As the plasma samples were prepared from different stock solutions, two independent stock solutions were analyzed after six months of storage at -80°C. The mean concentration of the stock solution compared to the nominal concentration was 88.5% and 87.7%. Data for bench-top, autosampler, freeze-thaw and long-term stability met the guideline requirements (Table S3). The results for inter laboratory cross validation are shown in Table S5.

Tables

Table S1: LC gradient elution scheme

Step	Time [min]	Flow rate [µL/min]	Mobile Phase A [%]	Mobile Phase B [%]	Valve position
0	0.00	400	90.0	10.0	to waste
1	2.00	400	90.0	10.0	
2	2.10	400	60.0	40.0	to MS
3	2.20	400	60.0	40.0	
4	5.75	400	25.0	75.0	
5	6.50	400	25.0	75.0	to waste
6	6.75	400	90.0	10.0	
7	7.50	400	90.0	10.0	

Table S2: Concomitant medication during CAB therapy

Drug substance	Dose	Application scheme
Amlodipine	5 mg	1-0-1
Calcitriol	0.25 µg	1-0-1
Carvedilol	25 mg	1-0-0-1
Clonidine	250 µg	0-0-0-1
Metyrapone	250 mg	2-2-2
Moxonidine	0.4 mg	0-0-1
Paracetamol	500 mg	1-1-1
Pregabalin	25 mg	0-0-1
Ramipril	2.5 mg	1-0-0
Sevelamer hydrochloride	800 mg	1-1-1
Torasemide	100 mg	1-1-0
Urapidil	60 mg	1-1-1

Table S3: Validation results for accuracy and precision, stability, and effect of hemolytic, icteric or lipemic plasma samples

Validation parameter	Nominal concentration or Specification	Level	Accuracy (%)	Precision (CV, %)
A&P *Intra-day (n=5)*	6 ng/mL	QC LLOQ	95.2	6.5
	18 ng/mL	QC L	106.7	7.8
	54 ng/mL	QC I	101.8	5.7
	440 ng/mL	QC M	103.7	9.1
	740 ng/mL	QC H	103.0	1.8
A&P *Inter-day (n=3)*	6 ng/mL	QC LLOQ	107.5	9.7
	18 ng/mL	QC L	107.5	9.1
	54 ng/mL	QC I	107.1	6.1
	440 ng/mL	QC M	106.6	6.8
	740 ng/mL	QC H	108.1	4.4
Bench-top stability	24 h room temperature	QC L	99.9	4.8
		QC H	99.9	3.9
Autosampler stability	4°C, 24 h	QC L	101.1	4.7
		QC H	101.3	6.8
Freeze-thaw stability	-20°C / room temperature	QC L	101.1	2.5
		QC H	97.3	3.7
Long-term stability	-80°C, 3 months	QC L	104.6	2.8
		QC H	105.4	2.3
H/I/L samples	hemolytic	QC L	107.2	4.6
		QC H	106.0	3.2
H/I/L samples	icteric	QC L	102.3	4.8
		QC H	108.6	1.9
H/I/L samples	lipemic	QC L	106.0	3.5
		QC H	107.7	6.8

Table S4: Validation results for matrix effect and recovery

Validation parameter	Level	IS-normalized MF	Precision (CV, %)
Matrix effect	QC L	1.01	5.5
	QC M	1.08	11.0
	QC H	1.10	10.6
		Recovery (%)	*Precision (CV, %)*
Recovery	QC L	94.5	6.1
	QC M	86.4	8.5
	QC H	87.1	4.7

Table S5: Cross validation results

Cross Validation	Radboud University (µg/mL)	University Hospital Würzburg (µg/mL)	Deviation (%)
QC XL	0.30	0.26	86.7
QC L	1.50	1.28	85.3
QC M	2.00	1.65	82.5
QC H	3.76	3.45	91.8
CAB Sample 1	2.44	2.14	87.7
CAB Sample 2	0.82	0.71	86.6
CAB Sample 3	0.34	0.30	88.2

Table S6: MAP calculation of individual PK parameters including measured plasma CAB concentrations compared to simulated values based on population data

	Individual parameters	Reference collective parameters
CL [L/h]	7.71	2.41
VC [L]	316.06	161.20
F1 [%]	63.11	69.80
KA [1/h]	3.21	0.76

3.2. Volumetric absorptive microsampling (VAMS) for the quantification of ten kinase inhibitors and determination of their *in vitro* VAMS-to-plasma ratio

Sebastian Zimmermann, Fatemeh Aghai, Bastian Schilling, Sabrina Kraus, Götz Ulrich Grigoleit, Charis Kalogirou, Maria-Elisabeth Goebeler, Pius Jung, Theo Pelzer, Hartwig Klinker, Nora Isberner, Oliver Scherf-Clavel

Copyright

https://doi.org/10.1016/j.jpba.2022.114623

Abstract

Personalized dosing of kinase inhibitors (KI) might be beneficial in oral anti-cancer therapy to overcome individual pharmacokinetic variability. Volumetric absorptive microsampling (VAMS) has emerged as an attractive alternative compared to conventional invasive sampling methods enabling remote and frequent specimen collection. Therefore, an LC-MS/MS VAMS method was developed and validated to monitor drug exposure of ten KI from 20 µL dried capillary blood. The assay includes the KI cabozantinib, dabrafenib, nilotinib, and osimertinib with a calibration range of 6-1500 ng/mL and afatinib, axitinib, bosutinib, lenvatinib, ruxolitinib and trametinib within a range of 2-500 ng/mL. Using acetonitrile containing isotope labelled internal standards (IS) as solid-liquid extraction solvent, analytes and IS were detected by multiple reaction monitoring (MRM) after electro-spray ionization (ESI) in positive ionization mode after chromatographic separation using a phenyl-hexyl column. The method was validated according to the FDA and EMA guidelines for bioanalytical method validation and in accordance with the guideline of the International Association for Therapeutic Drug Monitoring and Clinical Toxicology for dried blood spot-based methods. The calibration model was linear and reproducible for all KI ($R^2 > 0.994$). Furthermore, the validation demonstrated that the VAMS method is accurate, precise, and sensitive. The method fulfilled the acceptance criteria for matrix effects, recovery, carry over, selectivity as well as for the haematocrit effect and all substances proved to be stable in dried condition for at least six weeks at room temperature. *In vitro*

experiments using spiked venous blood were conducted to establish a VAMS-to-plasma conversion factor for each analyte for comparison of VAMS and plasma concentrations. The method was successfully used in a real-life setting demonstrating its applicability in clinical routine. VAMS concentrations of afatinib, cabozantinib, dabrafenib, nilotinib, ruxolitinib and trametinib were assessed in capillary blood samples collected from either trained healthcare professionals or patients at home.

1. Introduction

Since the introduction of imatinib 20 years ago, the arsenal of kinase inhibitors (KI) for treatment of cancer and other conditions has grown steadily. Today, more than 30 KI have been approved.

Like conventional cytostatic chemotherapy KI are burdened with a considerable rate of adverse drug reactions which may severely impair patient's quality of life and result in non-adherence and therapy discontinuation. Moreover, a relevant proportion of patients on KI therapy show disease progression after an initially good treatment response. Supra- or subtherapeutic drug exposure could be a potential cause. It has been shown in various studies that plasma levels of KI vary greatly between individuals despite receiving the same dosage and that large inter-individual variability can endanger treatment safety and efficacy [1].

Depending on the substance, reasons for varying drug exposure are manifold. Many KI exhibit pH-dependent solubility and are substrates of CYP enzymes and/or drug transporters leading to a substantial risk for drug-drug-interactions (DDI) depending on comedication. Other patient characteristics such as renal or hepatic impairment as well as the prevalence of genetic polymorphic enzymes may further influence drug exposure. Additionally, the oral mode application comes along with an increased risk for non-adherence.

Individualized consideration of drug exposure and dosage adaptation could be a promising approach to reduce the risks of dose-related adverse effects or sub-therapeutic exposure. Several investigations have demonstrated that therapeutic drug monitoring (TDM) of KI might be beneficial in clinical routine [2-4]. The most common approach is based on the analysis of plasma exposure requiring on-site patient visits, venipuncture and immediate sample processing. Due to limited pre-analytical stability

of some KI storage and shipment of plasma samples is associated with high logistical effort and costs if plasma level determination is not locally available.

Therefore, microsampling techniques, mostly as dried blood spots (DBS), have been investigated as an alternative sampling method for TDM over the past years and applicability has already been described for some KI [5]. However, the major disadvantage of DBS is the hematocrit (Hct) bias. The varying proportion of cellular components (mostly erythrocytes) in blood leads to heterogeneity of the drop volume and viscosity. Several investigations tried to achieve conformity by using a fixed radius of the filter spot, but blood viscosity led to variable, Hct-dependant spreading characteristics on the filter paper resulting in biased measurement results [6, 7].

Volumetric absorptive microsampling (VAMS) is a technique developed to reduce Hct-bias by sampling a defined, Hct-independent volume of capillary blood [8]. Blood is sampled after a finger prick, applied onto a polymeric tip and dried. Analytes absorbed to VAMS devices are usually more stable compared to conventional wet plasma samples and can be stored and shipped at room temperature. Thus, VAMS allows for blood sampling at-home without assistance of healthcare professionals and could be particularly beneficial for certain patient populations such as paediatric or immobile patients.

Yet, it should be noted, that using VAMS cannot completely overcome Hct bias, especially if a drug shows an extreme blood-to-plasma ratio indicating adsorption and distribution on/into erythrocytes or exclusion from intracellular space and lack of adsorption, respectively. Hence, capillary blood concentrations cannot be easily compared with plasma thresholds [9]. To convert capillary blood into plasma concentrations, a substance-specific blood-to-plasma coefficient must be determined. For some KI, a blood-to-plasma ratio (B/P) is provided in their European Public Assessment Reports (EPAR). However, B/P based VAMS-to-plasma conversion factors (V/P) taking into account further drug characteristics like concentration- or Hct-dependent distribution need to be developed and validated to compare VAMS concentrations with plasma thresholds. While conversion factors or other capillary blood-to-plasma conversion methods have been reported for some KI using DBS [10], no conversion factors have been established for VAMS.

In this work, we present the development and validation of a VAMS LC-MS/MS method for the quantification of afatinib (AFA), axitinib (AXI), bosutinib (BOS),

cabozantinib (CAB), dabrafenib (DAB), lenvatinib (LEN), nilotinib (NIL), osimertinib (OSI), ruxolitinib (RUX) and trametinib (TRA). *In vitro* V/P was determined at varying Hct levels to develop an experimental conversion factor from VAMS to plasma to be challenged in future clinical validation studies. In addition, authentic VAMS samples from patients treated with AFA, CAB, DAB, NIL, RUX or TRA were obtained and measured to confirm the clinical applicability of the method.

2. Experimental

2.1. Materials

AFA, BOS, CAB-S-malate and RUX were purchased from Biozol (Eching, Germany), AXI and LEN from Alsachim (Illkirch Graffenstaden, France) and OSI from TRC (Toronto, Canada). DAB mesylate, NIL and TRA were purchased from Sigma Aldrich (Steinheim, Germany). The isotope labeled standards (IS) AFA-d6, NIL-d6 and RUX-d9 were purchased from Biozol (Eching, Germany), the others, AXI-13C1-d3, BOS-d9, CAB-d4, DAB-d9, LEN-d5, OSI-13C1-d3 and TRA-13C6 from Alsachim (Illkirch Graffenstaden, France). LC-MS grade water, methanol (MeOH), acetonitrile (ACN), dimethyl sulfoxide (DMSO) and ammonium bicarbonate were obtained from VWR International (Darmstadt, Germany). All chemicals (reagents and analytes) were ordered in highest quality for LC-MS purposes. For microsampling, Mitra® devices were purchased from Neoteryx (Torrance, CA, USA). For the finger prick, safety lancets, type super with 1.5 mm penetration depth, were purchased from Sarstedt (Nümbrecht, Germany). Analyte-free human matrix, whole blood containing EDTA as anticoagulant and plasma, were ordered from the Bavarian Red Cross (Wiesentheid, Germany). For comparison of anticoagulant-free matrix with human whole blood containing either EDTA or heparin, whole blood was obtained after venipuncture of a volunteer using different blood collection monovettes with different types of anticoagulation (EDTA, lithium heparin, none) purchased from Sarstedt (Nümbrecht, Germany).

2.2. Instrumentation and data analysis

The LC-MS/MS system consisted of an Agilent 6460 series triple quadrupole linked to an Agilent 1260 HPLC system (Waldbronn, Germany). For chromatographic separation of all analytes a Waters XBridge Phenyl column (3.5 µm, 2.1 x 50 mm; Waters, Milford, MA, USA) was used as stationary phase. Mobile phase A consisted

of 10% MeOH (v/v) with 10 mM ammonium bicarbonate and mobile phase B of 90% MeOH (v/v) with 10 mM ammonium bicarbonate. Prior to the analytical run, the injection needle was flushed in the flush port for ten seconds with 90% ACN before the sample was drawn and 15 seconds after drawing, immediately before injection. Gradient elution was performed at a flow rate of 400 µL/min and started at 60% B. After 0.50 minutes at starting conditions, mobile phase B was increased to 80% by minute 2.00 and remained at 80% B until minute 5.00. From minute 5.00-5.25, mobile phase B was reduced to 60% B again. The acquisition ended after 6.00 minutes at starting conditions. Analytes and IS were all ionized in positive mode using Agilent Jet Stream ion source for electrospray ionization. Source parameters were set to a capillary voltage of 3500 V, a gas temperature of 300°C and gas flow of 10 L/min. Multiple reaction monitoring (MRM) was used for detection. All MRM transitions and further LC-MS/MS parameter are listed in supplementary data (SD) Table S1. Data were recorded via Agilent Masshunter Software B.08.00 (Waldbronn, Germany). Microsoft Excel 2016 (Microsoft Corporation, Redmond, WA, USA) was used for processing the exported .csv formats. Statistical evaluation for calculation of the inter-day precision and t-test for the stability comparison of different anticoagulants as well as graphical visualizations were performed using R Software 4.0.2 and RStudio version 1.3.1073 (with additional packages “ggplot2”, “mcr”, “readxl”, “tidyverse”, RStudio, Inc., Boston, MA, USA). Chemdraw Version 19.0.1.28 (PerkinElmer, Waltham, MA, USA) was used to generate demonstrated chemicals structures (SD Table S2).

2.3. Preparation of stock and working solutions

All Analytes were dissolved separately in DMSO to achieve individual stock solutions corresponding to a concentration of 1 mg/mL free base. A working solution was prepared including CAB, DAB, NIL and OSI for a high and AFA, AXI, BOS, LEN, RUX and TRA for a low concentration range. Therefore, 150 µL of the stock solutions of CAB, DAB, NIL and OSI and 50 µL of the stock solutions of AFA, AXI, BOS, LEN, RUX and TRA were diluted to a total volume of 5.0 mL in MeOH. Except for CAB-d4, IS were prepared in DMSO at a concentration of 1 mg/mL. CAB-d4 was prepared in ACN at the same concentration. An IS working solution at a concentration of 10 µg/mL each (LEN-d5, 2.5 µg/mL) was prepared in MeOH. All stock solutions and working solutions were stored in polypropylene tubes (1.5 mL and 5.0 mL, respectively) at -80°C.

2.4. Calibrator and quality control blood sampling

Calibrator (CR) and quality control (QC) samples were prepared from independent stock solutions. The working solutions were serially diluted in MeOH to obtain nine different calibrator solvent samples (CR-WS) and four different quality control solvent samples (QC-WS), each 20-fold more concentrated than the actual CR and QC samples (detailed concentrations see SD Table S3). For CR and QC preparation, 25 µL of the CR-WS or QC-WS samples were spiked to 475 µL human blood, containing EDTA as anticoagulant in order to limit the concentration of organic solvent. The resulting calibration ranged from 6 to 1500 ng/mL for high concentration analytes (CAB, DAB, NIL, OSI) including four QC levels at 6 ng/mL for the lower limit of quantification (LLOQ), 18 ng/mL for QC low (QC L), 120 ng/mL for QC medium (QC M) and 1125 ng/mL for the highest QC (QC H). Accordingly, the calibration curve of the low concentration analytes (AFA, AXI, BOS, LEN, RUX, TRA) was in the range of 2-500 ng/mL with QC LLOQ at 2 ng/mL, QC L at 6 ng/mL, QC M at 40 ng/mL and QC H at 375 ng/mL. Spiked blood samples were incubated for one hour at 37°C to mimic physiological distribution. For blood sampling the polymer surface of the sampling device was dipped into the freshly prepared liquid matrix of the CR or QC samples according to the instructions attached to the device. Samples were dried at room temperature for at least twelve hours protected from light. CR-WS and QC-WS solutions were stored in polypropylene tubes with 2.0 mL volume at -20°C. Blank EDTA blood and CR and QC samples were stored at 4°C. Blank blood was kept for no longer than three weeks at 2-8°C, CR and QC samples for no longer than one day.

2.5. Sample preparation

Dried blood samples were removed from the plastic handler and placed in a 2.0 mL polypropylene tube and rehydrated with 50 µL water for five minutes. 450 µL of extraction solution containing ACN and 0.1% IS working solution was added for protein precipitation. Physical extraction came from a subsequent 30 min vortexing procedure followed by centrifugation for five minutes at 4°C and 12,000 rcf. VAMS remained in the 2.0 mL polypropylene tube during these steps. After centrifugation, 300 µL were transferred to a 1.5 mL polypropylene tube and evaporated using an Eppendorf concentrator. The residue was dissolved in 200 µL of mobile phase (60/40, A/B, v/v), vortexed for five minutes, and centrifuged using the previous conditions. 180 µL were transferred into an HPLC vial with polypropylene insert. Injection volume was 40 µL. Both, sample preparation and analysis were performed at room temperature.

2.6. Analytical method validation

The method was validated according to the FDA and EMA guidelines for bioanalytical method validation [11, 12] and in accordance with the guideline of the International Association for Therapeutic Drug Monitoring and Clinical Toxicology for dried blood spot-based methods [13].

2.6.1. Calibration model and sensitivity

The measurement range was set to 2-500 ng/mL for AFA, AXI, BOS, LEN, RUX, TRA and 6-1500 ng/mL for CAB, DAB, NIL, OSI. Sensitivity is defined by the LLOQ of the method. Therefore, the analyte response should at least be fivefold the response of the zero calibrator. The calibration model was assessed after the analysis of nine CR. The analytes were quantified using a linear $\frac{1}{conc^2}$ weighted calibration curve. 75% of the CR should meet the acceptance criteria of ± 15% of the nominal concentration or ± 20% for the LLOQ. Calibration model and sensitivity were evaluated on five successive days.

2.6.2. Accuracy and precision

All four QC levels with five replicates each in combination with nine CR were analyzed on three consecutive days to evaluate accuracy and precision of the method for all analytes. Intra-day and inter-day accuracy should range within 15% of the nominal concentration for all QC levels above the LLOQ and within ± 20% for the LLOQ. Intra- and inter-day precision are expressed as coefficient of variance (CV) and should not exceed 15% for QC H, QC M and QC L and 20% for the LLOQ, respectively. Inter-day precision was evaluated according to a published method of Krouwer and Rabinowitz [14]. In addition, accuracy and precision were examined for robustness from different laboratory personal (n=3).

2.6.3. Carry over

The amount of system carryover was investigated by measuring the analyte signal in extracted blank samples (n=5) directly after the injection of the highest calibrator (upper limit of quantification). In extracted blank samples, the analyte signal should be within a maximum of 20% of the average LLOQ response and 5% of the average IS response.

2.6.4. Selectivity and hematocrit effect

Selectivity was evaluated by analysis of six drug-free blank samples from individual donors and compared to LLOQ samples. To ensure that no interference occurred in the respective donor samples at the respective retention times, the analyte signal should not exceed 20% of the average LLOQ response and 5% of the IS response. For the preparation of different Hct levels, 100 mL EDTA blood was centrifuged and separated into plasma and blood cells. The components were then pipetted together in the appropriate volume fractions to generate Hct levels of 0.55 (Hct high), 0.40 (Hct medium) and 0.30 (Hct low). The Hct-adjusted blood samples were each spiked with QC-WS solution according to Section 2.4 to generate QC samples and incubated for one hour at 37°C. CR samples were adjusted to Hct 0.45. The effect of Hct variation on accuracy and precision was evaluated after five-fold analysis of all four QC levels. Acceptance criteria were ± 15% for accuracy (± 20% LLOQ) and maximal 15% for CV (20% LLOQ).

2.6.5. Matrix effects, recovery and process efficiency

EDTA blood from six healthy donors was studied to determine matrix effects as well as the recovery and process efficiency of the method. To investigate the influences of different matrices, the blank matrices were spiked with analyte and IS both before (pre-extraction samples) and after extraction (post-extraction samples). Samples from each individual were analyzed at three concentration levels (QC H, QC M and QC L). For comparison, analytes and IS were also prepared in neat mobile phase 60/40 (A/B, v/v) (neat solution samples) with the same concentration as the matrix samples including dilution steps. To assess matrix effects, an IS normalized matrix factor (MF) was calculated for each level, donor and analyte (Eq. 1). The CV of the MF should not be greater than 15%.

$$MF = \frac{A_{(analyte;\, post-extraction)} / A_{(analyte;\, neat\ solution)}}{A_{(IS;\, post-extraction)} / A_{(IS;\, neat\ solution)}} \qquad (1)$$

The recovery was calculated as the quotient of the IS corrected peak area of the samples spiked before extraction and the corrected peak area quantified in samples spiked after extraction (Eq. 2).

$$Recovery\ [\%] = \frac{A_{(analyte;\, pre-extraction)} / A_{(IS;\, pre-extraction)}}{A_{(analyte;\, post-extraction)} / A_{(IS;\, post-extraction)}} \cdot 100 \qquad (2)$$

Similar to that, the process efficiency was calculated as the quotient of the IS corrected peak area of the samples spiked before extraction and the corrected peak area quantified in neat solution samples (Eq. 3).

$$Process\ efficiency\ [\%] = \frac{A_{(analyte;\ pre-extraction)}/A_{(IS;\ pre-extraction)}}{A_{(analyte;\ neat\ solution)}/A_{(IS;\ neat\ solution)}} \cdot 100 \quad (3)$$

Recovery and process efficiency do not need to be 100% but should be consistent and reproducible. All results should be within a maximum CV of 15%.

2.6.6. Stability

The stability of dried blood samples was evaluated after storage at room temperature protected from light for six weeks (19% relative humidity (rH)) and after stress tests at 60°C for two days (10% rH). For liquid matrix stability, VAMS QC were sampled with the VAMS device according to the sampling protocol (Section 2.4) after three days storage of the spiked blood matrix at 4°C. In addition, processed samples were stored after preparation at -20°C for six days to evaluate the post-preparation VAMS stability. Stability samples, for QC H and QC L were processed and compared with freshly prepared QC in quintuplicate. Liquid blood QC and processed samples were compared in duplicate for QC H, QC M and QC L. Stability was assessed in human whole blood samples anticoagulated with either EDTA or heparin and compared to whole blood samples without anticoagulation. After venipuncture, blood samples were subsequently spiked with QC-WS to obtain spiked QC H and QC L concentrations. Samples were homogenized by shaking for 15 s. The incubation period was omitted in all matrices to avoid clotting of anticoagulant-free blood. 10 VAMS samples from each matrix and concentration were obtained of which 5 were measured directly after drying for 24 h. The rest was kept at room temperature (22% rH) for 3 weeks before analyzing. For stability, the difference between day 0 and day 21 was assessed for each substance.

2.7. *In vitro* VAMS-to-plasma correlation

The VAMS-to-plasma correlation of all analytes was evaluated in an *in vitro* experiment. Pooled blood from eight donors was separated from liquid and cellular components and mixed yielding adjusted Hct levels of 0.55 (Hct high), 0.4 (Hct medium) and 0.3 (Hct low) as well as 0.45 for Hct-adjusted calibration as described in Section 2.6.4. 475 µL of the Hct-adjusted matrix was spiked with 25 µL of CR-WS and QC-WS solutions to generate eleven samples per Hct with different KI concentrations

(1500 ng/mL, 1125 ng/mL, 750 ng/mL, 420 ng/mL, 375 ng/mL, 180 ng/mL, 120 ng/mL, 40 ng/mL, 18 ng/mL, 12 ng/mL, 6 ng/mL for CAB, DAB, NIL, OSI and 500 ng/mL, 375 ng/mL, 250 ng/mL, 140 ng/mL, 125 ng/mL, 60 ng/mL, 40 ng/mL, 13.3 ng/mL, 6 ng/mL, 4 ng/mL, 2 ng/mL for AXI, AFA, BOS, LEN, RUX, TRA) covering the full calibration range of all analytes. Afterwards liquid blood samples were incubated, absorbed to VAMS devices and stored and processed as described in Sections 2.4 and 2.5. To determine plasma concentrations, corresponding liquid blood samples were centrifugated after sampling with VAMS at 3000 rcf for 15 min at 4°C to generate plasma. The plasma supernatant was subsequently transferred in a new cap and stored at -80°C until analysis. Plasma samples were processed according to Aghai et al. [15]. VAMS samples were analyzed and compared to the corresponding plasma samples. This *in vitro* assay was repeated once with a second batch of blood matrix. A linear model with interaction (Eq. 4) was fitted on the data in order to assess the influence of normalized Hct (normalized to the calibration value of 0.45) on the conversion from VAMS concentrations (C_{VAMS}) to plasma concentrations (C_{plasma}) resulting in the coefficients A, B, C and the Intercept.

$$C_{plasma} = A \cdot C_{VAMS} + B \cdot \frac{Hct}{0.45} + C \cdot \frac{Hct}{0.45} \cdot C_{VAMS} + Intercept \quad (4)$$

In cases where the interaction term was not statistically significant ($p > 0.01$), the interaction was removed to yield the simplified, Hct-independent model (Eq. 5).

$$C_{plasma} = A \cdot C_{VAMS} + Intercept \quad (5)$$

In the case of TRA, a concentration-dependent V/P ratio was observed without significant impact of the Hct. This was modeled by a second-degree polynomial (Eq. 6).

$$\frac{C_{VAMS}}{C_{Plasma}} = A \cdot \frac{1}{C_{VAMS}} + B \cdot \left(\frac{1}{C_{VAMS}}\right)^2 + Intercept \quad (6)$$

2.8. Collection of patient samples

The method was applied to evaluate the feasibility of the VAMS technology in a real-life setting in patients treated with either AFA, CAB, DAB/TRA, NIL or RUX. Capillary blood samples were collected from the fingertip. Four VAMS samples with four different sampling times were collected on a single day for each investigation (one sample per time point). The time points for collection of VAMS samples one to four were proposed to be between 9 a.m. and 12 p.m., between 12 p.m. and 3 p.m.,

between 3 p.m. and 6 p.m., and between 6 p.m. and 9 p.m., respectively. Patients documented the drug administration and sampling themselves. The first sample was collected during a routine patient visit by trained personnel. After demonstration of the sampling procedure collection and documentation of the other three samples was performed by the patient at home with individually scheduled sampling times. 20 µL of capillary blood were drawn onto the VAMS device after a finger prick and placed in an airtight and opaque bag with desiccant. Afterwards samples were sent back to the laboratory for analysis. This study was approved by the Ethics Commission of the University of Wuerzburg (ref199/18-am) and conducted in accordance with the declaration of Helsinki and the later amendments. Written informed consent was obtained from all patients.

3. Results and discussion

3.1. Method validation

3.1.1. Calibration model and sensitivity

The $\frac{1}{conc^2}$ weighted calibration curves were linear and reproducible over the validated range with a coefficient of determination (R^2) of ≥ 0.994 for all analytes. Every CR met the acceptance criteria with back-calculated accuracy ranging between a minimum of 89.9% (TRA K8 on validation day 4) and maximum of 114.5% (AFA K6 on validation day 2). The method was sensitive with all peak areas in LLOQ samples exceeding the minimum of the five-fold-response compared to the zero calibrator.

3.1.2. Accuracy and precision

The validation demonstrated the VAMS method to be accurate and precise for all four QC levels. Data on accuracy and precision are presented in Table 1. Inter-analyst variability was in accordance with the guideline's criteria. Back-calculated concentration and CV did not variate for any QC more than 15% (assessed for QC L, QC M and QC H in duplicate).

3.1.3. Carry over

Analyte signals in the corresponding blank samples did not exceed 20% of the LLOQ response with maximum carry over of 8.4% for OSI. The mean IS response in carryover samples was at most 0.1% of the average IS response for all ten KI.

Table 1 Accuracy and precision validation results.

Analyte	QC level	Intra-day accuracy and precision (n=5)		Inter-day precision (n=3)		
		Accuracy (%)	CV (%)	Within-day precision CV (%)	Between-day precision CV (%)	Total precision CV (%)
AFA	*LLOQ*	103.6	4.1	5.02	4.52	6.76
	L	92.3	4.0	4.08	4.27	5.91
	M	95.2	1.6	3.63	1.98	4.13
	H	100.8	2.7	3.30	6.36	7.17
AXI	*LLOQ*	108.2	4.4	5.94	2.06	6.29
	L	97.3	7.2	5.61	0.78	5.66
	M	103.4	5.2	3.92	3.89	5.52
	H	105.2	3.7	3.19	2.36	3.96
BOS	*LLOQ*	107.5	5.0	5.72	4.35	7.18
	L	105.4	3.5	4.41	0.00[a]	4.41
	M	104.8	1.5	3.70	1.52	4.00
	H	108.7	5.2	3.83	0.54	3.86
CAB	*LLOQ*	106.6	8.1	5.73	2.01	6.07
	L	102.4	4.4	4.79	0.00[a]	4.79
	M	99.9	3.1	3.18	2.52	4.05
	H	110.4	2.3	4.06	1.56	4.35
DAB	*LLOQ*	109.1	5.7	5.41	2.30	5.88
	L	99.7	3.4	3.60	2.08	4.16
	M	107.9	6.9	5.75	3.38	6.67
	H	106.7	4.5	3.87	0.67	3.93
LEN	*LLOQ*	104.6	3.1	5.68	6.35	8.52
	L	107.3	4.8	8.32	0.00[a]	8.32
	M	107.1	3.2	9.23	0.00[a]	9.23
	H	112.6	2.2	4.44	0.46	4.46
NIL	*LLOQ*	109.4	4.7	3.85	2.60	4.65
	L	102.0	3.4	4.11	0.00[a]	4.11
	M	99.7	2.0	2.97	2.72	4.03
	H	111.1	2.2	3.51	1.42	3.79
OSI	*LLOQ*	116.4	5.1	7.58	0.00[a]	7.58
	L	108.1	5.8	8.80	0.00[a]	8.80
	M	107.0	5.3	7.06	2.11	7.36
	H	114.6	3.2	7.91	3.16	8.51
RUX	*LLOQ*	103.0	3.9	4.42	3.66	5.74
	L	112.8	4.2	3.74	2.56	4.53
	M	107.5	1.1	2.34	2.21	3.22
	H	112.4	6.0	3.83	0.00	3.83
TRA	*LLOQ*	111.3	4.5	7.02	2.80	7.56
	L	91.6	7.5	7.24	7.78	10.63
	M	99.1	3.2	3.04	4.13	5.13
	H	113.0	3.4	4.95	6.90	8.49

AFA, Afatinib; AXI, Axitinib; BOS, Bosutinib; CAB, Cabozantinib; DAB, Dabrafenib; LEN, Lenvatinib; NIL, Nilotinib; OSI, Osimertinib; RUX, Ruxolitinib; TRA, Trametinib; QC, quality control; LLOQ, lower limit of quantification; L, low; M, medium; H, high; CV, coefficient of variance.

[a] Variance of day averages was less than weighted variance of pooled within-day precision - between-day precision was set to zero, according to Krouwer and Rabinowitz [14].

3.1.4. Selectivity and hematocrit effect

Individual blank blood samples showed no interference throughout all MRM chromatograms. No signal exceeded more than 1.0% of the average LLOQ response demonstrating the high selectivity of the method. The maximum analyte response was 0.7% for OSI. The blank IS response was less than 0.1% for all IS transitions. Analysis

of different Hct levels showed that all results were in accordance with the guideline's criteria (SD Table S4), indicating strong reproducibility of the method.

3.1.5. Matrix effects, recovery, and process efficiency

Calculated MF are presented in Table 2. The MF of OSI (0.85) deviates the most from the expected value of 1.0. This deviance was consistent in all three analyzed concentrations. All in all, the low variability of the results (CV < 15%) of all substances confirms the consistency of the MF for all KI.

High recovery (> 80% according to Xie et al.) is mandatory to achieve reproducible results during VAMS extraction [8, 16, 17]. The drying process of the blood samples causes the analytes to bind not only to the biomatrix but also to the polymeric surface of the VAMS devices. Especially for hydrophobic analytes, sufficient lipophilicity of the extraction solvent is necessary for extraction [16]. Various modifications were tested during method development to maximize recovery. Extraction solvents containing ethylacetate or ethylacetate/hexane (1:1, v/v) was inferior compared to MeOH or ACN. Especially for OSI, recovery was reproducibly increased with ACN compared to MeOH at different concentration levels (QC L and QC H). AXI, AFA, BOS, CAB, DAB, LEN, NIL, RUX and TRA reached the intended 80% recovery mark (Table 2). Despite achieving better results for OSI recovery after optimizing sample preparation, the mean recovery of OSI remained below 80% (68%). Xie et al. reported that inacceptable stability and Hct effects are related to a minor recovery rate [17]. The insufficient stability of OSI during stress test evaluation (Section 3.1.6) might have contributed to low recovery. However, OSI met the acceptance criteria with consistent and reproducible recovery results, which was demanded from the FDA and the International Association for Therapeutic Drug Monitoring and Clinical Toxicology making the VAMS method suitable for all KI.

The process efficiency (Eq. 3) corrects the recovery for matrix effects by taking into account the matrix factor. Therefore, differences between process efficiency and recovery are observed for analytes with matrix effects. Consequently, OSI showed 15% less analyte detection due to ion suppression. For all other substances no significant differences were observed (Table 2).

Table 2 Validation results for matrix effects, recovery and process efficiency.

Analyte	QC level	Matrix factor	CV (%)	Recovery (%)	CV (%)	Process efficiency (%)	CV (%)
AFA	*L*	0.94	3.8	79.9	4.1	75.3	4.8
	M	0.95	1.4	81.5	5.1	77.9	5.2
	H	0.96	1.4	79.6	4.0	76.1	3.3
AXI	*L*	0.97	5.8	99.4	6.8	95.8	4.9
	M	0.99	3.2	100.8	5.0	99.5	5.2
	H	0.99	1.3	101.4	3.6	100.8	3.9
BOS	*L*	0.98	6.3	91.8	4.1	90.3	7.2
	M	0.96	3.4	94.2	4.5	90.6	4.9
	H	0.97	2.3	94.2	3.7	91.2	3.7
CAB	*L*	1.03	3.4	106.3	3.2	109.5	4.5
	M	1.03	1.2	101.7	2.8	104.8	1.7
	H	1.00	1.3	107.9	0.2	108.1	0.7
DAB	*L*	1.01	2.2	112.7	3.5	114.0	2.4
	M	1.02	0.7	114.1	2.5	115.8	2.2
	H	1.00	1.4	110.0	2.0	110.1	2.6
LEN	*L*	0.99	0.4	93.0	3.7	91.9	3.6
	M	1.00	0.7	93.6	3.2	93.8	3.1
	H	1.00	0.7	94.4	2.3	94.2	2.6
NIL	*L*	0.99	3.0	98.2	4.6	97.6	5.2
	M	0.99	1.1	98.2	3.9	97.6	4.1
	H	1.00	0.8	98.2	2.8	97.8	3.0
OSI	*L*	0.84	2.7	68.1	3.2	56.9	4.8
	M	0.85	1.9	67.7	3.7	57.9	4.3
	H	0.86	1.1	68.9	7.9	59.3	8.0
RUX	*L*	0.99	1.8	99.5	3.5	98.3	3.1
	M	1.00	0.8	98.3	2.8	98.3	3.0
	H	0.99	0.6	99.1	2.8	98.1	2.8
TRA	*L*	0.99	9.5	98.7	9.4	96.8	7.1
	M	0.96	3.1	99.6	6.1	95.8	6.7
	H	0.99	2.1	98.8	2.7	97.3	1.8

AFA, Afatinib; AXI, Axitinib; BOS, Bosutinib; CAB, Cabozantinib; DAB, Dabrafenib; LEN, Lenvatinib; NIL, Nilotinib; OSI, Osimertinib; RUX, Ruxolitinib; TRA, Trametinib; QC, quality control; L, low; M, medium; H, high; CV, coefficient of variance.

3.1.6. Stability

All KI were stable at room temperature in dried condition for at least six weeks (19% rH). QC H and QC L samples were within ± 15% accuracy with a maximum CV of 7.2% (QC H) and 7.7% (QC L) for OSI (Table 3). Stability beyond six weeks is expected under the above-named conditions but has not been investigated, as a six-week interval is sufficient for feasibility of VAMS monitoring. Stress test evaluation of the dried VAMS samples at 60°C for two days (10% rH) showed that eight of ten analytes were stable. Back-calculated concentrations for AFA and OSI could not be determined in accordance with the guideline. Interestingly, both KI are irreversible inhibitors. Covalent bindings between the analytes and the surrounding surface, caused by increased molecule kinetics during 60°C stress test, may have contributed to instability.

Table 3 Stability results of VAMS, liquid blood matrix and processed samples.

Analyte	QC level	VAMS RT, 6 weeks (n=5)		VAMS 60°C, 2 days (n=5)		Liquid blood matrix 4°C, 3 days (n=2)		Processed samples -20°C, 6 days (n=2)	
		Accuracy (%)	Precision CV (%)	Accuracy (%)	Precision CV (%)	Accuracy (%)	Precision CV (%)	Accuracy (%)	Precision CV (%)
AFA	*L*	94.9	5.4	71.0[a]	8.1	59.2[a]	8.4	112.9	0.4
	M	-	-	-	-	59.3[a]	1.3	97.3	1.9
	H	99.8	3.0	76.7[a]	6.3	60.8[a]	3.5	105.7	3.0
AXI	*L*	102.7	4.1	89.3	5.3	100.2	8.3	103.1	0.0
	M	-	-	-	-	107.6	6.8	95.4	1.3
	H	110.2	4.8	99.1	3.3	113.9	0.1	104.9	1.6
BOS	*L*	103.4	2.2	89.5	2.4	101.6	9.0	104.2	0.5
	M	-	-	-	-	106.5	5.6	94.7	0.3
	H	110.3	6.4	101.9	3.7	108.7	3.7	102.2	2.8
CAB	*L*	100.0	3.9	85.4	3.8	97.8	7.4	101.6	0.1
	M	-	-	-	-	103.7	6.3	94.3	0.9
	H	105.9	5.6	94.9	3.8	105.7	3.4	100.1	1.1
DAB	*L*	106.5	2.1	85.0	3.6	98.9	7.6	99.6	1.7
	M	-	-	-	-	104.2	5.9	91.8	1.5
	H	113.7	5.5	92.5	4.2	105.1	4.0	99.5	1.8
LEN	*L*	96.1	2.9	90.2	3.7	89.6	8.5	111.7	1.1
	M	-	-	-	-	91.3	6.7	101.1	1.1
	H	99.8	5.4	99.4	3.8	93.0	3.3	106.5	1.1
NIL	*L*	101.0	4.1	89.6	2.5	104.7	7.9	107.3	2.0
	M	-	-	-	-	106.4	8.7	96.6	0.1
	H	104.9	5.6	93.7	2.2	109.0	3.3	99.1	1.6
OSI	*L*	90.5	7.7	n.a.[a]	n.a.	100.9	6.0	123.8[a]	4.3
	M	-	-	-	-	104.7	8.2	109.2	3.0
	H	96.1	7.2	n.a.[a]	n.a.	100.9	9.3	118.4[a]	1.4
RUX	*L*	109.5	3.5	91.7	4.5	104.2	7.9	107.6	1.6
	M	-	-	-	-	108.9	7.7	99.2	2.0
	H	114.5	6.1	103.3	3.5	111.9	3.9	106.2	2.7
TRA	*L*	112.3	3.3	94.4	4.1	105.6	4.1	111.7	4.0
	M	-	-	-	-	108.3	6.0	100.6	1.6
	H	114.2	6.2	101.3	4.0	112.2	2.3	107.2	1.1

[a] Accuracy outside the accepted range (100 ± 15%) AFA, Afatinib; AXI, Axitinib; BOS, Bosutinib; CAB, Cabozantinib; DAB, Dabrafenib; LEN, Lenvatinib; NIL, Nilotinib; OSI, Osimertinib; RUX, Ruxolitinib; TRA, Trametinib; RT, room temperature; QC, quality control; LLOQ, lower limit of quantification; L, low; M, medium; H, high; CV, coefficient of variance.

Additionally, the low recovery and process efficiency demonstrated for AFA and even more for OSI could have been the reason for different stability results (Table 3). Investigation of the post-preparation stability showed that nearly no instability occurred within six days when stored at -20°C, or was corrected by the IS for all substances despite OSI. The OSI concentration was calculated with an accuracy of 118.4% and 123.8% for the high and low QC, respectively. Differences in accuracy during storage at -20°C were not expected. However, it is recommended to immediately process and analyze OSI VAMS samples. Accuracy and precision were within the accepted limits for the other analytes (Table 3). Except for AFA, all analytes were stable in the liquid matrix at 4°C for three days, thus enabling quantification of all KI despite AFA in this time frame (Table 3). Stock and working solution stability have been evaluated in a previous study [15]. Accuracy was within ± 15% of the nominal concentration for all analytes except AFA and OSI. This could be explained by the missing incubation step that was necessary to avoid clotting. The concentrations could be measured with high precision and a CV less than 15% for all ten KI. CR and QC samples on this validation run prepared with one-hour incubation according to Section 2.4 showed accurate and precise results. Except for OSI (EDTA QC H and QC H without anticoagulation) and TRA (QC L without anticoagulation), the calculated concentrations do not deviate more than 15% from the initial concentrations (t0) (SD Table S5). A decrease could only be observed for TRA QC L whereas QC H yielded similar results. Thus, the type of anticoagulation (EDTA, heparin, none) did not significantly influence the concentration difference at week 3 vs t0. Therefore, no instability caused by different anticoagulation was observed.

3.2. *In vitro* VAMS-to-plasma ratio

The correlation between VAMS and plasma concentration was determined by *in vitro* studies. A VAMS-to-plasma conversion model using ordinary least squares regression was obtained for all 10 KIs (Table 4). For nine of the ten KI, V/P were constant over the entire calibration range and thus the conversion factor was independent of the VAMS concentration. In contrast, for TRA the V/P decreased with increasing VAMS concentration (Fig. S1) which was successfully implemented into the model by using a second-degree polynomial (Eq. 6). This may be related to the presence of a saturable binding site for TRA on blood cells. However, no supporting data was available in the literature for TRA. Yet, the lack of data might be due to the fact, that saturation occurred at high TRA concentrations (> 100 ng/mL) which usually

cannot be found in clinical samples [18]. Determined V/P values were compared to B/P values obtained from the literature, if available. Recently the B/P for BOS was published [19] and is in good agreement with our observations, 1.12 vs. 1.07, respectively. The calculated V/P for NIL (0.74) corresponds to the published values of 0.70 [19] and 0.71 [20], but in contrast, the determined value for LEN (0.82) deviates from the literature (0.60) [21]. For all other KI no B/P values were available. Half of the determined V/P values were < 1 (AXI, CAB, DAB, LEN, NIL), indicating higher concentrations in plasma than in intracellular compartments. RUX on the other hand, was more concentrated in cellular blood components (mean observed V/P of 2.51). Considering the intracellular location of JAK2, the main pharmacological target of RUX and its effects on dendritic cells and various lymphocytes [22], intracellular accumulation of RUX could be an explanation.

In general, it was observed that the greater the difference of V/P from 1, the more pronounced the effect of the Hct. No highly significant effect of Hct was observed for AFA, AXI, BOS and TRA which is in line with the theory of dilution or concentration by cellular components in VAMS (see Fig. 1). The fact that the analytical validation demonstrated the method to be Hct-independent for different Hct levels and concentrations (see Section 3.1.4) is a clear advantage over DBS where Hct variations may lead to unreproducible results. Yet, Hct might be necessary for VAMS-to-plasma conversion. The Hct dependency for recalculation of plasma concentration was demonstrated for CAB, DAB, LEN, NIL, OSI and RUX in our model. However, the extent to which individual Hct values are necessary for the recalculation compared with mean Hct values based on the study population for which the conversion is intended needs to be investigated. Data on target concentrations of KI is mostly limited to plasma concentrations. Few data on concentrations of KI in capillary blood have used dried blood spots [10] and no data on KI concentrations using VAMS is available. Therefore, our VAMS-to-plasma conversion model is crucial for comparing VAMS concentrations to plasma levels. Yet, the fact that only *in vitro* samples have been used is a clear limitation of our model. Future investigations with patient samples should be conducted to validate the here established conversion factor for clinical practice.

Table 4 Coefficients obtained from *in vitro* experiments for the conversion of VAMS to plasma concentrations.

Analyte	Coefficients				R^2	mean obs. V/P[a] (SD)
	A (SE)	B (SE)	C (SE)	Intercept (SE)		
AFA[b]	0.868 (0.009)	-	-	0.712 (1.878)	0.9920	1.13 (0.09)
AXI[b]	1.216 (0.011)	-	-	1.414 (2.317)	0.9932	0.82 (0.05)
BOS[b]	0.952 (0.009)	-	-	-0.736 (1.894)	0.9931	1.07 (0.07)
CAB	0.946 (0.074)	14.171 (48.975)	0.489 (0.077)	-10.688 (47.283))	0.9901	0.72 (0.07)
DAB	1.055 (0.050)	14.375 (34.185)	0.336 (0.052)	-13.120 (33.016)	0.9952	0.74 (0.06)
LEN	0.885 (0.039)	1.423 (8.841)	0.362 (0.041)	-0.268 (8.536)	0.9962	0.82 (0.07)
NIL	1.054 (0.045)	38.058 (30.430)	0.194 (0.047)	-19.615 (29.389)	0.9952	0.74 (0.08)
OSI	1.09 (0.073)	1.144 (48.607)	-0.255 (0.075)	-1.627 (46.945)	0.9740	1.23 (0.24)
RUX	0.591 (0.024)	0.272 (5.404)	-0.207 (0.025)	0.381 (5.218)	0.9865	2.51 (0.35)
TRA[c]	13.722 (0.873)	2.788 (0.873)	-	1.643 (0.113)	0.8185	1.64 (2.01)

AFA, Afatinib; AXI, Axitinib; BOS, Bosutinib; CAB, Cabozantinib; DAB, Dabrafenib; LEN, Lenvatinib; NIL, Nilotinib; OSI, Osimertinib; RUX, Ruxolitinib; TRA, Trametinib; SD, standard deviation; SE, standard error.

[a] Across all experiments not separated by Hct.

[b] VAMS/Plasma conversion was independent of Hct (Eq. 5).

[c] Concentration-dependent VAMS/Plasma ratio was modelled for TRA (Eq. 6).

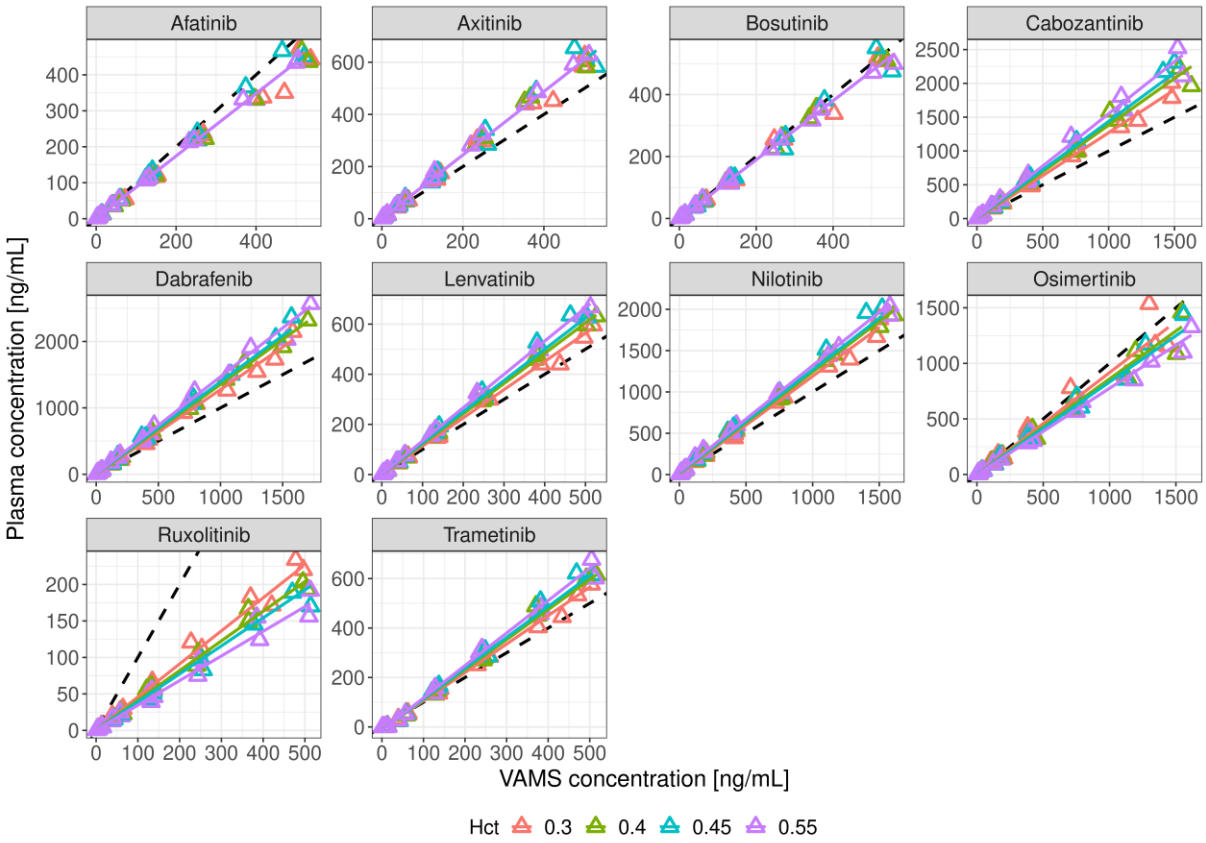

Fig. 1. Linear model fits and observed VAMS and Plasma concentrations resulting from the *in vitro* experiment. The dashed line represents a slope of 1 (Equal concentrations in VAMS and Plasma). A slope < 1 means enrichment in VAMS (e.g., Ruxolitinib); Trametinib showed non-linear behavior at low concentrations (see Section 3.2 and Fig. S1).

3.3. Feasibility of at-home sampling

24 VAMS samples of five patients treated with either AFA, CAB, NIL, RUX or a combination therapy of DAB and TRA were analyzed (n=4 for each analyte). AFA samples were collected from an 81-year-old female lung cancer patient receiving 20 mg once daily. CAB samples were collected from a 72-year-old male with renal cell carcinoma treated with 40 mg once daily. DAB and TRA samples were drawn from a 60-year-old woman with malignant melanoma (DAB 150 mg twice daily and TRA 2 mg once daily). NIL samples derived from a 75-year-old male patient diagnosed with chronic myeloid leukemia and was therapied with 300 mg twice daily, and RUX samples were taken from a 53-year-old female with chronic graft versus host disease treated with 10 mg twice daily. All patients were from Caucasian ethnicity and under therapy for more than twelve months without disruption, resulting in all measured values to be steady state concentrations. All samples were collected correctly. All VAMS devices were completely filled with capillary blood. No visible differences in sampling amount could be observed between samples taken during patient visits and

those taken at home. Neither undersampling (characterized by incompletely sampled VAMS devices resulting in visible blank material) nor oversampling (characterized by additional dried blood on top of the VAMS device) was detected which demonstrates that VAMS can be used in real-life, home-based scenarios. The measured concentrations were all within the validated calibration range without any chromatographic interference. Concentration-time profiles of VAMS and converted plasma concentrations are illustrated in Fig. 2.

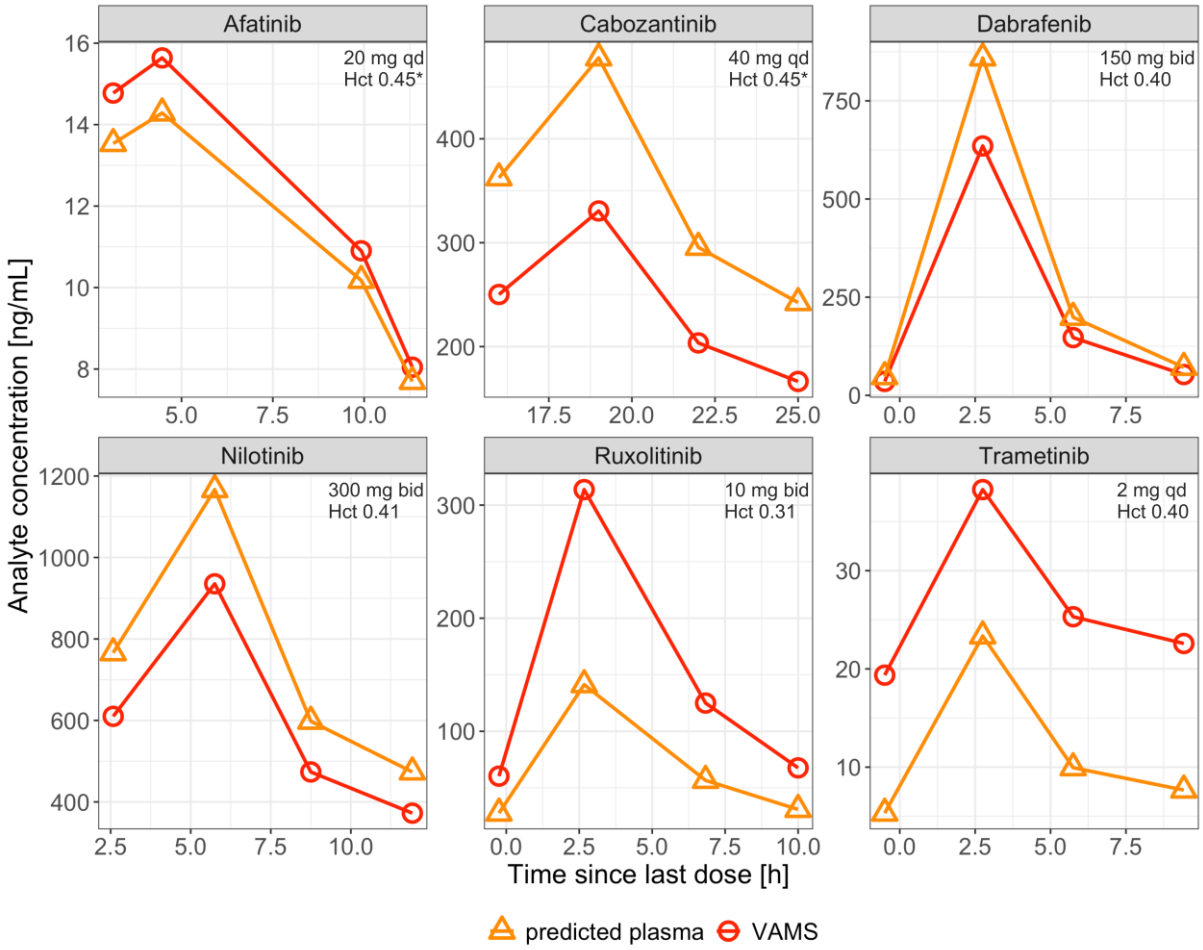

Fig. 2. VAMS concentration profile and corresponding predicted plasma concentration of one patient for each analyte using the obtained conversion factors. *No individual Hct available, assuming an Hct of 0.45. qd, once daily; bid, twice daily.

Data based on population pharmacokinetic studies showed the predicted plasma values to be in the range of reported plasma concentrations for AFA [23], NIL [24], DAB [25, 26] and TRA [18]. In addition to the population pharmacokinetic studies, reported AFA steady state plasma concentrations were 24.5 ng/mL (maximum drug concentration with a geometric CV of 88%, n=15) after an oral administration of 20 mg per day [27] and 11.5 ± 4.6 ng/mL, respectively, after analysis of three samples obtained from one patient [15] leading to the conclusion that the predicted plasma

concentrations, which ranged from 7.7 ng/mL to 14.3 ng/mL, were comparable to previously reported AFA plasma concentrations. After conversion from VAMS to plasma, NIL concentrations in this study were ranged from 474 ng/mL to 1168 ng/mL, respectively. Boons et al. published the measured NIL plasma concentrations from 20 patients with chronic myeloid leukemia mostly treated with 300 mg twice daily (17 of 20 patients) [28]. The reported NIL plasma concentrations were between 376 and 2663 ng/mL, demonstrating our conversion to be plausible. Plasma concentrations of DAB and TRA were monitored in 27 metastatic melanoma patients. 78% of the patients received the recommended starting dose of 150 mg DAB twice daily, 74% received 2 mg TRA daily. The analysis showed DAB and TRA steady state trough concentrations of 58.7 ± 61.1 ng/mL and 11.9 ± 4.1 ng/mL, respectively (mean ± SD), which were in accordance with our predicted plasma trough concentrations of 71.3 ng/mL and 7.7 ng/mL for DAB and TRA, respectively (> 9 h after dose intake) [29]. For patients with renal cell carcinoma, average CAB steady state concentrations were at 750 ng/mL (typical clearance 2.23 L/h, 40 mg daily dose) [30]. Converted plasma concentrations were found to be lower (242 ng/mL, 25 h after dose intake), which may indicate higher clearance for this patient and the need for further investigations. With an increased clearance of 3.3 L/h average steady state concentrations were 500 ng/mL and therefore closer to our calculated data. According to the METEOR trial [31] on which the study of Castellano et al. was based, elevated CAB clearance (4 L/h up to 7 L/h) was reported in 5% of patients. This may result in even lower CAB plasma concentrations compared to the reported high-clearance steady state concentration of 500 ng/mL [30]. Reported RUX steady state trough concentrations for healthy volunteers were in the range 20 ng/mL after the intake of 15 mg twice daily [32] or 16 ng/mL for a patient with myelofibrosis and 5 mg daily dose [33]. Calculated plasma concentrations based on the conversion model demonstrated in this study were comparable to those from healthy volunteers despite a lower dose (10 mg twice daily). However, due to the high variability of RUX drug exposure, converted concentrations found to be realistic for this patient. In most cases, plasma trough levels are used for drug monitoring. However, especially for drugs with a short elimination half-life, such as DAB (approx. 10 h) or RUX (approx. 3 h), unusually high peak concentrations might lead to dose-limiting adverse drug reactions despite trough levels within normal range. For other substances, e.g., Vancomycin, using area under the curve (AUC) to optimize dosing has already proven to be more

efficient than trough concentration [34]. Using minimally invasive sampling techniques like VAMS allows for more frequent sampling enabling determination of additional information on exposure such as peak concentrations or AUC.

4. Conclusion

In a recent publication, the use of VAMS for the quantification of KI has been demonstrated [35]. However, to the best of our knowledge, this is the first published VAMS method for determination of KI concentrations in patient samples collected from capillary blood and can be used as a tool to monitor drug concentrations in an alternative matrix. The method was successfully validated and proved to be feasible for samples collected by either healthcare professionals or patients at home. We were able to establish a VAMS-plasma-conversion factor based on *in vitro* samples to predict underlying plasma concentrations. Once the conversion holds true after clinical validation, TDM could be performed based on this minimally invasive approach. Thus, this analytical work provides the basis for further investigations of the VAMS method in a clinical setting.

Ethics approval

This study was approved by the Ethics Commission of the University of Wuerzburg (ref199/18-am) and conducted in accordance with the declaration of Helsinki and the later amendments. All participants and their authorized representatives gave their written informed consent and assent before inclusion in this study.

Funding

This study was supported by Hector Stiftung II gGmbH (Weinheim, Germany, Project MED 1807).

Declaration of Competing Interest

The authors declare the following financial interests/personal relationships which may be considered as potential competing interests: Oliver Scherf-Clavel, Nora Isberner and Hartwig Klinker received funding form the Hector Stiftung II gGmbH for the project “Individualized cancer therapy with kinase inhibitors using drug

monitoring – optimization by minimally invasive at-home sampling". Oliver Scherf-Clavel reports endowed professorship grant (Horphag research Ltd.). The remaining authors declare that the research was conducted in absence of any commercial or financial relationships that could be construed as a potential conflict of interest.

Acknowledgments

We would like to acknowledge our healthcare professionals Victoria Hamway, Michael Bolz, Theresa Hackl, Christina Funke, Miriam Müller, Lea Wörner, Annika Sachs dos Santos, Lubov Darst, Angelika Messner, Rima Isakson and Silke Ditzel, as well as the team of dermatology and pulmonology from the university hospital Wuerzburg for their support in organizing and collecting patient samples. We thank the patients who participated in this study.

References

[1] E. Chatelut, R. Bruno, M.J. Ratain, Intraindividual pharmacokinetic variability: focus on small-molecule kinase inhibitors, Clin. Pharmacol. Ther. 103 (6) (2018) 956–958.

[2] A. Mueller-Schoell, et al., Therapeutic drug monitoring of oral targeted antineoplastic drugs, Eur. J. Clin. Pharmacol. (2020).

[3] R.B. Verheijen, et al., Practical recommendations for therapeutic drug monitoring of kinase inhibitors in oncology, Clin. Pharmacol. Ther. 102 (5) (2017) 765–776.

[4] N. Widmer, et al., Review of therapeutic drug monitoring of anticancer drugs part two–targeted therapies, Eur. J. Cancer 50 (12) (2014) 2020–2036.

[5] S.P. Sulochana, et al., Review of DBS methods as a quantitative tool for anticancer drugs, Biomed. Chromatogr. 33 (1) (2019) e4445.

[6] J.D. Freeman, et al., State of the science in dried blood spots, Clin. Chem. 64 (4) (2018) 656–679.

[7] S. Velghe, L. Delahaye, C.P. Stove, Is the hematocrit still an issue in quantitative dried blood spot analysis? J. Pharm. Biomed. Anal. 163 (2019) 188–196.

[8] M.G.M. Kok, M. Fillet, Volumetric absorptive microsampling: current advances and applications, J. Pharm. Biomed. Anal. 147 (2018) 288–296.

[9] V. Londhe, M. Rajadhyaksha, Opportunities and obstacles for microsampling techniques in bioanalysis: special focus on DBS and VAMS, J. Pharm. Biomed. Anal. 182 (2020) 113102.

[10] V. Iacuzzi, et al., Dried blood spot technique applied in therapeutic drug monitoring of anticancer drugs: a review on conversion methods to correlate plasma and dried blood spot concentrations, Pharm. Res 38 (5) (2021) 759–778.

[11] European Medicine Agency. Guideline on bionalatyical method validation. 2012 May 30, 2020]; Available from: ⟨https://www.ema.europa.eu/en/documents/scientific-guideline/guideline-bioanalytical-method-validation_en.pdf⟩.

[12] Food and Drug Administration. Bioanalytical Method Validation Guidance for Industry. 2018 September 09, 2021]; Available from: ⟨https://www.fda.gov/files/ drugs/published/Bioanalytical-Method-Validation-Guidance-for-Industry.pdf⟩.

[13] S. Capiau, et al., Official international association for therapeutic drug monitoring and clinical toxicology guideline: development and validation of dried blood spot-based methods for therapeutic drug monitoring, Ther. Drug Monit. 41 (4) (2019) 409–430.

[14] J.S. Krouwer, R. Rabinowitz, How to improve estimates of imprecision, Clin. Chem. 30 (2) (1984) 290–292.

[15] F. Aghai, et al., Development and validation of a sensitive liquid chromatography tandem mass spectrometry assay for the simultaneous determination of ten kinase inhibitors in human serum and plasma, Anal. Bioanal. Chem. 413 (2) (2021) 599–612.

[16] Z. Ye, H. Gao, Evaluation of sample extraction methods for minimizing hematocrit effect on whole blood analysis with volumetric absorptive microsampling, Bioanalysis 9 (4) (2017) 349–357.

[17] I. Xie, et al., Extractability-mediated stability bias and hematocrit impact: High extraction recovery is critical to feasibility of volumetric adsorptive microsampling (VAMS) in regulated bioanalysis, J. Pharm. Biomed. Anal. 156 (2018) 58–66.

[18] D. Ouellet, et al., Population pharmacokinetics and exposure-response of trametinib, a MEK inhibitor, in patients with BRAF V600 mutation-positive melanoma, Cancer Chemother. Pharmacol. 77 (4) (2016) 807–817.

[19] N. Verougstraete, et al., Quantification of eight hematological tyrosine kinase inhibitors in both plasma and whole blood by a validated LC-MS/MS method, Talanta 226 (2021) 122140.

[20] European Medicine Agency. Tasigna: summary of product characteristics. 2007 March 07, 2021]; Available from: ⟨https://www.ema.europa.eu/en/documents/ product-information/tasigna-epar-product-information_en.pdf⟩.

[21] European Medicine Agency. Lenvima: summary of product characteristics. 2015 March 07, 2021]; Available from: ⟨https://www.ema.europa.eu/en/documents/ product-information/lenvima-epar-product-information_en.pdf⟩.

[22] E.M. Elli, et al., Mechanisms underlying the anti-inflammatory and immunosuppressive activity of ruxolitinib, Front Oncol. 9 (2019) 1186.

[23] M. Freiwald, et al., Population pharmacokinetics of afatinib, an irreversible ErbB family blocker, in patients with various solid tumors, Cancer Chemother. Pharmacol. 73 (4) (2014) 759–770.

[24] F.J. Giles, et al., Nilotinib population pharmacokinetics and exposure-response analysis in patients with imatinib-resistant or -intolerant chronic myeloid leukemia, Eur. J. Clin. Pharmacol. 69 (4) (2013) 813–823.

[25] D. Ouellet, et al., Population pharmacokinetics of dabrafenib, a BRAF inhibitor: effect of dose, time, covariates, and relationship with its metabolites, J. Clin. Pharmacol. 54 (6) (2014) 696–706.

[26] A. Puszkiel, et al., Clinical pharmacokinetics and pharmacodynamics of dabrafenib, Clin. Pharm. 58 (4) (2019) 451–467.

[27] S. Wind, et al., Clinical pharmacokinetics and pharmacodynamics of afatinib, Clin. Pharm. 56 (3) (2017) 235–250.

[28] C. Boons, et al., Dried blood spot sampling of nilotinib in patients with chronic myeloid leukaemia: a comparison with venous blood sampling, J. Pharm. Pharmacol. 69 (10) (2017) 1265–1274.

[29] M. Rousset, et al., Trough dabrafenib plasma concentrations can predict occurrence of adverse events requiring dose reduction in metastatic melanoma, Clin. Chim. Acta 472 (2017) 26–29.

[30] D. Castellano, et al., Exposure-response modeling of cabozantinib in patients with renal cell carcinoma: Implications for patient care, Cancer Treat. Rev. 89 (2020) 102062.

[31] T.K. Choueiri, et al., Cabozantinib versus everolimus in advanced renal cell carcinoma (METEOR): final results from a randomised, open-label, phase 3 trial, Lancet Oncol. 17 (7) (2016) 917–927.

[32] J.G. Shi, et al., The pharmacokinetics, pharmacodynamics, and safety of orally dosed INCB018424 phosphate in healthy volunteers, J. Clin. Pharmacol. 51 (12) (2011) 1644–1654.

[33] C. Pressiat, et al., Development and validation of a simultaneous quantification method of ruxolitinib, vismodegib, olaparib, and pazopanib in human plasma using liquid chromatography coupled with tandem mass spectrometry, Ther. Drug Monit. 40 (3) (2018) 337–343.

[34] B.T. Mogle, et al., Implementation of a two-point pharmacokinetic AUC-based vancomycin therapeutic drug monitoring approach in patients with methicillin-resistant Staphylococcus aureus bacteraemia, Int. J. Antimicrob. Agents 52 (6) (2018) 805–810.

[35] N. Verougstraete, C.P. Stove, Volumetric absorptive microsampling as a suitable tool to monitor tyrosine kinase inhibitors, J. Pharm. Biomed. Anal. 207 (2022) 114418.

Supplementary Material

Tables

Table S1. LC-MS/MS parameter

Name	IS	MS1 (m/z)	MS2 (m/z)	FRAG (V)	CE (V)	CELL ACC (V)	RET (min)
Afatinib	No	486.1	371.0	200	25	5	3.3
Afatinib-d6	Yes	492.1	371.0	200	25	5	3.3
Axitinib	No	387.0	356.2	200	26	7	1.7
Axitinib-13C1-d3	Yes	391.3	356.1	200	17	7	1.7
Bosutinib	No	532.0	141.3	200	22	7	3.0
Bosutinib-d9	Yes	541.0	150.1	200	22	7	3.0
Cabozantinib	No	502.2	391.1	200	35	3	3.7
Cabozantinib-d4	Yes	506.4	323.0	135	40	7	3.7
Dabrafenib	No	520.1	307.1	135	30	7	1.5
Dabrafenib-d9	Yes	529.0	316.1	135	30	7	1.5
Lenvatinib	No	427.0	369.8	185	29	1	1.4
Lenvatinib-d5	Yes	432.0	369.8	185	29	1	1.4
Nilotinib	No	530.0	289.1	135	30	7	3.6
Nilotinib-d6	Yes	536.1	295.0	135	30	7	3.6
Osimertinib	No	500.2	72.1	200	47	7	3.9
Osimertinib-13C1-d3	Yes	504.2	72.0	200	47	7	3.9
Ruxolitinib	No	307.0	186.0	135	30	7	1.1
Ruxolitinib-d9	Yes	316.1	186.0	135	30	7	1.1
Trametinib	No	616.0	490.9	200	35	7	4.0
Trametinib-13C6	Yes	622.0	496.9	200	35	7	4.0

Table S2. Chemical structure of the included kinase inhibitors, coloured Atoms indicate position of stable isotope label in the respective internal standard

Analyte	Chemical structure
Afatinib (AFA)	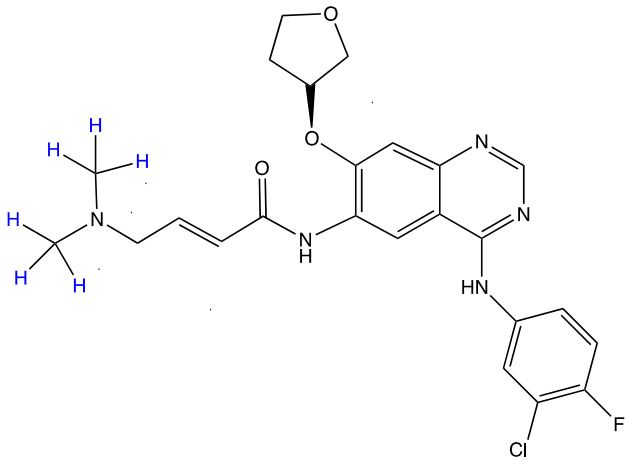
Axitinib (AXI)	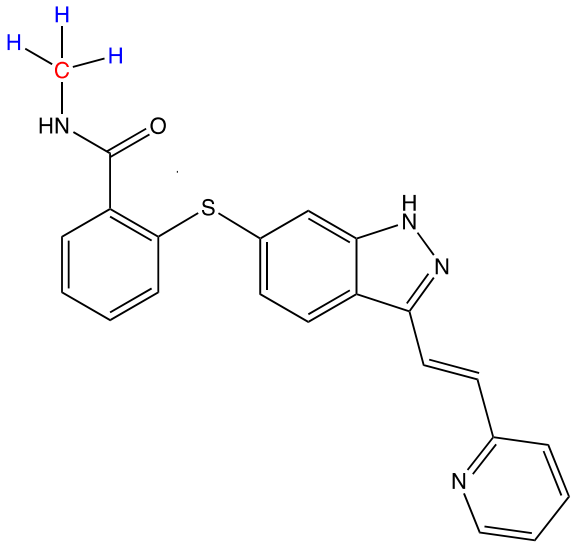
Bosutinib (BOS)	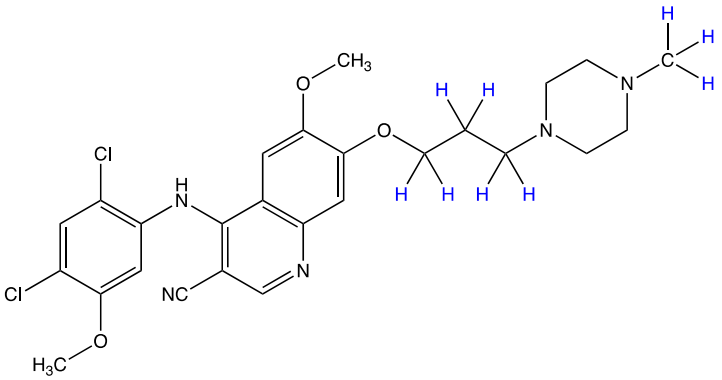

Cabozantinib (CAB)

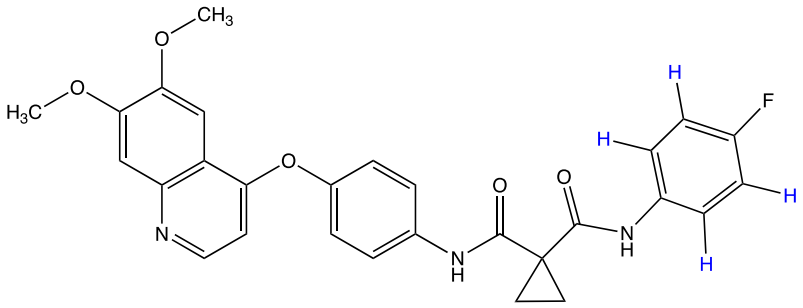

Dabrafenib (DAB)

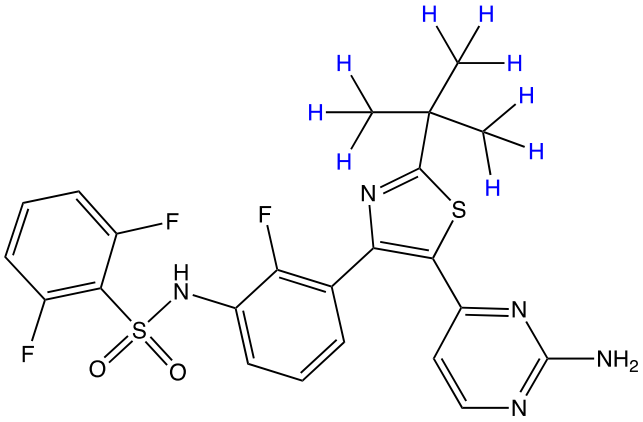

Lenvatinib (LEN)

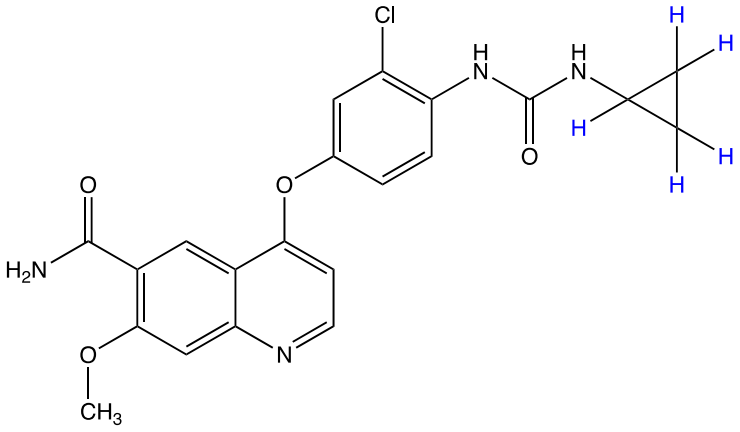

Nilotinib (NIL)

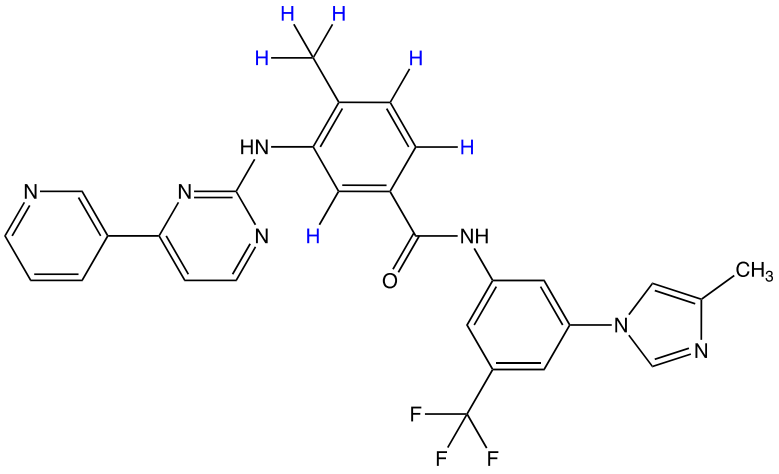

Osimertinib (OSI)

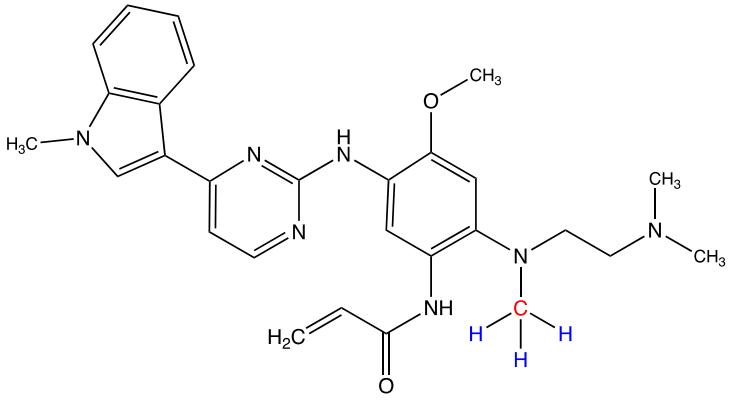

Ruxolitinib (RUX)

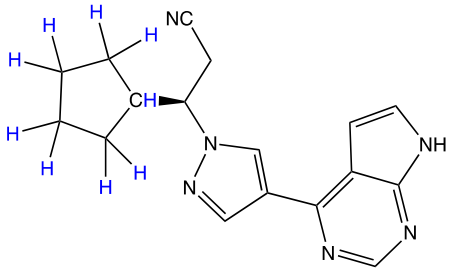

Trametinib (TRA)

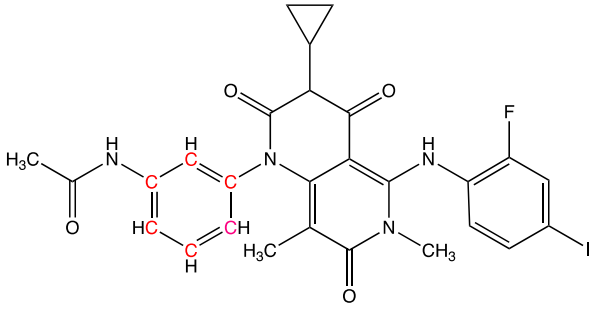

Table S3. Calibrator and quality control concentrations

Sample type	High concentration range [ng/mL] (CAB, DAB, NIL, OSI)	Low concentration range [ng/mL] (AXI, AFA, BOS, LEN, RUX, TRA)	Blood spiking (5%)	Sample type	High concentration range [ng/mL] (CAB, DAB, NIL, OSI)	Low concentration range [ng/mL] (AXI, AFA, BOS, LEN, RUX, TRA)
CR 1-WS	30000	10000	→	CR 1	1500	500
CR 2-WS	15000	5000	→	CR 2	750	250
CR 3-WS	7500	2500	→	CR 3	375	125
CR 4-WS	3600	1200	→	CR 4	180	60
CR 5-WS	2400	800	→	CR 5	120	40
CR 6-WS	800	267	→	CR 6	40	13.3
CR 7-WS	360	120	→	CR 7	18	6
CR 8-WS	240	80	→	CR 8	12	4
CR 9-WS	120	40	→	CR 9	6	2
QC H-WS	22500	7500	→	QC H	1125	375
QC M-WS	2400	800	→	QC M	120	40
QC L-WS	360	120	→	QC L	18	6
QC LLOQ-WS	120	40	→	QC LLOQ	6	2

AFA, Afatinib; AXI, Axitinib; BOS, Bosutinib; CAB, Cabozantinib; DAB, Dabrafenib; LEN, Lenvatinib; NIL, Nilotinib; OSI, Osimertinib; RUX, Ruxolitinib; TRA, Trametinib; CR, calibrator; QC, quality control; H, high; M, medium; L, low; LLOQ, lower limit of quantification; WS, working solution

Table S4. Validation results for hematocrit effects

Analyte	QC level	Hct 0.30 (n=5)		Hct 0.40 (n=5)		Hct 0.55 (n=5)	
		Accuracy (%)	Precision CV (%)	Accuracy (%)	Precision CV (%)	Accuracy (%)	Precision CV (%)
AFA	*LLOQ*	114.4	4.2	103.6	4.1	106.7	6.4
	L	102.6	3.5	92.3	4.0	97.4	3.4
	M	105.0	7.2	95.2	1.6	102.1	4.9
	H	101.0	2.0	100.8	2.7	94.5	3.4
AXI	*LLOQ*	95.3	7.4	97.3	6.1	90.0	5.6
	L	95.0	5.8	95.9	5.2	95.7	3.8
	M	97.5	2.5	93.5	4.1	96.0	1.6
	H	104.0	2.5	106.4	3.5	110.5	5.5
BOS	*LLOQ*	94.6	9.2	95.7	3.0	89.4	3.0
	L	102.7	6.4	100.7	4.9	101.3	2.0
	M	101.0	2.5	94.4	3.8	95.6	3.3
	H	107.0	2.5	105.1	4.4	110.5	6.3
CAB	*LLOQ*	105.5	3.6	83.2	2.2	108.4	6.0
	L	101.8	1.5	86.7	4.3	102.4	3.5
	M	102.8	4.4	97.7	2.2	104.0	3.2
	H	97.0	4.2	102.0	2.6	97.9	3.8
DAB	*LLOQ*	88.5	3.7	87.4	5.0	83.7	3.5
	L	91.2	5.3	91.4	3.2	91.7	3.8
	M	97.2	3.3	93.9	3.8	94.1	2.5
	H	102.5	3.3	104.4	4.2	108.4	6.2
LEN	*LLOQ*	96.5	2.3	90.2	3.9	85.3	4.9
	L	110.6	4.8	109.0	2.6	102.3	3.8
	M	106.2	2.3	101.7	3.9	96.6	2.9
	H	112.2	2.4	113.2	4.4	109.1	6.0
NIL	*LLOQ*	88.1	3.7	89.3	3.5	83.7	5.0
	L	102.8	3.9	102.8	4.2	102.8	2.6
	M	99.3	2.6	95.4	3.9	97.1	3.2
	H	105.2	2.8	106.7	4.2	111.2	5.8
OSI	*LLOQ*	111.2	4.6	112.0	0.7	114.8	4.3
	L	103.8	3.7	98.6	6.7	106.1	3.3
	M	105.5	5.2	105.9	2.2	111.3	4.5
	H	97.4	2.0	114.4	2.9	105.8	4.0
RUX	*LLOQ*	104.6	2.5	100.9	1.3	106.4	5.3
	L	104.3	2.4	96.0	3.6	103.4	1.8
	M	105.6	5.7	98.9	2.2	108.5	2.8
	H	100.1	4.2	108.8	3.0	101.7	2.9
TRA	*LLOQ*	107.3	9.7	111.3	4.5	110.1	7.4
	L	106.8	6.9	91.6	7.5	100.9	3.1
	M	106.8	6.0	99.1	3.2	108.1	4.4
	H	104.4	3.6	113.0	3.4	106.1	2.3

AFA, Afatinib; AXI, Axitinib; BOS, Bosutinib; CAB, Cabozantinib; DAB, Dabrafenib; LEN, Lenvatinib; NIL, Nilotinib; OSI, Osimertinib; RUX, Ruxolitinib; TRA, Trametinib; Hct, hematocrit; QC, quality control; LLOQ, lower limit of quantification; L, low; M, medium; H, high; CV, coefficient of variance

Table S5. Stability results for samples with different anticoagulation

Analyte	QC level	EDTA					Heparin					None				
		t0 [ng/mL]	CV (%)	3w [ng/mL]	CV (%)	Relative deviation (%)	t0 [ng/mL]	CV (%)	3w [ng/mL]	CV (%)	Relative deviation (%)	t0 [ng/mL]	CV (%)	3w [ng/mL]	CV (%)	Relative deviation (%)
AFA	*L*	4.0	1.7	4.3	5.5	7.5	3.9	4.3	4.1	6.0	5.1	4.0	9.2	3.8	7.8	-5.0
	H	265.9	7.9	292.9	9.6	10.2	232.7	3.5	247.9	10.3	6.5	213.5	3.8	232.2	8.6	8.8
AXI	*L*	5.3	4.7	5.5	3.9	3.8	5.2	6.6	5.5	5.2	5.8	5.6	9.0	5.1	4.2	-8.9
	H	407.7	4.3	409.0	1.8	0.3	396.3	6.8	361.3	7.9	-8.8	349.5	6.0	349.9	3.2	0.1
BOS	*L*	5.4	4.9	5.4	4.0	0.0	5.3	5.4	5.5	2.7	3.8	5.4	13.4	4.6	4.1	-14.8
	H	381.9	4.0	398.2	3.6	4.3	381.8	7.2	363.8	4.8	-4.7	324.0	5.3	329.6	1.9	1.7
CAB	*L*	16.0	5.4	15.9	5.2	-0.6	16.2	5.1	16.4	3.5	1.2	16.6	10.0	14.6	3.7	-12.0
	H	1143.6	4.7	1155.3	3.4	1.0	1134.9	6.8	1056.1	4.6	-6.9	994.2	4.5	978.6	2.4	-1.6
DAB	*L*	15.6	4.5	15.5	3.8	-0.6	15.8	7.0	16.0	2.4	1.3	16.6	10.0	14.7	3.4	-11.4
	H	1145.1	5.2	1147.7	2.6	0.2	1132.2	6.2	1043.4	4.5	-7.8	1013.1	6.3	976.6	1.6	-3.6
LEN	*L*	5.8	3.9	5.8	2.7	0.0	5.9	5.7	6.1	2.3	3.4	6.1	9.5	5.4	3.7	-11.5
	H	416.7	3.7	421.4	3.7	1.1	410.2	6.4	388.2	5.2	-5.4	362.8	5.1	359.2	1.6	-1.0
NIL	*L*	16.5	4.1	16.4	4.6	-0.6	16.9	5.6	16.9	3.0	0.0	17.0	10.0	15.4	4.5	-9.4
	H	1154.7	5.0	1139.2	4.5	-1.3	1155.2	6.8	1030.0	4.4	-10.8	995.3	4.8	945.3	1.4	-5.0
OSI	*L*	10.4	4.2	11.2	5.0	7.7	9.1	7.6	9.7	4.4	6.6	8.9	13.4	7.9	5.7	-11.2
	H	650.8	4.9	760.6	7.8	16.9	521.3	6.5	571.3	9.1	9.6	436.2	7.3	508.8	10.2	16.6
RUX	*L*	5.6	3.6	5.6	4.4	0.0	5.9	5.8	5.7	3.4	-3.4	5.9	5.6	5.1	4.7	-13.6
	H	401.9	4.1	397.9	3.3	-1.0	396.5	8.1	368.6	3.3	-7.0	366.0	5.0	362.3	1.8	-1.0
TRA	*L*	6.0	5.2	5.3	3.1	-11.7	5.8	8.2	5.3	8.4	-8.6	5.6	10.5	4.4	4.2	-21.4
	H	389.3	5.4	402.9	4.8	3.5	385.1	7.5	354.3	6.0	-8.0	329.4	5.9	334.2	3.6	1.5

AFA, Afatinib; AXI, Axitinib; BOS, Bosutinib; CAB, Cabozantinib; DAB, Dabrafenib; LEN, Lenvatinib; NIL, Nilotinib; OSI, Osimertinib; RUX, Ruxolitinib; TRA, Trametinib; QC, quality control; L, low; H, high; t0, initial calculated concentration; 3w, calculated concentration after three weeks; CV, coefficient of variance

Figures

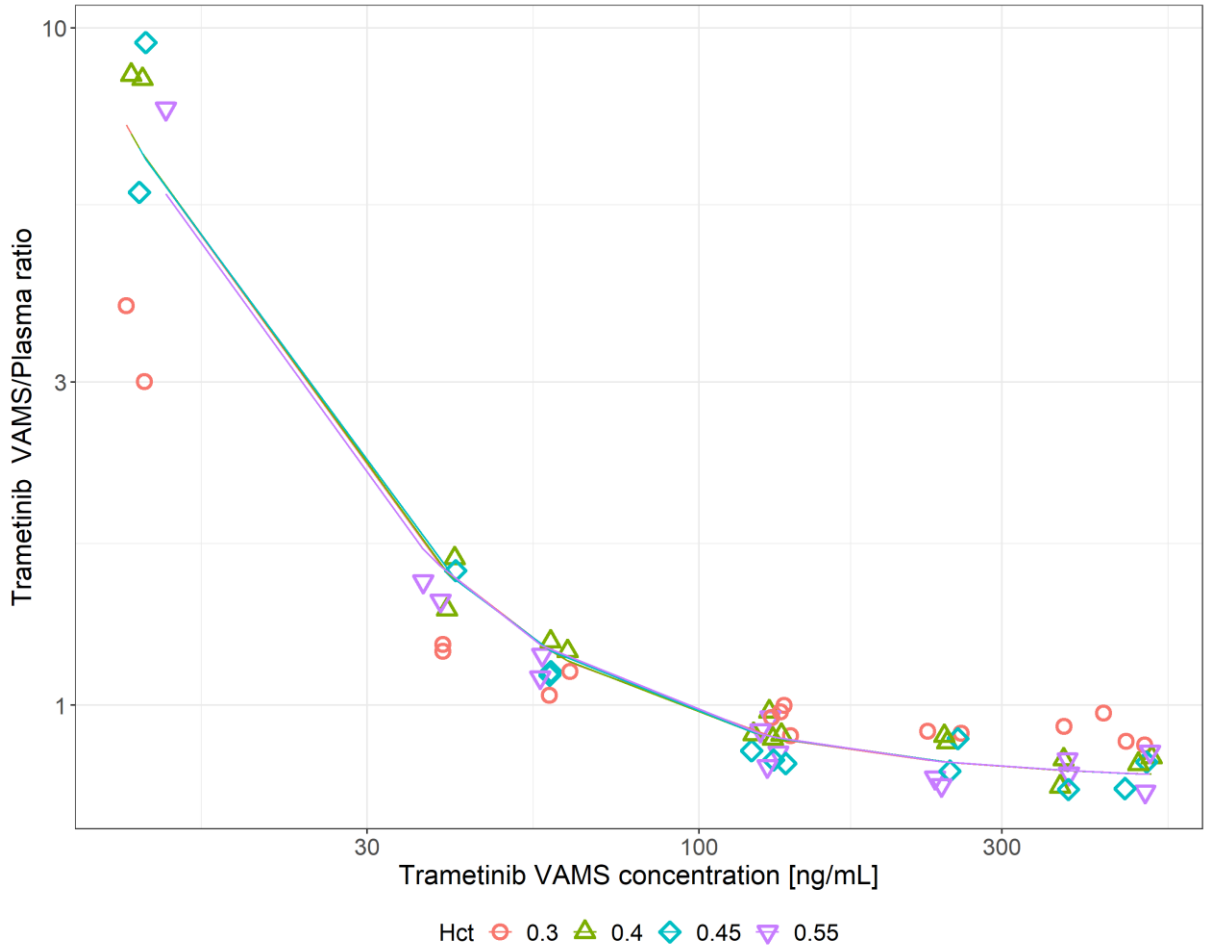

Figure S1. Non-linear relationship between VAMS-to-plasma ratio and VAMS concentration for observed for Trametinib

Further Reading

Alim, K., et al., *Interactions of janus kinase inhibitors with drug transporters and consequences for pharmacokinetics and toxicity.* Expert Opin Drug Metab Toxicol, 2021. **17**(3): p. 259-271.

Antunes, M.V., et al., *DBS sampling in imatinib therapeutic drug monitoring: from method development to clinical application.* Bioanalysis, 2015. **7**(16): p. 2105-2117.

Boons, C., et al., *Dried blood spot sampling of nilotinib in patients with chronic myeloid leukaemia: a comparison with venous blood sampling.* J Pharm Pharmacol, 2017. **69**(10): p. 1265-1274.

Boons, C., et al., *Feasibility of and patients' perspective on nilotinib dried blood spot self-sampling.* European journal of clinical pharmacology, 2019. **75**(6): p. 825-829.

de Wit, D., et al., *Dried blood spot analysis for therapeutic drug monitoring of pazopanib.* J Clin Pharmacol, 2015. **55**(12): p. 1344-50.

Denniff, P. and N. Spooner, *Volumetric absorptive microsampling: a dried sample collection technique for quantitative bioanalysis.* Anal Chem, 2014. **86**(16): p. 8489-95.

Elbin, C.S., et al., *The effect of preparation, storage and shipping of dried blood spots on the activity of five lysosomal enzymes.* Clin Chim Acta, 2011. **412**(13-14): p. 1207-12.

Evans, C., et al., *Implementing dried blood spot sampling for clinical pharmacokinetic determinations: considerations from the IQ Consortium Microsampling Working Group.* AAPS J, 2015. **17**(2): p. 292-300.

Fancher, K.M. and J.J. Pappacena, *Drug interactions with Bruton's tyrosine kinase inhibitors: clinical implications and management.* Cancer Chemother Pharmacol, 2020. **86**(4): p. 507-515.

Fogli, S., et al., *Drug-drug interactions in breast cancer patients treated with CDK4/6 inhibitors.* Cancer Treat Rev, 2019. **74**: p. 21-28.

Fogli, S., et al., *Optimizing treatment of renal cell carcinoma with VEGFR-TKIs: a comparison of clinical pharmacology and drug-drug interactions of anti-angiogenic drugs.* Cancer Treat Rev, 2020. **84**: p. 101966.

Garrison, D.A., et al., *Role of OATP1B1 and OATP1B3 in Drug-Drug Interactions Mediated by Tyrosine Kinase Inhibitors.* Pharmaceutics, 2020. **12**(9).

Groenland, S.L., et al., *Clinical Pharmacokinetics and Pharmacodynamics of the Cyclin-Dependent Kinase 4 and 6 Inhibitors Palbociclib, Ribociclib, and Abemaciclib.* Clin Pharmacokinet, 2020. **59**(12): p. 1501-1520.

Groenland, S.L., et al., *Exposure-Response Analyses of Anaplastic Lymphoma Kinase Inhibitors Crizotinib and Alectinib in Non-Small Cell Lung Cancer Patients.* Clin Pharmacol Ther, 2021. **109**(2): p. 394-402.

Iacuzzi, V., et al., *Development and validation of LC-MS/MS method for imatinib and norimatinib monitoring by finger-prick DBS in gastrointestinal stromal tumor patients.* PloS one, 2019. **14**(11): p. e0225225.

Irie, K., et al., *Development and validation of a method for gefitinib quantification in dried blood spots using liquid chromatography-tandem mass spectrometry: Application to finger-prick clinical blood samples of patients with non-small cell lung cancer.* J Chromatogr B Analyt Technol Biomed Life Sci, 2018. **1087-1088**: p. 1-5.

Kralj, E., et al., *Simultaneous measurement of imatinib, nilotinib and dasatinib in dried blood spot by ultra high performance liquid chromatography tandem mass spectrometry.* J Chromatogr B Analyt Technol Biomed Life Sci, 2012. **903**: p. 150-6.

Kucharczuk, C.R., A. Ganetsky, and J.M. Vozniak, *Drug-Drug Interactions, Safety, and Pharmacokinetics of EGFR Tyrosine Kinase Inhibitors for the Treatment of Non-Small Cell Lung Cancer.* J Adv Pract Oncol, 2018. **9**(2): p. 189-200.

Lankheet, N.A.G., et al., *Optimizing the dose in cancer patients treated with imatinib, sunitinib and pazopanib.* Brit J Clin Pharmaco, 2017. **83**(10): p. 2195-2204.

Mano, Y., K. Kita, and K. Kusano, *Hematocrit-independent recovery is a key for bioanalysis using volumetric absorptive microsampling devices, Mitra.* Bioanalysis, 2015. **7**(15): p. 1821-9.

Nijenhuis, C.M., et al., *Quantifying vemurafenib in dried blood spots using high-performance LC-MS/MS.* Bioanalysis, 2014. **6**(23): p. 3215-24.

Nijenhuis, C.M., et al., *The Use of Dried Blood Spots for Pharmacokinetic Monitoring of Vemurafenib Treatment in Melanoma Patients.* J Clin Pharmacol, 2016. **56**(10): p. 1307-12.

Picard, S., et al., *Trough imatinib plasma levels are associated with both cytogenetic and molecular responses to standard-dose imatinib in chronic myeloid leukemia.* Blood, 2007. **109**(8): p. 3496-9.

Spooner, N., et al., *A device for dried blood microsampling in quantitative bioanalysis: overcoming the issues associated blood hematocrit.* Bioanalysis, 2015. **7**(6): p. 653-9.

Wilhelm, A.J., J.C. den Burger, and E.L. Swart, *Therapeutic drug monitoring by dried blood spot: progress to date and future directions.* Clin Pharmacokinet, 2014. **53**(11): p. 961-73.

Zhao, D., et al., *Pharmacokinetic-Based Drug-Drug Interactions with Anaplastic Lymphoma Kinase Inhibitors: A Review.* Drug Des Devel Ther, 2020. **14**: p. 1663-1681.

3.3. Clinical validation and assessment of feasibility of volumetric absorptive microsampling (VAMS) for monitoring of nilotinib, cabozantinib, dabrafenib, trametinib, and ruxolitinib

Sebastian Zimmermann, Fatemeh Aghai-Trommeschlaeger, Sabrina Kraus, Götz Ulrich Grigoleit, Anja Gesierich, Bastian Schilling, Charis Kalogirou, Maria-Elisabeth Goebeler, Max Kurlbaum, Hartwig Klinker, Nora Isberner, Oliver Scherf-Clavel

Copyright

https://doi.org/10.1016/j.jpba.2023.115311

Abstract

Volumetric absorptive microsampling (VAMS) has emerged as a minimally invasive alternative to conventional sampling. However, the applicability of VAMS must be investigated clinically. Therefore, the feasibility of at-home sampling was investigated for the kinase inhibitors nilotinib, cabozantinib, dabrafenib, trametinib and ruxolitinib and evaluated regarding the acceptance of at-home microsampling, sample quality of at-home VAMS and incurred sample stability. In addition, clinical validation including three different approaches for serum level predictions was performed. For this purpose, VAMS and reference serum samples were collected simultaneously. Conversion of VAMS to serum concentration was based either on a linear regression model, a hematocrit-dependent formula, or using a correction factor. During the study period 591 VAMS were collected from a total of 59 patients. The percentage of patients who agreed to perform VAMS at home ranged from 50.0% to 84.6% depending on the compound. 93.1% of at-home VAMS were collected correctly. Regarding the drug stability in dried capillary blood, no stability issues were detected between on-site and at-home VAMS. Linear regression showed a strong correlation between VAMS and reference serum concentrations for nilotinib, cabozantinib, dabrafenib and ruxolitinib (r 0.9427-0.9674) and a moderate correlation for trametinib (r 0.5811). For clinical validation, the acceptance criteria were met for all three approaches for three of the five kinase inhibitors. Predictive performance was not improved by using individual

hematocrit instead of population hematocrit and was largely independent of conversion model. In conclusion, VAMS at-home has been shown to be feasible for use in routine clinical care and serum values could be predicted based on the measured VAMS concentration for nilotinib, cabozantinib, and dabrafenib.

Graphical Abstract

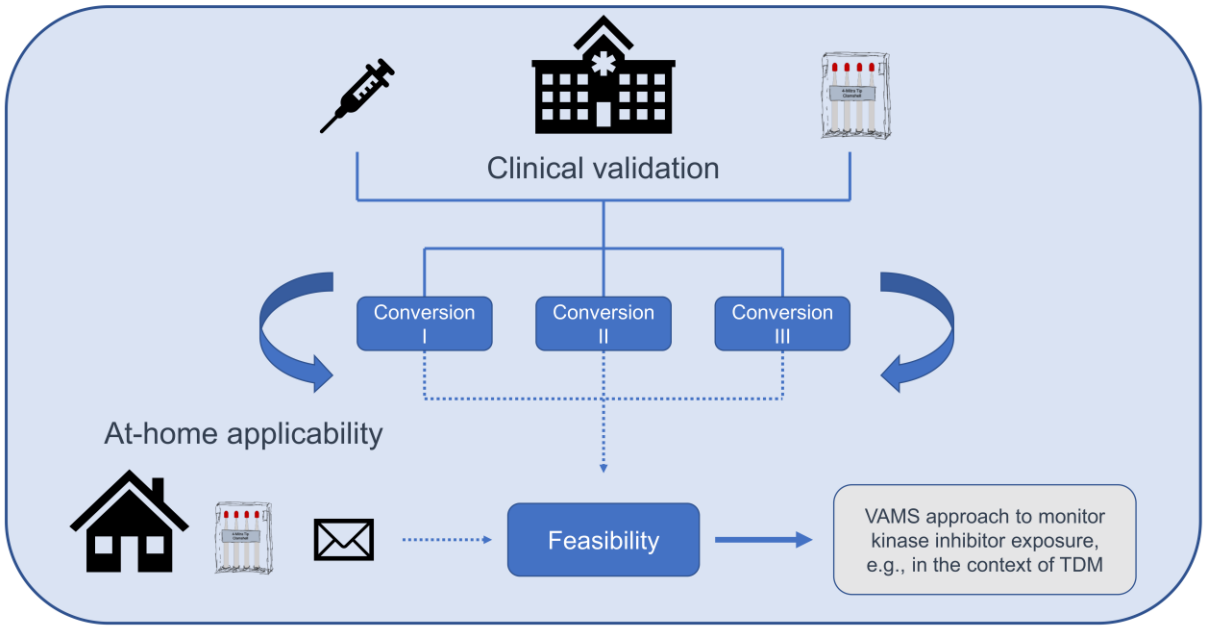

1. Introduction

Kinase inhibitors (KI) have become an important part in the treatment of patients with different malignant and non-malignant diseases. However, all KI have high interindividual pharmacokinetic variability [1], e.g., due to cytochrome (CYP) P450-mediated metabolism, and oral uptake with food effects on the bioavailability [2, 3]. Inadequate drug exposure has been observed in 50% of the patients treated with different KI for various cancers [4]. Even though several studies have provided evidence for the benefits of therapeutic drug monitoring (TDM) of KI, TDM and precision dosing is not part of routine clinical care [4-10]. Whereas an exposure-response relationship has been established for some KI, e.g., nilotinib (NIL) [11-15], data on the effects of exposure on outcome and toxicity are exploratory and partially inconclusive for other compounds [10]. To provide the basis for recommendations on TDM, exploratory monitoring in large cohorts should be performed to further investigate the associations of KI exposure with efficacy and toxicity and to establish target

concentrations. For KI with existing evidence for precision dosing, e.g., imatinib [5, 10], routine TDM should be made accessible easily to lower burdens for implementation in routine clinical care. For determination of drug exposure of KI, usually serum or plasma samples are collected by venipuncture in the outpatient setting. However, conventional sampling comes along with several disadvantages. It is often not possible to obtain trough levels due to conflicts between the patient's dosing schedule and the appointment. Collecting samples at different time intervals to receive more accurate pharmacokinetic (PK) parameters is difficult [16]. Additionally, venipuncture is an invasive procedure which may be uncomfortable for certain populations (e.g., children, patients with difficult veins) and requires trained staff [17]. To lower these burdens, microsampling techniques using dried matrix methods (DMM) which allow self-sampling of small amounts of capillary blood at home are an alternative [16, 17]. To this end, volumetric absorptive microsampling (VAMS) can be used. It is a certified in vitro diagnostic device that allows hematocrit-independent capillary blood sampling [18]. It is less straining for the patients, allows for more frequent sampling and is already used for monitoring exposure of other drugs such as anticonvulsants [19]. Samples can be sent to the laboratory for analysis by mail without need for special conditions regarding storage or shipment [16, 18]. However, to ensure adequate sampling quality, patients need proper instructions and support. Furthermore, existing data on the exposure of KI and proposed targets are expressed as serum or plasma concentrations. As whole blood concentrations are analyzed when using VAMS, the distribution of the compound between plasma and blood cells needs to be considered and capillary blood concentrations must be converted into serum concentrations prior to interpretation [20, 21]. Therefore, methods to convert VAMS to serum or plasma concentrations need to be validated by simultaneous collection of VAMS and serum samples to provide reliable results for precision dosing. However, no standard procedure for conversion of DMM concentrations has been established so far [20]. Although some VAMS methods have been developed in recent years for the quantification of KI concentrations, clinical application has been sparse and none of the investigations included the clinical validation of the conversion method [22-24]. Therefore, this study investigated the clinical applicability of VAMS and performed clinical validation of the VAMS method for the quantification of NIL, cabozantinib (CAB), dabrafenib (DAB), trametinib (TRA), and ruxolitinib (RUX). Different VAMS-to-serum conversion methods were tested regarding their predictive performance.

2. Material and methods

2.1. Study population

This non-interventional prospective study was conducted at the University Hospital of Würzburg between March 2020 and March 2022. The study was approved by the Ethics Commission of the University of Würzburg (ref199–18-am). Patients treated with NIL for Philadelphia chromosome positive (ph+) CML, with CAB for renal cell carcinoma, with DAB or a combination therapy of DAB and TRA for unresectable or BRAFV600-mutated metastatic melanoma, or with RUX for steroid-refractory acute or chronic graft-versus-host disease (GvHD) after allogeneic stem cell transplantation qualified for inclusion. The minimum age was 18 years and the minimum life expectancy two months. Patients with severe ($\geq$ III) skin GvHD were not included. Patients participated either in only on-site sampling or additionally in at-home sampling. Patients were eligible for at-home sampling if they were considered cognitively and motorically capable to perform self-sampling. Written informed consent was obtained from all patients.

2.2. Sample collection

At each routine patient visit, venous whole blood was collected by venipuncture to determine the reference serum concentration (S_{ref}) of the respective KI (serum container manufactured by Sarstedt (Nümbrecht, Germany)). 20 µL of capillary blood was collected immediately after venipuncture by trained staff using Mitra® VAMS devices from Neoteryx (Torrance, CA, USA). The VAMS was collected after a finger prick using safety lancets, type “super” with 1.5 mm penetration depth (Sarstedt, Nümbrecht, Germany). The VAMS procedure was standardized according to a previously defined sampling protocol and did not differ between clinic and at-home collection. The sampling protocol included the cleaning and warming of the hands, as well as the disinfection of the puncture area. After the finger prick, the first drop was discarded, and the VAMS was collected. Finally, treated band-aid was applied. The on-site VAMS were collected by trained staff and remained in the clinic (V_{ref}). Patients who participated in at-home sampling received training including in self-sampling the collection of a VAMS under observation (V_{P1}), Additionally, a detailed manual was handed out. Patients were asked to collect three additional samples at-home at prespecified time slots: 12-3 p.m. (V_{P2}), 3-6 p.m. (V_{P3}), and 6-9 p.m. (V_{P4}). Sample V_{P1} along with three unused VAMS ($V_{P2–4}$) was taken home by the patient. The sample

collection was not linked to their drug intake. Thus, a trough value was not necessarily determined. Time of sampling and last administration of the respective compound was documented on a specific form. The VAMS device and the form were sent to the laboratory by mail.

2.3. Bioanalysis

VAMS quality was assessed by visual inspection. Incorrectly sampled devices were excluded from the analysis. Two criteria for incorrect sampling were previously defined. First, insufficient sampling of the VAMS characterized by visible unsampled (white) surface reaching at least the outer verge of the VAMS. Second, oversampling, determined by the presence of additional dried matrix on top of the already completely sampled VAMS surface (Supplementary data (SD) Fig. S1). VAMS were analyzed by tandem mass spectrometry (LC-MS/MS) at the Institute for Pharmacy and Food Chemistry in Würzburg using a validated bioanalytical method [23]. The sample preparation was performed with acetonitrile for protein precipitation with an additional shaking procedure for physical extraction. The supernatant was evaporated afterwards and reconstituted with mobile phase. Serum concentrations were determined at the Core Unit Clinical Mass Spectrometry at the University Hospital Würzburg using a validated LC-MS/MS method [25]. Protein precipitation was also used for serum sample preparation. Positive electrospray ionization in combination with multiple reaction monitoring mode was used at both laboratories for the detection of the analytes and isotope labeled standards. The calibration range was identical between the VAMS and serum method with a lower limit of quantification (LLOQ) of 6 ng/mL for NIL, CAB and DAB and 2 ng/mL for RUX and TRA. Both methods were validated in terms of linearity, sensitivity, accuracy and precision, selectivity, carry over, matrix effect, recovery, and stability. Method robustness and dilution integrity was also investigated for the serum method whereas the VAMS method was additionally validated regarding the hematocrit effect. Both methods fulfilled the criteria of FDA and EMA guidelines on bioanalytical method validation. Hematocrit (Hct) was assessed as part of the clinical routine at the University Hospital Central Laboratory.

2.4. Outpatient applicability

Applicability of the method for at-home sampling was investigated separately for each compound. VAMS acceptance rate, sample quality of at-home VAMS and incurred sample stability were assessed. Acceptance rate for at-home sampling was

calculated as the ratio [%] of the number of patients who agreed to perform at-home sampling at least once after a VAMS was collected on-site to the total number of patients who agreed to perform VAMS (on-site and at-home). Sample quality was calculated as the ratio [%] between correctly sampled at-home VAMS and the total number of collected at-home VAMS. Incurred sample stability was determined by comparing the measured concentrations between the on-site (V_{ref}) and the corresponding take-home sample (V_{P1}).

2.5. Prediction of reference concentration

The back calculation of serum concentration (C_{pred}) was performed using three different approaches, which have already been described for DMM of anticancer drugs [20]. First, the prediction was performed on the basis of a linear regression model using the slope and intercept of the Passing-Bablok regression (conversion method 1). In addition, a Hct-dependent formula was used for conversion of VAMS to serum concentrations according to Eq. 1. Additionally, ρ (rho) (affinity of the respective drug to blood cells) and f_u (unbound fraction of the analyte in human plasma) were taken into account (conversion method 2). ρ can be calculated from the blood-to-plasma concentration ratio (F_p, Eq. 2) [20]. *In vitro* VAMS data were used for this investigation, and the previous equation was converted to Eq. 3. Therefore, a VAMS-specific blood-to-plasma concentration ratio (V/P) was used for ρ calculation [23]. Additionally, nonlinear least square regression based on the obtained VAMS and serum samples was used for TRA and RUX for the prediction of ρ. Prediction was performed with the individual Hct values and the median Hct of the corresponding population.

$$C_{pred} = \frac{C_{VAMS}}{(1 - Hct) + Hct \cdot \rho \cdot f_u} \quad (1)$$

$$F_p = \frac{C_{WB}}{C_{plasma}} = 1 + Hct \cdot (f_u \cdot \rho - 1) \quad (2)$$

$$\rho = \frac{Hct + V/P - 1}{Hct \cdot f_u} \quad (3)$$

These calculations were compared with the third conversion method which included a correction factor (CF) for VAMS to serum concentration conversion (Eq. 4 and Eq. 5).

$$CF = median\left[\frac{C_{serum}}{C_{VAMS}}\right] \quad (4)$$

$$C_{pred} = C_{VAMS} \cdot CF \quad (5)$$

2.6. Data analysis and statistical evaluation

Clinical validation was performed by correlating the drug concentrations in capillary blood and serum. Patient V_{ref} samples with missing corresponding serum sample (S_{ref}) were excluded from the analysis. Particularly at peak concentrations, even small differences between the time of venipuncture and VAMS collection might increase the variability and thus affect the correlation model. Therefore, peak concentrations of DAB (0-4 h post-dose) and RUX (0-2 h post-dose) were excluded from the clinical validation analysis due to their short half-life [26, 27]. The correlation between VAMS and serum concentration was assessed by Passing-Bablok regression with a 95% confidence interval and Pearson's r was calculated for evaluation. Passing-Bablok regression was also applied to correlate VAMS and serum concentrations in TRA subgroups as an exploratory approach to identify covariates contributing to variability (female, male, and male with body-mass index (BMI) < 35 kg/m^2). The correlation was interpreted as follows: 0.0-0.3 weak, 0.3-0.7 moderate, 0.7-1.0 strong. For conversion methods 1 and 3, a k-fold cross validation was performed. Therefore, the data set was randomly divided into a training and validation set with a 90/10 split. The conversion factors from both methods were applied to the independent validation set to statistically validate the conversion method. The k-fold cross validation procedure was repeated ten times (k=10). The predictive performance was assessed by calculation of the median percentage predictive error (MPPE, Eq. 6) and the median absolute percentage predictive error (MAPE, Eq. 7).

$$MPPE = median\left[\frac{C_{pred} - C_{serum}}{C_{serum}}\%\right] \quad (6)$$

$$MAPE = median\left[\frac{\left|C_{pred} - C_{serum}\right|}{C_{serum}}\%\right] \quad (7)$$

A deviation of less than 15% was defined as an acceptance criterion for MPPE and MAPE. According to the EMA guideline for cross validation studies, at least 66.7% of the predicted values should range within 20% of the actual value [28]. This threshold was applied as a secondary acceptance criterion to account for bioanalytical imprecision. The conversion method was considered valid only if MPPE, MAPE and

20% imprecision criteria were within the acceptance limits. Bland-Altman plots were generated for visualization of the association of predicted with actual serum concentration with ± 1.96 standard deviations as upper and lower limits. Microsoft Excel 2016 (Microsoft Corporation, Redmond, WA, USA) was used for data processing. For statistical analysis and graphical illustration, R Software 4.0.2 and R Studio version 1.3.1073 (RStudio, Inc., Boston, MA, USA) were used with additional packages: ggplot2, readxl, mcr, BlandAltmanLeh, tidyverse and plotrix.

3. Results

3.1. Volumetric absorptive microsampling of kinase inhibitors

In total, 591 VAMS were collected during the study period. Hereof, 231 samples were collected on-site for clinical validation and 360 VAMS were collected by the patients at home. Samples were derived from 59 patients. Ten patients received NIL, 18 patients CAB, 13 RUX, 17 patients received a combination therapy of DAB and TRA, and one patient received only DAB. Baseline characteristics of the study population are shown in SD Table S1. The acceptance rate for at-home sampling ranged from 50.0% to 84.6% depending on the compound. In sum, 37 of 59 (62.7%) patients agreed and performed VAMS at-home. Of the 360 VAMS sent by mail, 335 were sampled correctly (93.1%). The remaining 25 (6.9%) samples were classified as under- or oversampled. Additionally, one one-site VAMS was insufficiently sampled. Analyte-specific VAMS acceptance rate, sample quality of at-home VAMS, and mean VAMS concentrations for all compounds are presented in Table 1. No information was available on devices lost in the mail. No data were excluded due to sample preparation errors or analytical batch rejection. Eleven VAMS were excluded after analysis as their concentrations were below the lower limit of quantification (LLOQ) or above the upper limit of quantification (ULOQ) (five DAB samples, five RUX samples and one NIL sample). Incurred sample stability was investigated for 90 samples (SD Fig. S2). Mean relative deviation in KI concentration between V_{ref} and V_{P1} did not exceed more than 7.5% (CAB) (Table 2).

Table 1 Volumetric absorptive microsampling data for all analytes.

Analyte	Acceptance rate		Sample quality of at-home VAMS		VAMS		Mean concentration [ng/mL]	Concentration range [ng/mL]
	Total number of Patients	Ratio [%]	Total sample number	Ratio [%]	Total on-site samples (V_{ref})	Total at-home samples (V_{P1-P4})		
NIL	6/10	60.0	58/63	92.1	44	63	604.9	80.0-1386.7*
CAB	11/18	61.1	76/88	86.4	41	88	335.0	88.5-870.5
DAB	9/18	50.0	82/86	95.3	84	86	76.3	6.2-439.1**
TRA	9/17	52.9	78/82	95.1	77	82	30.1	6.5-53.7
RUX	11/13	84.6	119/123	96.7	62	123	89.4	2.9-346.2**
Overall	37/59	62.7	335/360	93.1	231	360		

* One value was excluded because of VAMS concentration above the ULOQ (1744.3 ng/mL)
** Peak concentrations were not considered. 5 values were excluded for DAB and for RUX because of VAMS concentrations below the LLOQ

Table 2 Incurred sample stability.

Analyte	Number of samples analyzed	Mean relative deviation [%] (min – max)	Median storage time [d] (min – max)
NIL	10	-2.8 (-11.8-3.6)	31.0 (4-82)
CAB	28	-7.5 (-31.1-22.8)	32.5 (1-71)
DAB	10	-1.8 (-20.6-12.0)	24.0 (18-46)
TRA	20	-1.1 (-28.3-19.1)	25.0 (11-57)
RUX	22	1.9 (-7.4-20.7)	19.0 (4-54)

The data given refer to all samples used for evaluation. VAMS concentrations below the LLOQ or above the ULOQ, DAB and RUX peak concentrations and incorrectly sampled VAMS were not considered for analysis.

3.2. Predictive performance

189 paired samples (S_{ref} and V_{ref}) were collected and used for clinical validation comprising at least 40 pairs for each compound (Table 3). 26 V_{ref} samples were excluded due to missing corresponding serum values (three samples for NIL, one for CAB, 15 for DAB, 14 for TRA, and seven for RUX). In addition, 28 DAB and 10 RUX samples were excluded as concentrations were considered peak concentrations or below LLOQ. Passing-Bablok regression showed a strong correlation between VAMS and reference serum concentrations for NIL, CAB, DAB, and RUX and a moderate correlation for TRA (Fig. 1). The correlation increased after analysis of the TRA male subgroup (correlation coefficient of 0.6429, n=44). Consequently, the female population showed higher variability between VAMS and serum concentrations (correlation coefficient 0.5022, n=19). A male subgroup without strong obesity was able to be correlated with a correlation coefficient of 0.7581 (n=39) (SD Fig. S3). Predictive performances for all analytes and conversion methods are presented in Table 4. Individual Hct did not improve predictive performance compared to population Hct. For NIL, CAB and DAB the acceptance criteria MPPE and MAPE were met with all three approaches and the predictions were in line with the EMA criteria (Fig. 2). TRA and RUX serum values could not be predicted according to the previously defined acceptance criteria (SD Fig. S4 and S5).

Table 3 Clinical validation data.

Analyte	Number of sample pairs	Conversion Method 1			Conversion Method 2			Conversion Method 3
		Slope (95% CI)	Intercept (95% CI)	Correlation coefficient	ρ (rho)	f_u	Hct (95% CI)	CF (95% CI)
NIL	41	1.478 (1.246-1.635)	150.874 (56.961-242.819)	0.9427	7.62×10^{-3}	0.020	0.420 (0.405 – 0.431)	1.757 (1.690 – 1.874)
CAB	40	1.848 (1.664-2.008)	-0.057 (-70.603-36.167)	0.9627	8.46×10^{-4}	0.003	0.394 (0.370 – 0.405)	1.852 (1.788 – 1.973)
DAB	41	1.785 (1.538-2.122)	0.414 (-5.559-4.759)	0.9674	1.00×10^{-3}	0.003	0.396 (0.391 – 0.403)	1.809 (1.688 – 1.918)
TRA	63	0.453 (0.329-0.616)	-2.713 (-7.452-1.280)	0.5811	201.50*	0.026	0.396 (0.389 – 0.403)	0.373 (0.338 – 0.401)
RUX	45	0.715 (0.657-0.826)	0.110 (-2.600-3.021)	0.9466	60.20*	0.030	0.343 (0.323 – 0.361)	0.737 (0.619 – 0.926)

CI, confidence interval; ρ, drug affinity to blood cells; f_u, unbound fraction of the drug; Hct, hematocrit; CF, correction factor
* ρ was estimated using nonlinear least square regression

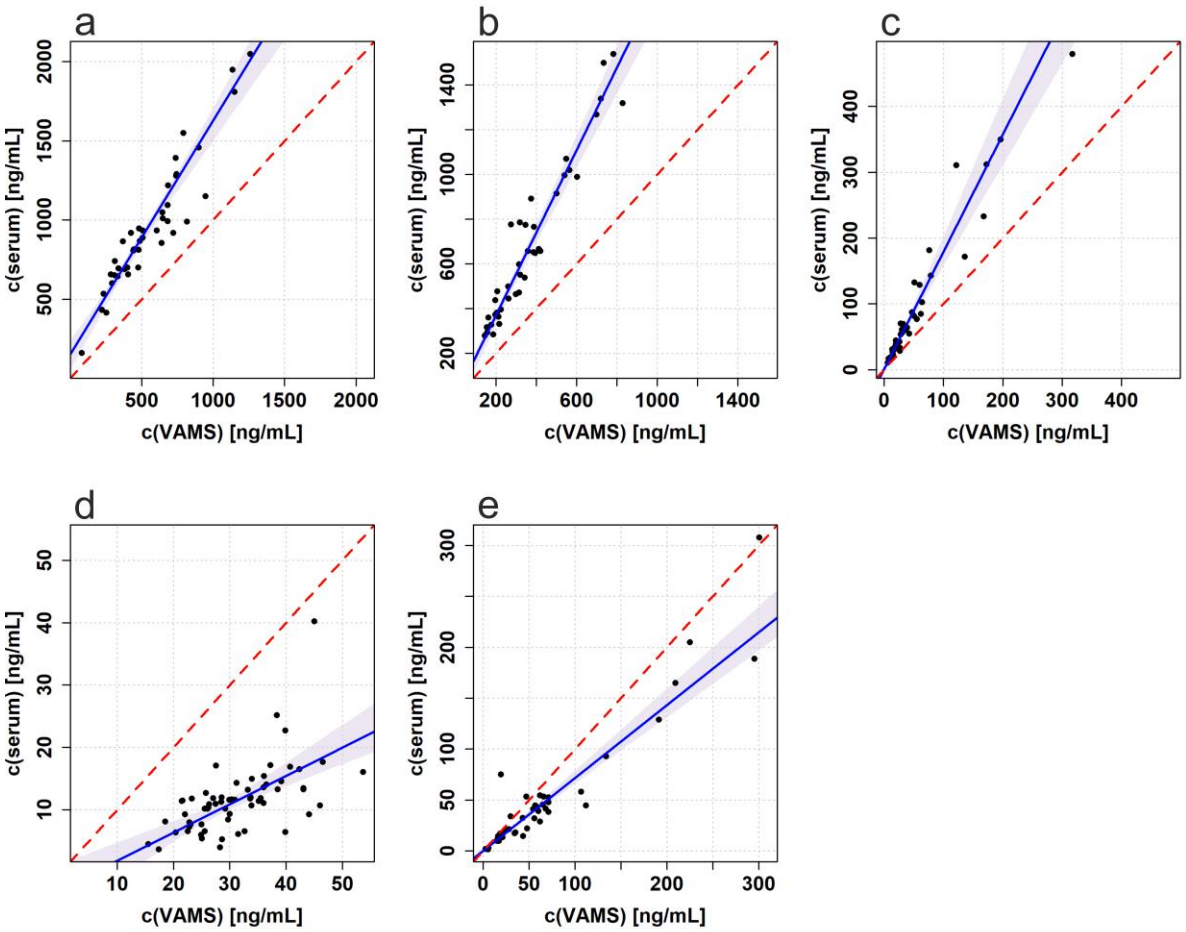

Fig. 1. Passing-Bablok regression analysis and observed VAMS and serum concentrations for NIL (a), CAB (b), DAB (c), TRA (d) and RUX (e). Blue solid line, regression line; red dashes line, identity; blue shadowed area, 95% CI of the regression line.

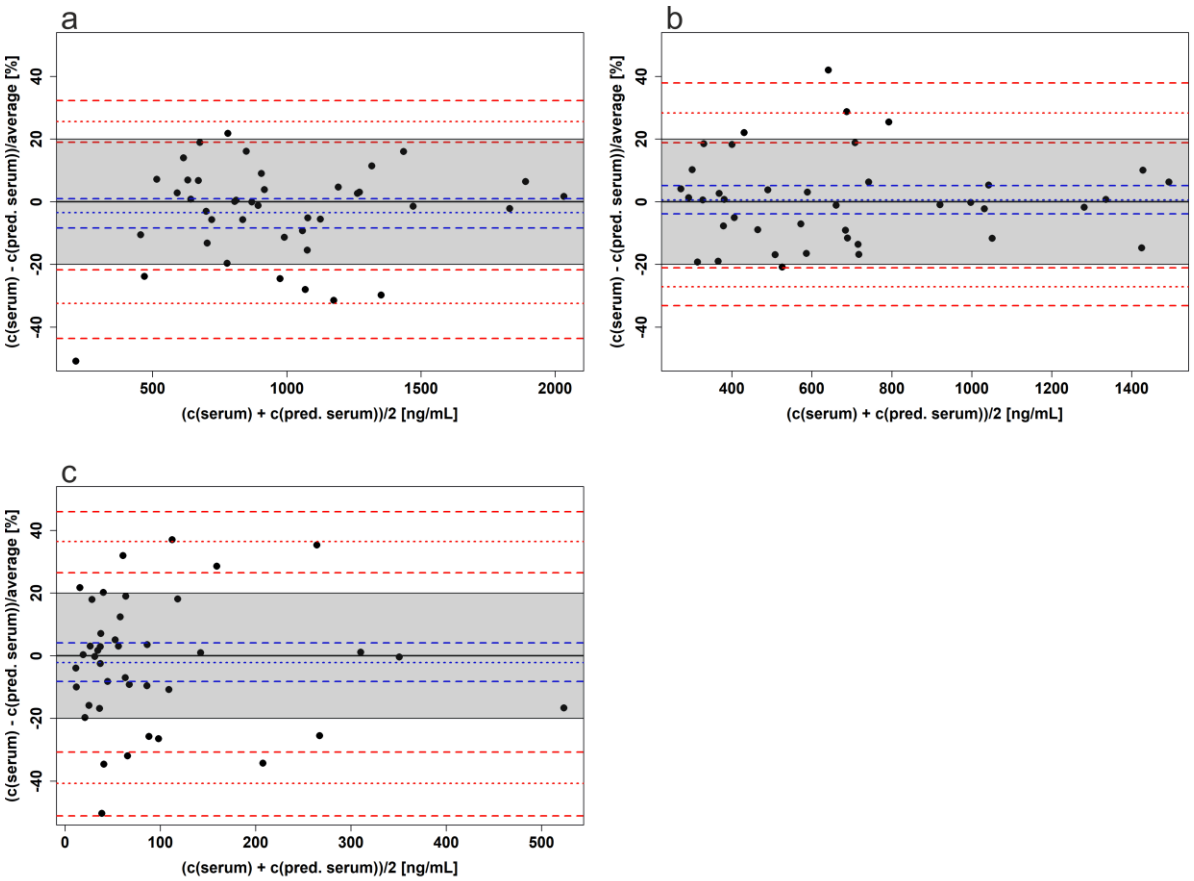

Fig. 2. Bland-Altman plot for NIL (a), CAB (b) and DAB (c). Prediction of serum level concentration was performed using the Passing-Bablok regression parameters (conversion method 1). Solid black line, zero; dotted blue line, mean; dashed blue line, 95% CI of the mean; dotted red lines, upper and lower limit of agreement; dashed red lines, 95% CI of the upper and lower lines of agreement. Gray area, ± 20% accuracy limits.

Table 4 Predictive performance.

Analyte	Evaluation criteria	Conversion method 1* (95% CI)	Conversion method 2		Conversion method 3* (95% CI)
			Population Hct	Individual Hct	
NIL	MPPE [%]	7.5 (-4.3-19.4)	-1.9	-3.7	8.0 (-4.1-20.0)
	MAPE [%]	10.8 (1.3-20.2)	10.4	11.9	12.4 (3.3-21.5)
	Predictions within reference range [%]	77.5 (54.4-100.6)	80.5	85.4	75.0 (53.1-96.9)
CAB	MPPE [%]	5.1 (-2.9-13.1)	-10.9	-10.4	5.3 (-2.3-12.8)
	MAPE [%]	10.6 (5.5-15.7)	10.9	12.4	10.1 (5.0-15.2)
	Predictions within reference range [%]	80.0 (61.7-98.3)	82.5	77.5	82.5 (63.4-101.6)
DAB	MPPE [%]	1.6 (-5.3-8.4)	-8.5	-7.2	1.5 (-5.3-8.2)
	MAPE [%]	10.5 (3.1-17.9)	11.1	12.6	10.0 (2.8-17.3)
	Predictions within reference range [%]	72.5 (52.1-92.9)	68.3	65.9	72.5 (52.1-92.9)
TRA	MPPE [%]	0.5 (-10.2-11.1)	0.0	8.4	3.2 (-7.4-13.8)
	MAPE [%]	18.3 (9.9-26.7)	18.0	16.9	18.9 (10.6-27.2)
	Predictions within reference range [%]	61.7 (45.3-78.1)	58.7	58.7	61.7 (43.7-79.6)
RUX	MPPE [%]	3.0 (-12.7-18.6)	6.7	9.5	3.6 (-11.2-18.4)
	MAPE [%]	23.8 (12.2-35.4)	16.9	15.1	18.7 (9.6-27.7)
	Predictions within reference range [%]	55.0 (31.0-79.0)	51.1	53.3	62.5 (33.0-92.0)

* Data correspond to the evaluation after 10-fold cross validation

MPPE, median percentage predictive error; MAPE, median absolute percentage predictive error; Hct, hematocrit

4. Discussion

At-home sampling was accepted by the majority of patients (62.7%). However, remarkable differences were observed between the different compounds. Whereas only 50.0% of the DAB patients participated in at-home sampling, 84.6% of RUX patients participated. The fact that patients with GvHD are under very close medical observation might have increased their motivation to participate in at-home sampling. The findings are in line with previous investigations assessing the feasibility of a dried blood spot (DBS) method for NIL [29]. Here, the ratio of preference for at-home DBS sampling to venipuncture was 60.7%. Additionally, it must be considered that monitoring results did not influence treatment decisions. Preference for microsampling over standard venipuncture may increase if patients benefit directly. The fact that 93.1% of at-home VAMS were sampled correctly, supports the applicability of at-home sampling. The observed sampling quality is comparable to the results of another VAMS study investigating at-home applicability [30] and even better than the previous DBS results for NIL [29]. Only 25 of 360 at-home VAMS from 17 patients were over- or undersampled. Interestingly, there was only one patient who failed to properly collect VAMS more than twice and sent four VAMS of poor quality. However, it should be noted that three of these four samples were taken during the first at-home sampling occasion. Sample quality of at-home VAMS of this patient improved after additional training. This indicates that sufficient instructions are crucial for implementation of at-home sampling and that feedback and additional training might increase sample quality. Our data showed that at-home storage and shipment of VAMS is no limitation to the implementation in clinical routine. Storage conditions of outpatient VAMS may differ substantially from conditions of on-site samples which are stored under predefined conditions in terms of temperature, humidity, or light exposure. Even though the samples were stored and shipped during all seasons the agreement between VAMS collected and stored on-site and VAMS stored at-home and shipped back was nearly 100% for NIL, DAB, TRA and RUX. A lower result was only detected for CAB, but still within the margins of acceptance (SD Fig. S2). Similar results were reported in a previous publication assessing in vitro stability of VAMS [23].

In our study, the slope obtained by Passing-Bablok regression significantly differed from 1 for all compounds indicating either exclusion from blood cells or accumulation in blood cells. None of the drugs was evenly distributed among cellular

and non-cellular blood constituents. Therefore, a suitable conversion method of VAMS to serum concentration is necessary if VAMS should be used to predict serum trough concentrations. We were able to demonstrate that individual Hct values are not required for the conversion, because using population Hct values resulted in comparable concentrations for all compounds. For patient populations with homogenous Hct, the inclusion of individual Hct values may increase variability, as the individual Hct may be subject of analytical variabilities. This may explain why the predictive performance of CAB and DAB slightly decreased when using individual instead of population Hct. These results are consistent with previous findings, which also suggest that Hct is not solely responsible for the variability between different sampling strategies [20, 31]. This is an advantage when it comes to self-sampling at-home without simultaneous Hct measurement. However, especially in patients with advanced malignant diseases or GvHD Hct is likely to be less stable than in the general population, e.g. because patients receive blood transfusions or intravenous fluids. In these cases, individual Hct measurements may be necessary. However, the method must be validated before it can be applied in clinical routine. With the information from the in vitro experiments and the population Hct value, the serum concentration can be calculated without the need for further data or patient samples. Interestingly, with the prediction of ρ according to Eq. 3, this only worked for NIL, CAB and DAB whereas predictive performance was poor for TRA and RUX. This may be due to the high variability of the VAMS-to-plasma ratio, which was used for the calculation of ρ. The determined value for ρ was suitable for NIL, CAB and DAB, but not for RUX and TRA. As a result, in vitro studies provide initial insights (what to expect from in vivo evaluation) but must be confirmed by clinical investigations for each compound. The estimation via nonlinear least square regression on the other hand requires a data set for paired VAMS and serum concentrations, which is usually not available. In our case, it might also be biased as it is calculated from and applied to the same data set. However, for TRA and RUX this approach was more appropriate because the predictions of serum levels were consistent with the results of the other conversion methods. Regardless of the method that was used for back calculation, there were only little differences in the predictive performance for each analyte. Therefore, we conclude that the quality of the data is more important than the conversion method. Nevertheless, a certain dispersion between measured and predicted serum concentrations can be observed for NIL, CAB, and DAB (Fig. 2). The extent to the

bioanalytical imprecision may be explained by patient-specific factors, such as comedication or time differences between VAMS and serum sample collection. In addition, different laboratory equipment and mass spectrometers as well as different analysts also contribute to an increased variability.

To increase data quality, VAMS and serum samples must ideally be collected at the same time. From a practical point of view, this is difficult to implement, especially in a real-life setting. Even small variations in time between VAMS and serum sample collection may lead to high variability exceeding the limits of acceptability of predictive performance. This is particularly distinct for analytes with a low half-life, e.g., DAB or RUX [26, 27]. The low half-life of eight and three hours, respectively, led to a high variability between VAMS and serum concentrations, which was most evident at peak levels. Therefore, only a subset of DAB and RUX sample pairs that did not contain peak concentrations was used for the clinical validation. It is likely that DAB peak levels could have been predicted if the samples could have been taken at the same time as the variability would have been lower. However, this could not be investigated due to the exploratory nature of the study. Additionally, patients receiving RUX for GvHD after allogeneic stem cell transplantation often show anemia as a side effect of RUX therapy or as part of their underlying disease (empirical probabilities 0.69) [27]. Thus, it is not surprising that the Hct in this patient collective had the lowest value and the greatest dispersion. Although the cellular fraction was only one third of the blood volume, the measured VAMS concentration was 1.4-fold higher compared to the serum level. In 7 µL blood cells, which were measured on average per VAMS for this investigation, the amount of RUX was thus higher than in the remaining 13 µL of plasma. Small differences in blood cell count thus have a greater impact on predictive performance than in patient collectives with higher Hct or drugs with lower blood cell affinity. However, despite the high correlation between VAMS and serum concentrations and the exclusion of systematically biased peak levels, predicted serum concentrations did not meet the acceptance requirements. The largest data set of 63 sample pairs was available to validate the conversion methods for TRA. In addition, the Hct of the melanoma patients was subject to only minor variation and the half-life of 5.3 days is rather long compared to RUX [32]. Nevertheless, the predictions were imprecise for TRA and did not meet the acceptance criteria. Interestingly, for one patient no prediction was acceptable even though 10 samples were measured (5 VAMS and 5 serum, VAMS concentration ranges from 28.2 to 39.9 ng/mL). Unexpectedly, serum

concentrations were always overpredicted with MAPE and MPPE of approximately 100. However, this observation could not be confirmed for DAB. This patient was male and overweight with a BMI of 38.6 kg/m^2. Due to chronic inflammation, obesity is linked to atherosclerosis, metabolic syndrome, and alternated blood count, e.g., elevated Hct [33, 34]. In our case, Hct did not explain the significant deviation of the prediction from measured concentrations suggesting that other factors are decisive. In other obese patients with a BMI < 35 kg/m^2, back calculation of serum levels was acceptable in some cases, or MAPE but not MPPE exceeded 15%, indicating over- and underprediction in the same way. It is important to note that obesity significantly improves progression-free survival in patients with metastatic melanoma treated with DAB and TRA [35]. The authors of the investigation hypothesized that increased concentrations of a hormonal mediator such as oestradiol might explain the association. This would explain why no association between overall survival and BMI was observed in female patients. Information on hormone concentrations in our patient population was not available. A relationship between variability between VAMS and serum concentrations and estrogen levels seems conceivable, as evaluation with Passing-Bablok regression was better in describing the data in the male subgroup than in the female subgroup or the whole collective (SD Fig. S3). Since McQuade et al. demonstrated that overall survival was nearly doubled in obese male, it can be assumed that our patient actually had above-average concentrations. Future studies should investigate the role of estrogens on the distribution of TRA between blood and plasma and analyze effects on drug exposure. Additionally, exposure-response analyses should investigate if VAMS concentrations of TRA are better for prediction of outcome than plasma concentrations.

5. Conclusion

The real-life applicability of the VAMS method was demonstrated in this non-interventional prospective study for NIL, CAB, DAB, TRA, and RUX. By applying a fully validated VAMS method to clinical samples in the outpatient setting, the patients' acceptance of at-home microsampling, sample quality of at-home VAMS and incurred sample stability was evaluated. Thereby, VAMS at-home has been shown to be feasible for use in routine clinical care. In case of NIL, CAB, and DAB, serum concentrations could be predicted based on the measured VAMS concentration, making the VAMS method suitable as a minimally invasive alternative to conventional

sampling, particularly in the context of TDM. As collection of VAMS allows sampling at different time intervals, other pharmacokinetic parameters despite trough concentrations can be considered for decision making, e.g. AUC or C_{max}. With a suitable pharmacokinetic model, which also includes capillary blood concentrations, even more precise predictions could be made regarding underlying plasma or serum concentrations. Thereby, patients at risk for under- or overdosing can be identified earlier, and therapy can individually be adjusted to increase therapy response, safety, and quality of life.

Compliance with ethical standards

This study was approved by the Ethics Commission of the University of Würzburg (ref199/18-am) and conducted in accordance with the declaration of Helsinki and the later amendments. All participants and their authorized representatives gave their written informed consent and assent before inclusion in this study.

Funding

This study was supported by Hector Stiftung II gGmbH (Weinheim, Germany, Project MED 1807).

Declaration of Competing Interest

The authors declare the following financial interests/personal relationships which may be considered as potential competing interests. Bastian Schilling reports a relationship with Novartis that includes: board membership, consulting or advisory, and travel reimbursement. Maria-Elisabeth Goebeler reports a relationship with Novartis, AMGEN, Gemoab, BMS, Roche and Janssen-Cliag that includes: board membership. Oliver Scherf-Clavel reports a relationship with Horphag Research that includes: endowed professorship funding.

Acknowledgments

We would like to acknowledge Victoria Hamway, Michael Bolz, Theresa Hackl, Christina Funke, Miriam Müller, Lea Wörner, Annika Sachs dos Santos, Lubov Darst, Angelika Messner, Rimma Isakson and Silke Ditzel, as well as the team of the Department of Dermatology from the University Hospital Würzburg for their support in

organizing and collecting patient samples. We thank Sabine Kendl and Martin Fassnacht for LC-MS/MS measurement of serum samples. Lastly, we would like to thank the patients who participated in this study.

References

[1] N.P. van Erp, H. Gelderblom, H.J. Guchelaar, Clinical pharmacokinetics of tyrosine kinase inhibitors, Cancer Treat. Rev. 35 (2009) 692–706.

[2] G.D.M. Veerman, et al., Clinical implications of food-drug interactions with smallmolecule kinase inhibitors, Lancet Oncol. 21 (2020) e265–e279.

[3] M. Herbrink, et al., Variability in bioavailability of small molecular tyrosine kinase inhibitors, Cancer Treat. Rev. 41 (2015) 412–422.

[4] S.L. Groenland, et al., Therapeutic drug monitoring-based precision dosing of oral targeted therapies in oncology: a prospective multicenter study, Ann. Oncol. 33 (2022) 1071–1082.

[5] E. Cardoso, et al., Therapeutic Drug Monitoring of Targeted Anticancer Protein Kinase Inhibitors in Routine Clinical Use: A Critical Review, Ther. Drug Monit. 42 (2020) 33–44.

[6] R.B. Verheijen, et al., Practical recommendations for therapeutic drug monitoring of kinase inhibitors in oncology, Clin. Pharm. Ther. 102 (2017) 765–776.

[7] N. Widmer, et al., Review of therapeutic drug monitoring of anticancer drugs part two–targeted therapies, Eur. J. Cancer 50 (2014) 2020–2036.

[8] J.M. Janssen, et al., Pharmacokinetic targets for therapeutic drug monitoring of small molecule kinase inhibitors in pediatric oncology, Clin. Pharm. Ther. 108 (2020) 494–505.

[9] S.L. Groenland, et al., Therapeutic drug monitoring of oral anticancer drugs: the dutch pharmacology oncology group-therapeutic drug monitoring Protocol for a Prospective Study, Ther. Drug Monit. 41 (2019) 561–567.

[10] A. Mueller-Schoell, et al., Therapeutic drug monitoring of oral targeted antineoplastic drugs, Eur. J. Clin. Pharm. 77 (2021) 441–464.

[11] R.A. Larson, et al., Population pharmacokinetic and exposure-response analysis of nilotinib in patients with newly diagnosed Ph+ chronic myeloid leukemia in chronic phase, Eur. J. Clin. Pharm. 68 (2012) 723–733.

[12] F.J. Giles, et al., Nilotinib population pharmacokinetics and exposure-response analysis in patients with imatinib-resistant or -intolerant chronic myeloid leukemia, Eur. J. Clin. Pharm. 69 (2013) 813–823.

[13] N. Fukuda, et al., Relationship between achievement of major molecular response or deep molecular response and nilotinib plasma concentration in patients with chronic myeloid leukemia receiving first-line nilotinib therapy, Cancer Chemother. Pharm. 89 (2022) 609–616.

[14] F.J. Giles, et al., Nilotinib exposure-response analysis in patients with imatinibresistant or-intolerant chronic myeloid leukemia (CML), Blood 116 (2010) 890.

[15] C. Tanaka, et al., Clinical pharmacokinetics of the BCR-ABL tyrosine kinase inhibitor nilotinib, Clin. Pharm. Ther. 87 (2010) 197–203.

[16] N. Verougstraete, et al., Therapeutic drug monitoring of tyrosine kinase inhibitors using dried blood microsamples, Front Oncol. 12 (2022), 821807.

[17] V. Londhe, M. Rajadhyaksha, Opportunities and obstacles for microsampling techniques in bioanalysis: special focus on DBS and VAMS, J. Pharm. Biomed. Anal.182 (2020), 113102.

[18] N. Spooner, et al., A device for dried blood microsampling in quantitative bioanalysis: overcoming the issues associated blood hematocrit, Bioanalysis 7 (2015) 653–659.

[19] A. D'Urso, et al., Therapeutic drug monitoring of antiseizure medications using volumetric absorptive microsampling: where are we? Pharm. (Basel) 14 (2021).

[20] V. Iacuzzi, et al., Dried blood spot technique applied in therapeutic drug monitoring of anticancer drugs: a review on conversion methods to correlate plasma and dried blood spot concentrations, Pharm. Res 38 (2021) 759–778.

[21] S. Capiau, et al., Official international association for therapeutic drug monitoring and clinical toxicology guideline: development and validation of dried blood spotbased methods for therapeutic drug monitoring, Ther. Drug Monit. 41 (2019) 409–430.

[22] N. Verougstraete, C.P. Stove, Volumetric absorptive microsampling as a suitable tool to monitor tyrosine kinase inhibitors, J. Pharm. Biomed. Anal. 207 (2022), 114418.

[23] S. Zimmermann, et al., Volumetric absorptive microsampling (VAMS) for the quantification of ten kinase inhibitors and determination of their in vitro VAMS-toplasma ratio, J. Pharm. Biomed. Anal. 211 (2022), 114623.

[24] P. Opitz, et al., Development and validation of a bioanalytical method for the quantification of axitinib from plasma and capillary blood using volumetric absorptive microsampling (VAMS) and on-line solid phase extraction (SPE) LC-MS, J. Pharm. Biomed. Anal. 221 (2022), 115033.

[25] F. Aghai, et al., Development and validation of a sensitive liquid chromatography tandem mass spectrometry assay for the simultaneous determination of ten kinase inhibitors in human serum and plasma, Anal. Bioanal. Chem. 413 (2021) 599–612.

[26] European Medicine Agency. Tafinlar: summary of product characteristics. 2013 July 19, 2021]; Available from: https://www.ema.europa.eu/en/documents/product-information/tafinlar-epar-product-information_en.pdf.

[27] European Medicine Agency. Jakavi: summary of product characteristics. 2012 September 18, 2020]; Available from: https://www.ema.europa.eu/en/documents/product-information/jakavi-epar-product-information_en.pdf.

[28] European Medicine Agency. Guideline on bionalatyical method validation. 2012 May 30, 2020]; Available from: https://www.ema.europa.eu/en/documents/scientific-guideline/guideline-bioanalytical-method-validation_en.pdf.

[29] C.C. Boons, et al., Feasibility of and patients' perspective on nilotinib dried blood spot self-sampling, Eur. J. Clin. Pharmacol. 75 (2019) 825–829.

[30] K. Van Uytfanghe, L. Heughebaert, C.P. Stove, Self-sampling at home using volumetric absorptive microsampling: coupling analytical evaluation to volunteers' perception in the context of a large scale study, Clin. Chem. Lab Med 59 (2021) e185–e187.

[31] R.B. Verheijen, et al., Development and clinical validation of an LC-MS/MS method for the quantification of pazopanib in DBS, Bioanalysis 8 (2016) 123–134.

[32] European Medicine Agency. Mekinist: summary of product characteristics. 2014 March 13, 2022]; Available from: https://www.ema.europa.eu/en/documents/product-information/mekinist-epar-product-information_en.pdf.

[33] G.S. Hotamisligil, Inflammation and metabolic disorders, Nature 444 (2006) 860–867.

[34] H.R. Jeong, et al., Positive associations between body mass index and hematological parameters, including RBCs, WBCs, and platelet counts, in Korean children and adolescents, Children (Basel) 9 (2022).

[35] J.L. McQuade, et al., Association of body-mass index and outcomes in patients with metastatic melanoma treated with targeted therapy, immunotherapy, or chemotherapy: a retrospective, multicohort analysis, Lancet Oncol. 19 (2018) 310–322.

Supplementary Material

Tables

Table S1 Baseline characteristics of the study population

Baseline characteristics	n=59
CML	
Patients	10 (16.9%)
Age (years)	64 (35-85)
Sex (number (%))	
Male	4 (40%)
Female	6 (60%)
Hematocrit (L/L)	0.42 (0.34-0.49)
Nilotinib daily dose (mg)	600 (450-600)
Malignant melanoma	
Patients	18 (30.5%)
Age (years)	63 (50-78)
Sex (number (%))	
Male	13 (72.2%)
Female	5 (27.8%)
Hematocrit (L/L)	0.39 (0.30-0.48)
Dabrafenib daily dose (mg)	300 (200-300)
Trametinib daily dose (mg)	2 (1-2)
RCC	
Patients	18 (30.5%)
Age (years)	68 (53-80)
Sex (number (%))	
Male	10 (55.6%)
Female	8 (44.4%)
Hematocrit (L/L)	0.40 (0.30-0.47)
Cabozantinib daily dose (mg)	40 (20-60)
GvHD	
Patients	13 (22.0%)
Age (years)	49 (23-72)
Sex (number (%))	
Male	7 (53.8%)
Female	6 (46.2%)
Hematocrit (L/L)	0.34 (0.19-0.48)
Ruxolitinib daily dose (mg)	20 (10-20)

Value for age, Hct and daily dose are median values. Paraphrases represent the range for age, Hct and daily dose.
CML, chronic myeloid leukemia; RCC, renal cell carcinoma; GvHD, graft versus host disease

Figures

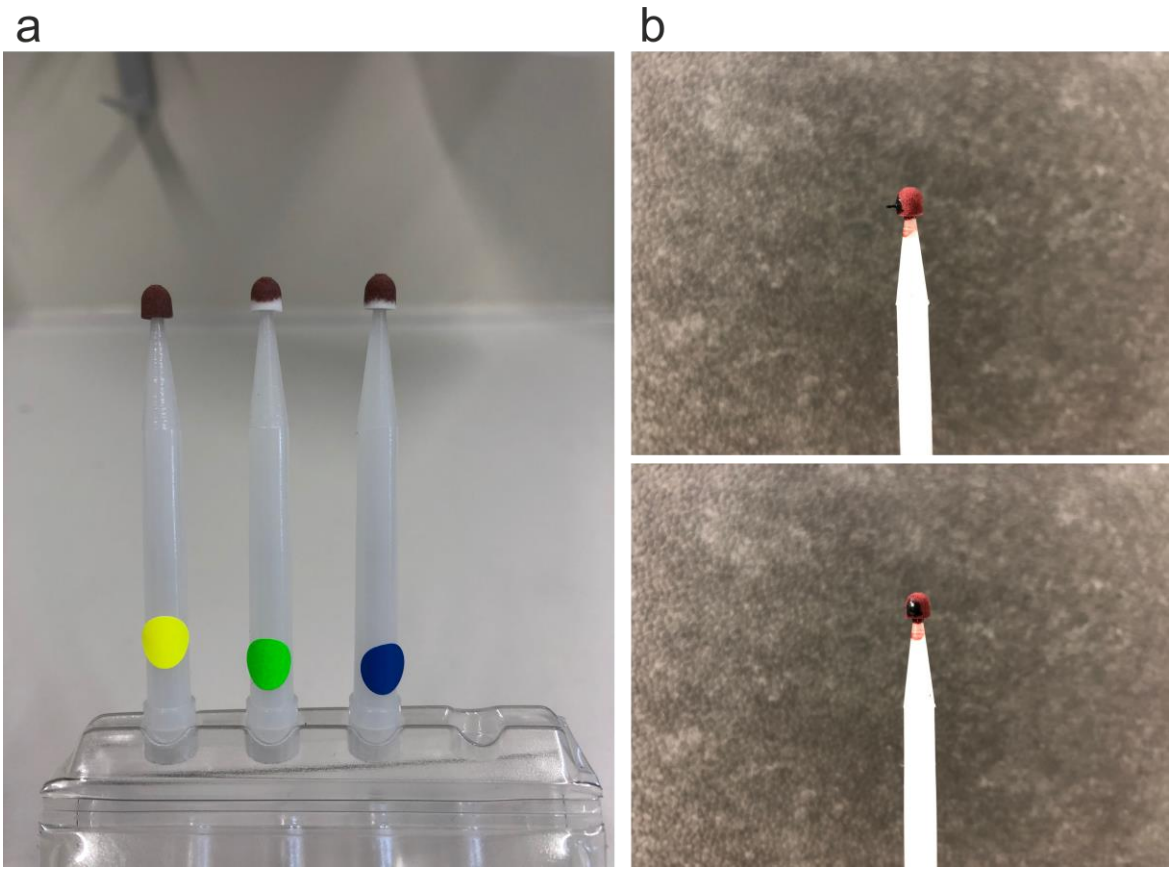

Fig. S1 Examples of VAMS devices incorrectly sampled. a: green and blue marked VAMS were undersampled, white polymeric surface not completely covered with capillary blood (yellow VAMS collected correctly), color indicates different time points for collection; b: Device was oversampled, view in profile (top) and central (bottom), dried matrix on top of the already completely sampled VAMS surface

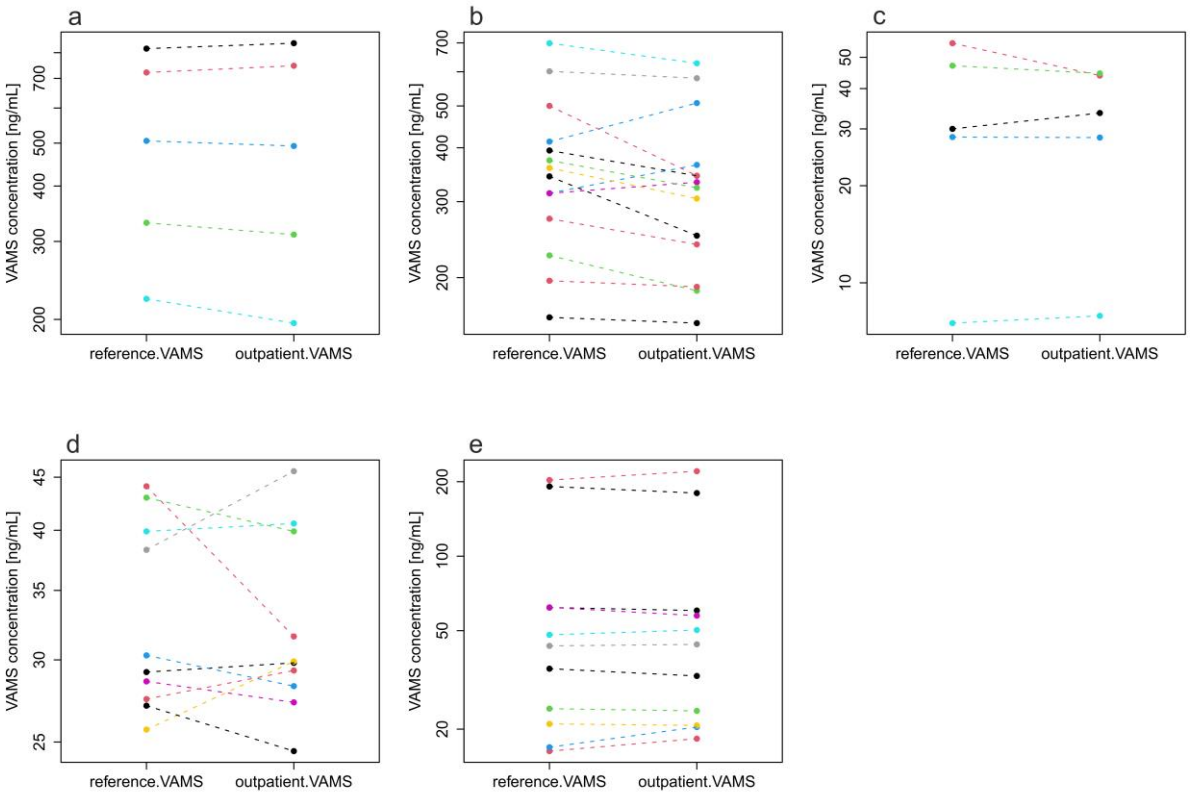

Fig. S2 Ladder plot for VAMS concentration deviation between reference VAMS (left) and outpatient VAMS (right) for a: nilotinib; b: cabozantinib; c: dabrafenib; d: trametinib; e: ruxolitinib. VAMS concentration in logarithmic scale

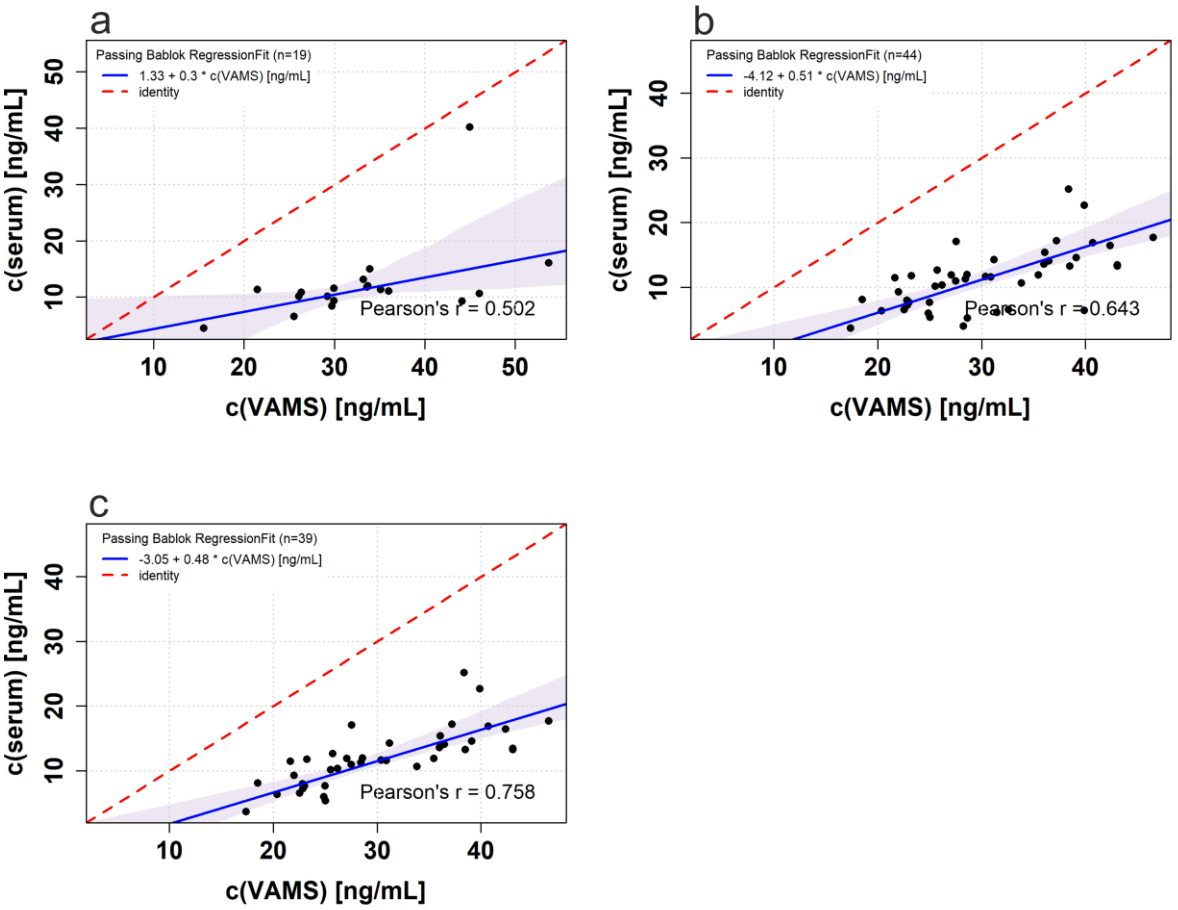

Fig. S3 Passing-Bablok regression analysis and observed VAMS and serum concentrations for TRA in female (a), male (b), and male with BMI < 35 kg/m^2 (c) subgroups. Blue solid line, regression line; red dashes line, identity; blue shadowed area, 95% CI of the regression line

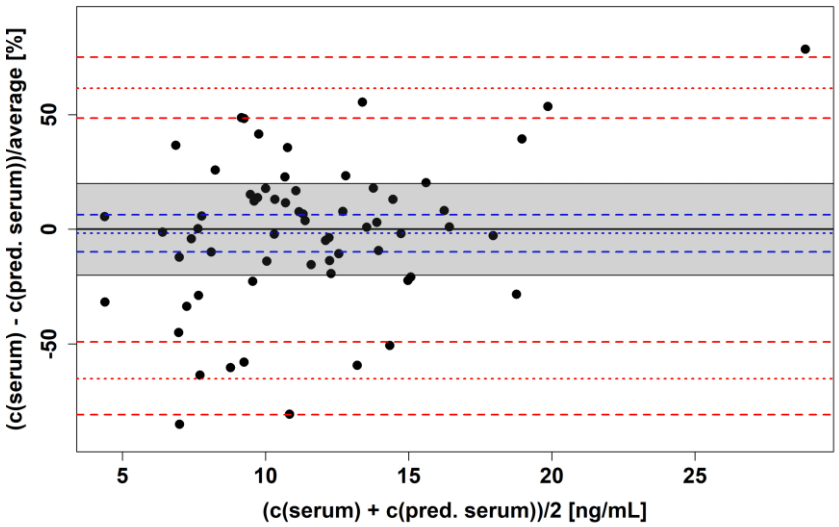

Fig. S4 Bland-Altman plot for TRA. Prediction of serum level concentration was performed through statistical analysis (conversion method 1). Solid black line, zero; dotted blue line, mean; dashed blue line, 95% CI of the mean; dotted red lines, upper and lower limit of agreement; dashed red lines, 95% CI of the upper and lower lines of agreement. Gray area, ± 20% accuracy limits

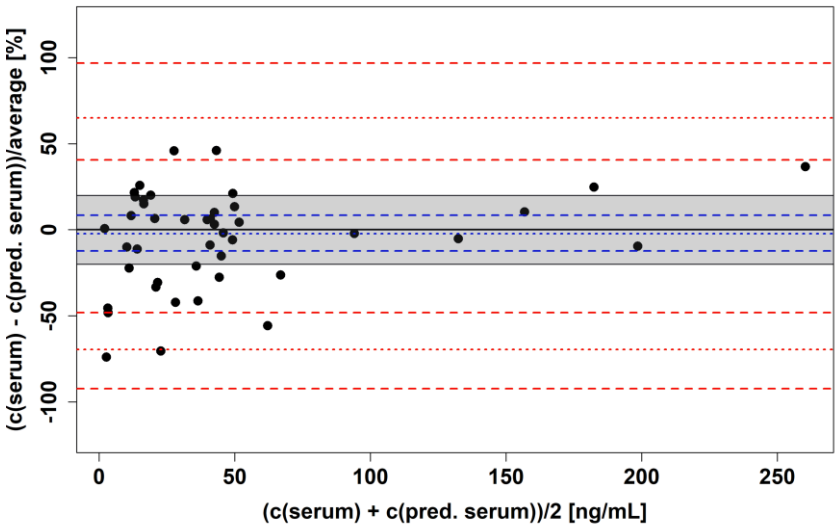

Fig. S5 Bland-Altman plot for RUX. Prediction of serum level concentration was performed through statistical analysis (conversion method 1). Solid black line, zero; dotted blue line, mean; dashed blue line, 95% CI of the mean; dotted red lines, upper and lower limit of agreement; dashed red lines, 95% CI of the upper and lower lines of agreement. Gray area, ± 20% accuracy limits

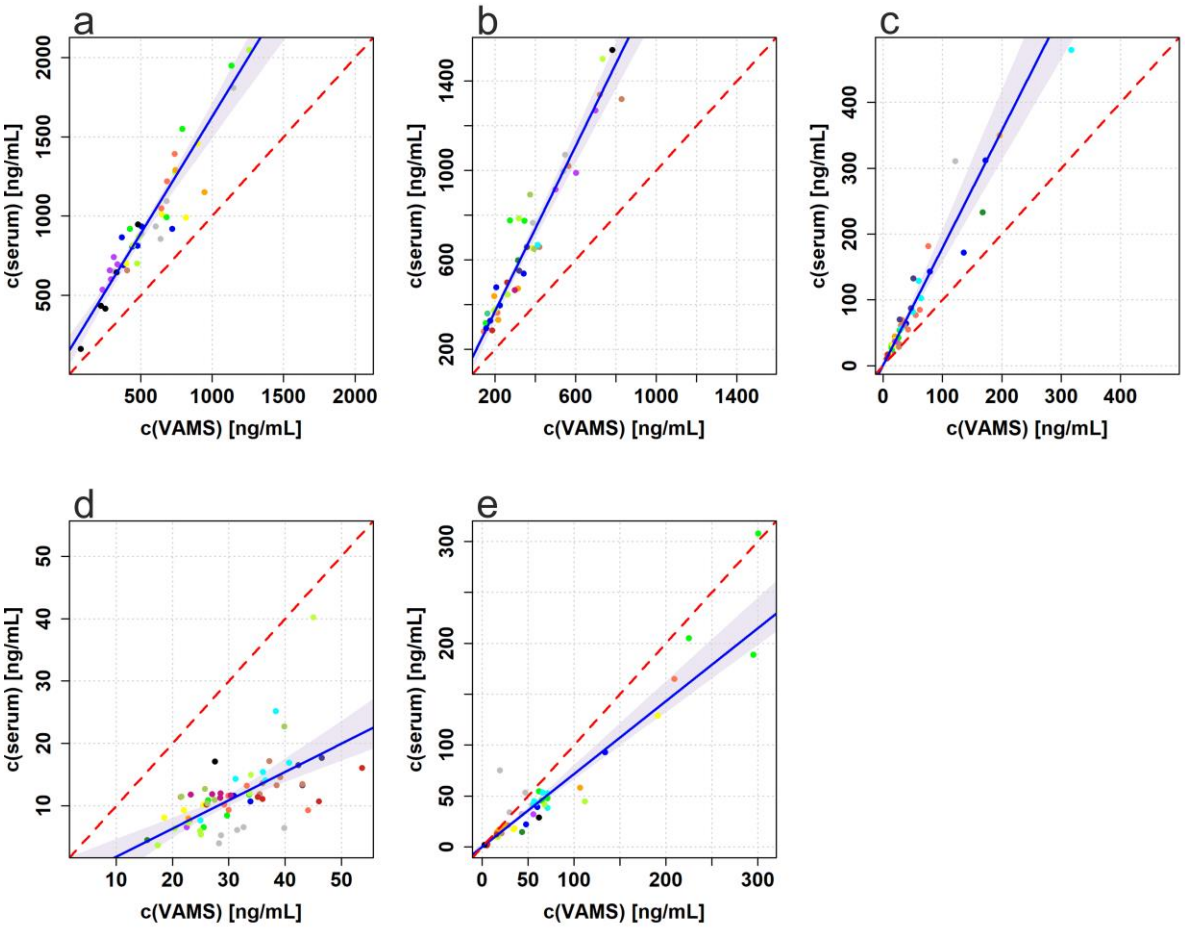

Fig. S6 Passing-Bablok regression analysis and observed VAMS and serum concentrations for NIL (a), CAB (b), DAB (c), TRA (d) and RUX (e). Colored dots, individuals; blue solid line, regression line; red dashes line, identity; blue shadowed area, 95% CI of the regression line

4. Final Discussion

4.1. Challenges for clinical implementation

The translation from bench to bedside is characterized by many barriers. Science must lead to evidence first, evidence-based approaches must be represented in guidelines, and guidelines must be considered in patient therapy. In sum, it may take an average of 17 years for implementation of healthcare approaches into clinical practice [1, 2]. The main reason why TDM is not performed in oncology for most of the drugs is the lack of exposure-response data and missing prospective studies showing clinical benefit [1]. Since exposure-response relationship studies are usually not required for regular approval, most of the information is only collected post-approval in the academic environment [1]. This is a strong limitation for the clinical implementation of TDM and was also the case for the use of CAB in ACC. Although safety and efficacy were investigated [3], there is no information on exposure-response for this off label use and, as a result, there are no target thresholds for CAB in ACC which could be considered for dose adjustment. However, information was available from a different malignancy. The exposure-response data for CAB in RCC were used for interpretation. Consequently, no regular TDM was applied for the critically ill patient, but the clinical outcome was assessed in relation to the drug exposure as an additional indicator.

As resources are limited, the laboratory capacity plays an important role in routine TDM. Patient samples must be analyzed in a timely manner [4]. Complex sample processing is difficult to manage within short turnaround times especially considering that 60-80% of the overall time required for bioanalysis is spent on sample preparation [5, 6]. To meet the demands for TDM, efficient bioanalytical methods must be available [4]. To reduce the sample preparation time and to overcome this barrier, an online SPE was used for purification of the biological samples. Therefore, protein precipitation and sample dilution were the only manual steps required, which makes the bioanalytical method capable for high throughput analysis.

Particularly in special populations such as critically ill, there is an increasing interest in TDM [1, 7]. Based on physiological alterations, e.g., through renal impairment, hemodialysis, altered protein binding or concomitant medication with high DDI potential, those patients must be given special consideration when administrated KI. Drug monitoring of CAB was feasible to demonstrate that the observed ACC patient

has lower drug exposure than expected. This study may raise awareness that drug monitoring of KI might be beneficial in special populations. In addition, it might provide measures to overcome existing barriers to accelerate implementation in clinical practice. So far, however, there is no approval for CAB for the investigated indication, making clinical trials for this indication mandatory first.

4.2. Harmonization of regulatory guidelines

The bioanalytical method for quantification of CAB in plasma samples as well as the VAMS method for simultaneous quantification of ten KI have been validated according to the regulatory guidelines of EMA [8] and FDA [9]. Since both authorities have slightly different perspectives on the requirements for bioanalysis, there are differences in their guidelines. Increasing the complexity, depending on the area of application, the LC-MS/MS method must also meet the requirements of other national authorities, such as ANVISA in Brazil, NMPA in China, or MHLW/PMDA in Japan. Therefore, a harmonized consensus was reached. On January 21, 2023, the ICH M10 guideline became effective in Europe [10], superseding the previous EMA guideline and is currently under implementation or has already been implemented in other countries.

With the adaptation towards a harmonized approach, the extent of a validation changes. In contrast to the previous guidelines, the batch size must now be considered, which will later be analyzed during routine analysis. Regarding the evaluation of any trends over time, accurate and precise analysis of QC samples should be demonstrated over the entire run. To enable reinjection of extracted samples, which is permitted in justified cases such as instrumental errors, reinjection reproducibility should be demonstrated. Both, batch size validity and reinjection reproducibility, were not investigated during method validation, neither for plasma nor for VAMS. Less strict, however, are the acceptance criteria for A&P runs. If the within-run acceptance criteria are not met in any A&P run, an overall estimate should be calculated in all A&P runs for each QC level. Other differences concern the matrix effect, which should now be investigated in terms of accuracy and precision or sample stability, which can be extrapolated to lower temperatures without further validation. According to the FDA guideline, evaluation of whole blood stability during method development can be useful (to avoid analyte loss due to instability during blood draw) and should be revalidated, if necessary. However, this was not mandatory and was

also only a case-by-case recommendation according to the EMA. With the new implementation, whole blood stability should now be included either during method development or validation. This was not investigated during CAB plasma method validation. The VAMS method, including CAB as analyte, has been fully validated in EDTA blood and there was no evidence of any stability issues. Therefore, it is not expected that there was any analyte decrease after blood sample collection.

According to ICH M10, QC samples for stability investigation should be prepared in bulk for each concentration tested and divided into a minimum of three aliquots for each investigation. Even if this process was not described in the applied guidelines, no other approach would have been feasible for VAMS as each sample needs to be prepared from freshly spiked blood and can only be analyzed once. The plasma samples were prepared from spiked blank matrix and also aliquoted and stored until analysis. However, it cannot be guaranteed that the samples were analyzed from three different aliquots per QC level and condition.

The CAB plasma method was cross validated with another laboratory in the Netherlands, evaluating the percentage deviation between the measurements. Compared to the previous EMA approach, the harmonized approach does not include specific acceptance criteria for cross validation. Agreement between two methods can now be assessed differently, for example using Bland-Altman plots or Deming regression. Regarding VAMS, also two distinct methods have been compared to each other, investigating the recalculation of VAMS to serum concentration. This approach differs from the CAB plasma cross validation, as *different* methods were used in *different* laboratories for the analysis of *different* sample types (serum vs. VAMS). However, according to the novel guideline this falls under the definition of a cross validation and the bias was assessed as recommended.

The LC-MS/MS methods for quantification of plasma CAB and VAMS KI concentrations were successfully validated. With the international consensus, future bioanalytical methods will no longer be validated according to FDA and EMA. As the scope of these guidelines refers to approval studies, it must be critically questioned whether full validation according to FDA, EMA, or ICH M10 is appropriate for the purpose of TDM. In order to fulfill the purpose of the method, the IATDMCT guideline [11] was taken into account for VAMS. A consideration of the GTFCh [12], ICH Q2(R2) [13] or Q14 [14] guidelines would also have been advisable. However, the extent of a

validation does not determine the quality of a method. Even if some of the experiments are not performed, the methods are not any worse. Conversely, a comprehensive validation does not improve an analytical method either. It is more important to control the performance of the bioanalytical method during sample analysis than to increase the criteria for method validation [15]. Even extended acceptance criteria might not interfere with the scientific conclusions that are drawn from the data [15]. Therefore, parameters and criteria used for validation should always reflect the aim of the subsequent measurement.

4.3. Towards home-based microsampling

In the outpatient setting, it is difficult to determine plasma levels at any time. Only in a few scenarios, for example in critically ill patients with inpatient treatment, multiple samples can be taken at all possible times. To enable the same flexibility in outpatient settings, analyzing drug concentrations at any timepoint without having to wait for the next appointment, minimally invasive methods were investigated. Therefore, VAMS was used in this thesis. With the collection of capillary blood, VAMS addresses a different matrix than conventional sampling techniques. Although the development and validation of the respective bioanalytical method involves greater effort because of extraction difficulties or hematocrit effects, it is rather factors such as the quality of patient training, the correct autonomous sampling, patient commitment, or correct documentation that influence VAMS outcome and make implementation difficult. Possibly the greatest obstacle is the interpretation of the VAMS concentrations. The plasma concentration can theoretically be calculated, e.g., using Eq. 9 from Section 1.3.3. For certain scenarios, the equation can even be simplified. For example, for drugs with very high protein binding (f_u~0), most of the molecules are bound to plasma proteins. Since the amount of substance in whole blood is “diluted” by blood cells, the plasma concentration can be calculated based on the whole blood concentration and Hct [16, 17]. Therefore, Eq. 9 (Section 1.3.3) can be used without the second term from the denominator as it nearly equals 0. This is also the case for large hydrophilic molecules with no partitioning into blood cells [18]. However, the formula that is used (e.g., Eq. 9, Section 1.3.3) may be less relevant since it could be shown in the specific case of Section 3.3 that the results are not dependent on how the underlying concentration was calculated. Different approaches may be used for

recalculation, offering additional flexibility for implementation of home-based microsampling.

On the other hand, there are certain scenarios where the determination of capillary blood concentrations may be superior to plasma or serum concentrations. The calcineurin inhibitor tacrolimus, which is used as an immunosuppressant in solid organ transplantation, is extensively bound to erythrocytes [18-20]. High inter- and intraindividual pharmacokinetic variability and a narrow therapeutic index justify the demand for TDM, but plasma concentrations are less than 1% of the whole blood concentration [20]. Therefore, unlike usual, TDM of tacrolimus is based on whole blood concentrations. Cyclosporine and everolimus are also highly bound to erythrocytes and, at least for the latter, TDM should be performed on whole blood concentrations as accumulation in erythrocytes interferes with the determination of plasma levels [16, 18, 19, 21]. VAMS concentrations may also be beneficial for other compounds, such as TRA, which showed a strong overestimation after recalculation of serum levels in a severely obese male, the same collective for which significant improvement in therapy was observed, but prior to further interpretation, this needs to be investigated.

One of the main advantages of VAMS is the collection of multiple samples enabling AUC determination. Steady state trough concentrations are not always appropriate as target thresholds for TDM. Compared to trough level dosing, for example, AUC-based dosing reduces the toxicity and treatment duration of the glycopeptide antibiotic vancomycin [22]. A previous study came to the same result, but only two samples were used to determine the AUC, one at peak and one at trough concentration [23]. Despite the fact that usually approximately 10-15 samples are necessary to predict 80% of the total AUC [24], it was also reported for other drugs that only a few blood samples (limited sampling strategy) are sufficient for accurate and precise prediction of individual PK parameter values [24-30]. The collection of a few samples at home (e.g., VAMS) can be managed with high patient acceptance and good quality [31] and was demonstrated as part of this work (Section 3.3).

4.4. Overall conclusion

Nearly every process of cell life is regulated through kinase-mediated phosphorylation [32]. Although previous studies with KI showed negative results for the treatment of ACC, further research is ongoing as kinases are also overexpressed in ACC tissues. Pharmacodynamics, whether a drug (e.g., KI) inhibits specific pathways, is essential for its consideration as potential treatment, but pharmacokinetics is decisive for safety and efficacy. It could be shown in the ACC case report that treatment success should be evaluated also in terms of drug exposure. Therefore, drug monitoring of KI warrants inclusion in future studies on ACC, especially considering the DDI potential with mitotane or methyrapone. With limited capacities in most clinical laboratories, simple bioanalytical methods are crucial for putting this conclusion into practice.

A valid method that meets the requirements of the EMA and FDA should in principle also meet those of ICH M10, but it is not the scope of the guidelines to be applied in TDM. From an ethical perspective, however, it is necessary to provide valid results. Thus, a full validation of any bioanalytical method that should be used for drug monitoring is reasonable and appropriate, even in academia.

The use of healthcare approaches in the home environment to monitor own physical constitution is not uncommon, considering that in addition to blood glucose, blood pressure, or heart rate, for example, a single-lead electrocardiogram can be generated in any situation [33]. As this trend continues, VAMS may be an appreciated home-based alternative for autonomous TDM. Accurate and precise bioanalysis, reliable stability even under real-life conditions, and valid conversion of VAMS concentrations to serum values for CAB, NIL, and DAB recommend its use for KI drug monitoring. Multiple sampling paves the way for AUC-based dosing. Furthermore, it could be shown that VAMS is feasible for its clinical application and should be investigated prospectively in the context of TDM.

References

[1] Stojanova, J., Carland, J.E., Murnion, B., Seah, V., Siderov, J., and Lemaitre, F., Therapeutic drug monitoring in oncology - What's out there: A bibliometric evaluation on the topic. *Frontiers in Oncology*, 2022. **12**: p. 959741.

[2] Morris, Z.S., Wooding, S., and Grant, J., The answer is 17 years, what is the question: understanding time lags in translational research. *Journal of the Royal Society of Medicine*, 2011. **104**(12): p. 510-20.

[3] Kroiss, M., Megerle, F., Kurlbaum, M., Zimmermann, S., Wendler, J., Jimenez, C., et al., Objective Response and Prolonged Disease Control of Advanced Adrenocortical Carcinoma with Cabozantinib. *The Journal of Clinical Endocrinology and Metabolism*, 2020. **105**(5): p. 1461-1468.

[4] Groenland, S.L., Mathijssen, R.H.J., Beijnen, J.H., Huitema, A.D.R., and Steeghs, N., Individualized dosing of oral targeted therapies in oncology is crucial in the era of precision medicine. *European Journal of Clinical Pharmacology*, 2019. **75**(9): p. 1309-1318.

[5] Armenta, S., Esteve-Turrillas, F.A., Garrigues, S., and Guardia, M.d.l., Smart materials for sample preparation in bioanalysis: A green overview. *Sustainable Chemistry and Pharmacy*, 2021. **21**: p. 100411.

[6] Nováková, L., Challenges in the development of bioanalytical liquid chromatography–mass spectrometry method with emphasis on fast analysis. *Journal of Chromatography A*, 2013. **1292**: p. 25-37.

[7] Clark, W. and Dasgupta, A. (2016) Clinical Challenges in Therapeutic Drug Monitoring: Special Populations, Physiological Conditions and Pharmacogenomics. Elsevier.

[8] European Medicine Agency. Guideline on bionalatyical method validation. https://www.ema.europa.eu/en/documents/scientific-guideline/guideline-bioanalytical-method-validation_en.pdf Accessed May 30, 2020.

[9] Food and Drug Administration. Bioanalytical Method Validation Guidance for Industry. https://www.fda.gov/files/drugs/published/Bioanalytical-Method-Validation-Guidance-for-Industry.pdf Accessed September 09, 2021.

[10] International Council for Harmonisation of Technical Requirements for Pharmaceuticals for Human Use. Bioanalytical method validation and study sample analysis M10 https://database.ich.org/sites/default/files/M10_Guideline_Step4_2022_0524.pdf Accessed July 03, 2023.

[11] Capiau, S., Veenhof, H., Koster, R.A., Bergqvist, Y., Boettcher, M., Halmingh, O., et al., Official International Association for Therapeutic Drug Monitoring and Clinical Toxicology Guideline: Development and Validation of Dried Blood Spot-Based Methods for Therapeutic Drug Monitoring. *Therapeutic Drug Monitoring*, 2019. **41**(4): p. 409-430.

[12] Gesellschaft für Toxikologische und Forensische Chemie. Guidelines for quality assurance in forensic-toxicological analyses; Appendix B - Requirements for the validation of analytical methods. https://www.gtfch.org/cms/images/stories/files/Appendix%20B%20GTFCh%20020090601.pdf Accessed March 06, 2024.

[13] International Council for Harmonisation of Technical Requirements for Pharmaceuticals for Human Use. Validation of analytical procedures Q2(R2). https://database.ich.org/sites/default/files/ICH_Q2%28R2%29_Guideline_2023_1130.pdf Accessed March 06, 2024.

[14] International Council for Harmonisation of Technical Requirements for Pharmaceuticals for Human Use. Analytical procedure development Q14. https://database.ich.org/sites/default/files/ICH_Q14_Guideline_2023_1116.pdf Accessed March 06, 2024.

[15] Timmerman, P., White, S., McDougall, S., Kall, M.A., Smeraglia, J., Fjording, M.S., and Knutsson, M., Tiered approach into practice: scientific validation for chromatography-based assays in early development - a recommendation from the European Bioanalysis Forum. *Bioanalysis*, 2015. **7**(18): p. 2387-2398.

[16] Iacuzzi, V., Posocco, B., Zanchetta, M., Gagno, S., Poetto, A.S., Guardascione, M., and Toffoli, G., Dried Blood Spot Technique Applied in Therapeutic Drug Monitoring of Anticancer Drugs: a Review on Conversion Methods to Correlate Plasma and Dried Blood Spot Concentrations. *Pharmaceutical Research*, 2021. **38**(5): p. 759-778.

[17] de Wit, D., den Hartigh, J., Gelderblom, H., Qian, Y., den Hollander, M., Verheul, H., et al., Dried blood spot analysis for therapeutic drug monitoring of pazopanib. *The Journal of Clinical Pharmacology*, 2015. **55**(12): p. 1344-50.

[18] Rowland, M. and Emmons, G.T., Use of dried blood spots in drug development: pharmacokinetic considerations. *The AAPS Journal*, 2010. **12**(3): p. 290-3.

[19] Emmons, G. and Rowland, M., Pharmacokinetic considerations as to when to use dried blood spot sampling. *Bioanalysis*, 2010. **2**(11): p. 1791-6.

[20] Sikma, M.A., Van Maarseveen, E.M., Hunault, C.C., Moreno, J.M., Van de Graaf, E.A., Kirkels, J.H., et al., Unbound Plasma, Total Plasma, and Whole-Blood Tacrolimus Pharmacokinetics Early After Thoracic Organ Transplantation. *Clinical Pharmacokinetics*, 2020. **59**(6): p. 771-780.

[21] Shipkova, M., Hesselink, D.A., Holt, D.W., Billaud, E.M., van Gelder, T., Kunicki, P.K., et al., Therapeutic Drug Monitoring of Everolimus: A Consensus Report. *Therapeutic Drug Monitoring*, 2016. **38**(2): p. 143-69.

[22] Neely, M.N., Kato, L., Youn, G., Kraler, L., Bayard, D., van Guilder, M., et al., Prospective Trial on the Use of Trough Concentration versus Area under the Curve To Determine Therapeutic Vancomycin Dosing. *Antimicrobial Agents and Chemotherapy*, 2018. **62**(2).

[23] Finch, N.A., Zasowski, E.J., Murray, K.P., Mynatt, R.P., Zhao, J.J., Yost, R., et al., A Quasi-Experiment To Study the Impact of Vancomycin Area under the Concentration-Time Curve-Guided Dosing on Vancomycin-Associated Nephrotoxicity. *Antimicrobial Agents and Chemotherapy*, 2017. **61**(12).

[24] Abdul-Aziz, M.H., Alffenaar, J.C., Bassetti, M., Bracht, H., Dimopoulos, G., Marriott, D., et al., Antimicrobial therapeutic drug monitoring in critically ill adult patients: a Position Paper. *Intensive Care Medicine*, 2020. **46**(6): p. 1127-1153.

[25] Alnaim, L., Therapeutic drug monitoring of cancer chemotherapy. *Journal of Oncology Pharmacy Practice*, 2007. **13**(4): p. 207-21.

[26] Kim, E.J., Oh, J., Lee, K., Yu, K.S., Chung, J.Y., Hwang, J.H., et al., Pharmacokinetic Characteristics and Limited Sampling Strategies for Therapeutic Drug Monitoring of Colistin in Patients With Multidrug-Resistant Gram-Negative Bacterial Infections. *Therapeutic Drug Monitoring*, 2019. **41**(1): p. 102-106.

[27] Padulles Caldes, A., Colom, H., Caldes, A., Cerezo, G., Torras, J., Grinyo, J.M., and Lloberas, N., Optimal sparse sampling for estimating ganciclovir/valganciclovir AUC in solid organ transplant patients using NONMEN. *Therapeutic Drug Monitoring*, 2014. **36**(3): p. 371-7.

[28] van den Elsen, S.H.J., Sturkenboom, M.G.G., Akkerman, O.W., Manika, K., Kioumis, I.P., van der Werf, T.S., et al., Limited Sampling Strategies Using Linear Regression and the Bayesian Approach for Therapeutic Drug Monitoring of Moxifloxacin in Tuberculosis Patients. *Antimicrobial Agents and Chemotherapy*, 2019. **63**(7).

[29] Alsultan, A., An, G., and Peloquin, C.A., Limited sampling strategy and target attainment analysis for levofloxacin in patients with tuberculosis. *Antimicrobial Agents and Chemotherapy*, 2015. **59**(7): p. 3800-7.

[30] Wicha, S.G., Märtson, A.-G., Nielsen, E.I., Koch, B.C.P., Friberg, L.E., Alffenaar, J.-W., et al., From Therapeutic Drug Monitoring to Model-Informed Precision Dosing for Antibiotics. *Clinical Pharmacology & Therapeutics*, 2021. **109**(4): p. 928-941.

[31] Van Uytfanghe, K., Heughebaert, L., and Stove, C.P., Self-sampling at home using volumetric absorptive microsampling: coupling analytical evaluation to volunteers' perception in the context of a large scale study. *Clinical Chemistry and Laboratory Medicine*, 2021. **59**(5): p. e185-e187.

[32] Cohen, P., The origins of protein phosphorylation. *Nature Cell Biology*, 2002. **4**(5): p. E127-30.

[33] Spaccarotella, C.A.M., Migliarino, S., Mongiardo, A., Sabatino, J., Santarpia, G., De Rosa, S., et al., Measurement of the QT interval using the Apple Watch. *Scientific Reports*, 2021. **11**(1): p. 10817.

5. Summary

The aim of the present work was to improve drug monitoring in patients with various diseases in the context of precision medicine. This was pursued through the development and validation of mass spectrometric methods for determining the drug concentrations of kinase inhibitors and their clinical application. Besides conventional approaches to determine plasma level concentrations, the focus was also on alternative sampling techniques using volumetric absorptive microsampling (VAMS).

A conventional LC-MS/MS method was developed for the determination of cabozantinib in human EDTA plasma and validated according to the guidelines of the European and United States drug authorities (EMA, FDA). The method met the required criteria for linearity, accuracy and precision, selectivity, sensitivity, and stability of the analyte. Validation was also performed for dilution integrity, matrix effect, recovery, and carry-over, with results also in accordance with the requirements. The importance of monitoring the exposure of cabozantinib was demonstrated by a clinical case report of a 34-year-old female patient with advanced adrenocortical carcinoma who also required hemodialysis due to chronic kidney failure. Expected cabozantinib plasma concentrations were simulated for this off-label use based on a population pharmacokinetic model. It was shown that the steady state trough levels were much lower than expected but could not be explained by hemodialysis. Considering the critical condition and potential drug-drug interaction with metyrapone, a substance the patient had taken among several others during the observation period, individual pharmacokinetics could consequently not be estimated without drug monitoring.

In addition, a VAMS method for simultaneous determination of ten kinase inhibitors from capillary blood was developed. This microsampling technique was mainly characterized by the collection of a defined volume of blood, which could be dried and subsequently analyzed. The guidelines for bioanalytical method validation of the EMA and FDA were also used for this evaluation. As the nature of dried blood samples differs from liquid matrices, further parameters were investigated. These include the investigation of the hematocrit effect, process efficiency, and various stability conditions, for example at increased storage temperatures. The validation showed that the developed method is suitable to analyze dried matrix samples accurate, precise, and selective for all analytes. Apart from the stability tests, all acceptance criteria were met. The decreased stability of two analytes was probably

due to the reproducible but reduced recovery. *In vitro* studies provided results on the VAMS-to-plasma correlation to predict the analyte distribution between both matrices, at least in an exploratory manner. It revealed a heterogeneous picture of analytes with different VAMS-to-plasma distributions. Furthermore, the analysis of 24 patient samples indicated the applicability of at-home VAMS. Both should be confirmed later as part of the clinical validation.

The clinical investigation of the VAMS method pursued two objectives. On the one hand, the simultaneous collection of VAMS and serum samples should enable a conversion of the determined concentrations and, on the other hand, the feasibility of autonomous microsampling at home should be examined more closely. For the former, it could be shown that different conversion methods are suitable for converting VAMS concentrations into serum levels. The type of conversion was secondary for the prediction. However, the previously defined criteria could not be fulfilled for all five kinase inhibitors investigated. The framework conditions of the study led to increased variability, especially for analytes with short half-life. A low and varying hematocrit, caused by the underlying disease, also made prediction difficult for a specific patient collective. For the second objective, investigating the feasibility of VAMS, different aspects were considered. It could be shown that the majority of patients support home-based microsampling. The acceptance is likely to increase even further when microsampling is no longer part of a non-interventional study, but participation is accompanied by targeted monitoring and subsequent adjustment of the therapy. The fact that additional training increases understanding of the correct sampling procedure is also a source of confidence. Demonstrated stability during storage under real-life conditions underlines the practicality of this sampling technique.

Taken together, mass spectrometric methods for both plasma and VAMS could be developed and validated, and their clinical application could be successfully demonstrated. The availability of simple bioanalytical methods to determine kinase inhibitor exposure could improve access to prospective studies and thus facilitate the implementation of routine therapeutic drug monitoring.

6. Zusammenfassung

Ziel der vorliegenden Arbeit war es, den Einsatz des Drug Monitorings bei Patienten mit verschiedenen Erkrankungen im Rahmen der Präzisionsmedizin zu erleichtern. Dies wurde durch die Entwicklung und Validierung massenspektrometrischer Methoden zur Bestimmung der Wirkstoffkonzentrationen von Kinaseinhibitoren und deren klinische Anwendung verfolgt. Dabei standen neben konventionellen Ansätzen zur Bestimmung der Plasmaspiegelkonzentration auch alternative Entnahmetechniken in Form von „Volumetric Absorptive Microsampling (VAMS)“ im Mittelpunkt.

Eine solche konventionelle LC-MS/MS-Methode wurde zur Bestimmung von Cabozantinib in humanem EDTA-Plasma entwickelt und nach den Richtlinien der europäischen und US-amerikanischen Arzneimittelbehörden (EMA, FDA) validiert. Die Methode erfüllte die geforderten Kriterien bezüglich Linearität, Richtigkeit und Präzision, Selektivität, Sensitivität und Stabilität des Analyten. Die Validierung erfolgte auch hinsichtlich Verdünnungsintegrität, Matrixeffekt, Wiederfindung, und Analyt-Verschleppung, deren Ergebnisse ebenso in Übereinstimmung mit den Vorgaben standen. Die Bedeutung der Expositionsüberwachung von Cabozantinib wurde anhand eines klinischen Fallberichts einer 34-jährigen Patientin mit fortgeschrittenem Nebennierenrindenkarzinom, die aufgrund chronischen Nierenversagens zudem dialysepflichtig war, gezeigt. Die erwartbaren Cabozantinib-Plasmakonzentrationen wurden für diesen Off-Label-Use basierend auf einem populations-pharmakokinetischen Modell simuliert. Es zeigte sich, dass die Steady-State-Talspiegel wesentlich niedriger waren als angenommen, sich aber nicht durch die Hämodialyse erklären ließen. Unter Berücksichtigung des kritischen Gesundheitszustandes und möglicher Arzneimittelinteraktionen mit Metyrapon, einer Substanz, die die Patientin neben einigen anderen während des Beobachtungszeitraums eingenommen hatte, konnte die individuelle Pharmakokinetik folglich nicht ohne Arzneistoffspiegelmessung abgeschätzt werden.

Darüber hinaus konnte eine VAMS-Methode zur simultanen Bestimmung von zehn Kinaseinhibitoren aus Kapillarblut entwickelt werden. Dieses Mikrosampling-Verfahren zeichnete sich vor allem durch die Entnahme eines definierten Blutvolumens aus, welches getrocknet und anschließend analysiert werden konnte. Auch hierbei wurden die Richtlinien für bioanalytische Methodenvalidierung der EMA und FDA zur

Beurteilung herangezogen. Da sich die Beschaffenheit der Trockenblutproben von flüssigen Matrices unterscheidet, wurden weitere Einflussfaktoren untersucht. Dazu gehören die Untersuchung des Hämatokrit-Effekts, der Prozesseffizienz und verschiedener Stabilitätsbedingungen, zum Beispiel bei erhöhten Lagertemperaturen. Die Validierung zeigte, dass die entwickelte Methode in der Lage ist Trockenmatrixproben für alle Analyten richtig, präzise und selektiv zu messen. Von den Stabilitätsuntersuchungen abgesehen wurden alle Akzeptanzkriterien erfüllt. Die verminderte Stabilität von zwei Analyten ist vermutlich durch die zwar reproduzierbare, aber geringere Wiederfindungsrate zu begründen. *In vitro* Untersuchungen lieferten Ergebnisse über die VAMS-zu-Plasma-Korrelation, um die Analytverteilung zwischen beiden Matrizes zumindest exploratorisch vorherzusagen. Dabei zeigte sich ein heterogenes Bild von Analyten mit unterschiedlicher VAMS-zu-Plasma-Verteilung. Darüber hinaus zeigten die Messungen von 24 Patientenproben die Anwendbarkeit von VAMS im häuslichen Umfeld. Beides sollte später im Rahmen der klinischen Validierung bestätigt werden.

Die klinische Untersuchung der VAMS-Methode verfolgte zweierlei Ziele. Zum einen sollte durch die zeitgleiche Entnahme von VAMS und Serumproben eine Umrechnung der ermittelten Konzentrationen ermöglicht und zum anderen die Durchführbarkeit der eigenständigen Mikroprobenentnahme zuhause genauer überprüft werden. Für Ersteres konnte gezeigt werden, dass verschiedene Umrechnungsmethoden geeignet sind, VAMS-Konzentrationen in Serumspiegel umzurechnen. Die Art der Umrechnung war für die Vorhersage zweitrangig. Allerdings konnten nicht für alle fünf untersuchten Kinaseinhibitoren die zuvor festgelegten Kriterien erfüllt werden. Die Rahmenbedingungen der Studie führten vor allem bei Analyten mit geringer Halbwertszeit zu einer erhöhten Variabilität. Ein geringer und schwankender Hämatokritwert, bedingt durch die zugrundeliegende Erkrankung, erschwerte zudem die Vorhersage bei einem bestimmten Patientenkollektiv. Für das zweite Ziel, die Durchführbarkeit von VAMS zu untersuchen, wurden verschiedene Aspekte betrachtet. Es konnte gezeigt werden, dass die Mehrheit der Patienten die häusliche Mikroprobenentnahme befürwortet. Die Akzeptanz dürfte sogar noch weiter steigen, wenn die Mikroprobenentnahme nicht mehr nur Teil einer nicht-interventionellen Studie ist, sondern die Teilnahme mit einer gezielten Überwachung und anschließenden Anpassung der Therapie einhergeht. Zuversichtlich stimmte auch die Tatsache, dass ein zusätzliches Training das Verständnis für die korrekte

Durchführung erhöht. Dass sich die Stabilität auch bei der Lagerung unter Realbedingungen zeigen ließ, unterstreicht die Praxistauglichkeit dieser Sampling-Technik.

Insgesamt konnten sowohl für Plasma als auch VAMS massenspektrometrische Methoden entwickelt, validiert und deren klinische Anwendung erfolgreich demonstriert werden. Die Verfügbarkeit von simplen bioanalytischen Methoden zur Bestimmung der Kinaseinhibitor-Exposition könnte den Zugang zu prospektiven Studien und damit die Einführung von routinemäßigem Therapeutischen Drug Monitoring erleichtern.

7. Appendix

7.1. List of abbreviations

Abbreviation	Description
A&P	Accuracy and precision
ABL	Abelson murine leukemia viral oncogene encoded tyrosine kinase
ACC	Adrenocortical carcinoma
ACN	Acetonitrile
ADC	Antibody drug conjugate
ADP	Adenosine diphosphate
AE	Adverse effect
AFA	Afatinib
ANOVA	Analysis of variance
ANVISA	Brazilian Health Regulatory Agency
APCI	Atmospheric pressure chemical ionization
API	Atmospheric pressure ionization
ATP	Adenosine triphosphate
AUC	Area under the concentration-time curve
AXI	Axitinib
AXL	*AXL* gene encoded receptor tyrosine kinase
B/P	Blood-to-plasma concentration ratio, see also F_p
BC	Blood cells
BCR	Breakpoint cluster region protein encoded by the *BCR* gene
BCRP	Breast cancer resistance protein
bid	Twice a day
BMI	Body mass index
BOS	Bosutinib
BRAFV600	Mutation at codon 600 (valin) of the proto-ongogene *BRAF*
CAB	Cabozantinib
CE	Collision energy
CELL ACC	Cell accelerator voltage
CF	Correction factor
CI	Confidence interval
CID	Collision-induced dissociation
CL	Clearance

C_{max}	Maximum concentration
CML	Chronic myeloid leukemia
CR	Calibrator
CV	Coefficient of variance
CYP	Cytochrome P450 isoenzyme
DAB	Dabrafenib
DBS	Dried blood spot
DC	Direct current
DDI	Drug-drug interaction
DFG	Asp-Phe-Gly
DMM	Dried matrix method
DMSO	Dimethyl sulfoxide
DNA	Deoxyribonucleic acid
ED_{50}	Median effective dose
EDTA	Ethylenediaminetetraacetic acid
EGFR	Epidermal growth factor receptor
EMA	European Medicine Agency
ENSAT	European Network for the Study of Adrenal Tumors
EPAR	European Public Assessment Reports
ESI	Electrospray ionization
F1	Fraction in first absorption depot
FDA	United States Food and Drug Administration
FDG	18-fluorodeoxyglucose
FKBP12	FK-binding protein 12
F_p	Blood-to-plasma concentration ratio, see also B/P
FRAG	Fragmentor voltage
f_u	Fraction unbound
GIST	Gastrointestinal stromal tumors
GTFCh	Society of Toxicological and Forensic Chemistry
GvHD	Graft versus host disease
Hct	Hematocrit
HER	Human epidermal growth factor receptor
H/I/L	Hemolytic, icteric, lipemic
HILIC	Hydrophilic interaction chromatography
HPLC	High performance liquid chromatography
IATDMCT	International Association for Therapeutic Drug Monitoring and Clinical Toxicology

ICH	International Council for Harmonisation of Technical Requirements for Pharmaceuticals for Human Use
IS	Isotope-labeled internal standard
ISR	Incurred sample reanalysis
JAK	Janus kinase
K	Calibrator, see also CR
KA	Absorption rate constant
KI	Kinase inhibitor
LC	Liquid chromatography
LC-MS/MS	Liquid chromatography with tandem mass spectrometry
LD_{50}	Median lethal dose
LEN	Lenvatinib
LLE	Liquid-liquid extraction
LLOQ	Lower limit of quantification
m/z	Mass to charge ratio
MAP	Maximum a posteriori
MAPE	Median absolute percentage predictive error
MCMC	Markov chain Monte Carlo
MDS	Myelodysplastic syndrome
MEK	MAPK/ERK kinase
MeOH	Methanol
MET	Hepatocyte growth factor receptor kinase
MF	Matrix factor
MHLW/PMDA	Japanese Pharmaceuticals and Medical Devices Agency
MIPD	Model-informed precision dosing
MPD	Myeloproliferative disease
MPPE	Median percentage predictive error
MRM	Multiple reaction monitoring
MS	Mass spectrometry
MS/MS	Tandem mass spectrometry
MTC	Medullary thyroid carcinoma
mTOR	Mammalian target of rapamycin
NIL	Nilotinib
NLME	Nonlinear mixed effects
NMPA	Chinese National Medical Products Administration
NP	Normal phase
NSCLC	Non-small-cell lung cancer

OAT	Organic anion transporter
OSI	Osimertinib
P-gp	P-glycoprotein
PD	Pharmacodynamics
PDGFR	Platelet-derived growth factor receptor
PET	Positron emission tomography
Ph	Philadelphia chromosome
PI	Prediction interval
PK	Pharmacokinetics
popPK	Population pharmacokinetics
PP	Protein precipitation
QC	Quality control
qd	Once a day
QqQ	Triple quadrupole mass spectrometer
r	Correlation coefficient
R^2	Coefficient of determination
RA	Rheumatoid arthritis
RCC	Renal cell carcinoma
RET	Retention time, may also be used for *RET* proto-oncogene encoded receptor tyrosine kinase
RF	Radiofrequency
rH	Relative humidity
ROCK	Rho-kinase
RP	Reversed phase
RUX	Ruxolitinib
SALLE	Salting-out assisted liquid-liquid extraction
SD	Standard deviation, may also be used for supplementary data
SDC	Supplemental Digital Content
SLE	Supported liquid extraction
SPE	Solid phase extraction
TDM	Therapeutic drug monitoring
TKI	Tyrosine kinase inhibitor
TNM	Tumor, node, metastasis
TOF	Time-of-flight mass spectrometer
TRA	Trametinib
ULOQ	Upper limit of quantification
V/P	VAMS-to-plasma concentration ratio

VAMS	Volumetric absorptive microsampling
VC	Volume of central compartment
VEGF	Vascular endothelial growth factor
VEGFR	Vascular endothelial growth factor receptor
VKORC	Vitamin K epoxide reductase complex
WB	Whole blood
WS	Working solution
η	Random effects
ρ	Drug affinity to blood cells

7.2. List of kinase inhibitors

Year*	Drug	Primary target	Therapeutic indication
1999	Sirolimus	FKBP12/ mTOR	Kidney transplants, Lymphangioleiomyomatosis
2001	Imatinib	BCR-Abl	Ph+ CML or ALL, ASM, CEL, GIST, dermatofibrosarcoma protuberans, MDS/ MPD, hypereosinophilic syndrome
2003	Gefitinib	EGFR	NSCLC with exon 19 deletions or exon 21 substitutions
2004	Erlotinib	EGFR	NSCLC, pancreatic cancer
2005	Sorafenib	VEGFR1/2/ 3	HCC, RCC, DTC
2006	Sunitinib	VEGFR2	GIST, PNET, RCC
	Dasatinib	BCR-Abl	Ph+ CML or ALL
2007	Nilotinib	BCR-Abl	Ph+ CML
	Lapatinib	EGFR, ErbB2/ HER2	HER2-positive breast cancer
	Temsirolimus	FKBP12/ mTOR	RCC
2009	Everolimus	FKBP12/ mTOR	HER2-negative breast cancer, PNET, RCC, angiomyolipomas, Sub-ependymal giant cell astrocytomas
	Pazopanib	VEGFR1/2/ 3	RCC, soft tissue sarcomas
2011	Crizotinib	ALK, ROS1	ALK or ROS1-postive NSCLC, ALCL, inflammatory myofibroblastic tumors
	Ruxolitinib	JAK1/2/3, Tyk	Myelofibrosis, polycythemia vera, atopic dermatitis, GvHD
	Vandetanib	VEGFR2	MTC
	Vemurafenib	B-Raf	BRAFV600E melanomas, Erdheim-Chester disease
2012	Axitinib	VEGFR 1/2/3	RCC
	Bosutinib	BCR-Abl	Ph+ CML
	Cabozantinib	RET, VEGFR2	MTC, RCC, HCC
	Ponatinib	BCR-Abl	Ph+ CML or ALL
	Regorafenib	VEGFR1/2/ 3	Colorectal cancer, GIST, HCC
	Tofacitinib	JAK3	Rheumatoid arthritis, psoriatic arthritis, ulcerative colitis
2013	Afatinib	ErbB1/2/4	NSCLC, squamous NSCLC
	Dabrafenib	B-Raf	BRAFV600 mutation melanomas, NSCLC, and ATC
	Ibrutinib	BTK	CLL, MCL, MZL, GvHD

	Trametinib	MEK1/2	BRAFV600E/K melanoma, BRAFV600E NSCLC
2014	Ceritinib	ALK	ALK-positive NSCLC resistant to crizotinib
	Idelalisib	PI3Kδ	CLL in combination with rituximab, FL, SLL
	Nintedanib	FGFR1/2/3	Idiopathic pulmonary fibrosis
2015	Alectinib	ALK, RET	ALK-positive NSCLC
	Cobimetinib	MEK1/2	BRAFV600E/K melanomas in combination with vemurafenib
	Lenvatinib	VEGFR, RET	DTC
	Osimertinib	EGFR T970M	NSCLC with exon 19 deletions or exon 21 substitutions
	Palbociclib	CDK4/6	Estrogen receptor- and HER2-positive breast cancers
2017	Brigatinib	ALK	ALK-positive NSCLC
	Copanlisib	PI3Kδ	FL
	Midostaurin	Flt3	AML, mastocytosis, mast cell leukemia
	Neratinib	ErbB2/ HER2	HER2-positive breast cancer
	Netarsudil	ROCK1/2	Glaucoma
	Ribociclib	CDK4/6	Combination therapy for breast cancer
	Abemaciclib	CDK4/6	Combination therapy or monotherapy for breast cancer
	Acalabrutinib	BTK	MCL, CLL, SLL
2018	Baricitinib	JAK1/2	RA
	Binimetinib	MEK1/2	Combination therapy with encorafenib for BRAFV600E/K melanomas
	Dacomitinib	EGFR	EGFR-mutant NSCLC
	Duvelisib	PI3Kδ	CLL, SLL, FL
	Encorafenib	B-Raf	Combination therapy with binimetinib for BRAFV600E/K melanomas
	Fostamatinib	Syk	Chronic immune thrombocytopenia
	Gilteritinib	Flt3	AML with *FLT3* mutations
	Larotrectinib	TRKA/B/C	Solid tumors with NTRK fusion proteins
	Lorlatinib	ALK	ALK-positive NSCLC
2019	Alpelisib	PI3Kα	Combination therapy with fulvestrant for breast cancer
	Entrectinib	TRKA/B/C, ROS1	Solid tumors with NTRK fusion proteins, ROS1-positive NSCLC
	Erdafitinib	FGFR1/2/ 3/4	Urothelial bladder cancer
	Fedratinib	JAK2	Myelofibrosis

	Pexidartinib	CSF1R	Tenosynovial giant cell tumors
	Upadacitinib	JAK1	Rheumatoid arthritis, psoriatic arthritis, atopic dermatitis
	Zanubrutinib	BTK	MCL
2020	Avapritinib	PDGFRα	GIST with PDGFRα exon 18 mutations
	Capmatinib	MET	NSCLC with MET exon 14 skipping
	Pemigatinib	FGFR2	Cholangiocarcinoma with FGFR2 fusions or other rearrangements
	Pralsetinib	RET	RET-fusion NSCLC, MTC, DTC
	Ripretinib	Kit, PDGFRα	Fourth-line treatment for GIST
	Selpercatinib	RET	RET fusion NSCLC, thyroid cancers, RET mutant MTC
	Selumetinib	MEK1/2	Neurofibromatosis type I
	Tucatinib	ErbB2/ HER2	Combination second-line treatment for HER2-positive breast cancer
2021	Asciminib	BCR-Abl	Ph+ CML
	Belumosudil	ROCK2	GvHD
	Infigratinib	FGFR2	Cholangiocarcinomas with FGFR2 fusions or other rearrangements
	Mobocertinib	EGFR	NSCLC with EGFR-positive exon 20 insertions
	Tepotinib	MET	NSCLC with MET mutations
	Tivozanib	VEGFR2	Third-line treatment of RCC
	Trilaciclib	CDK4/6	Chemotherapy-induced myelosuppression
	Umbralisib**	PI3Kδ, CK1ε	MZL, FL
2022	Abrocitinib	JAK1	Atopic dermatitis
	Futibatinib	FGFR2	cholangiocarcinomas with FGFR2 fusions or other rearrangements
	Pacritinib	JAK2	Myelofibrosis
	Deucravacitinib	TYK2	Moderate-to-severe plaque psoriasis
2023	Capivasertib	HER2	Hormone receptor positive, HER2-negative breast cancer
	Fruquintinib	VEGFR2	Metastatic colorectal cancer
	Leniolisib	PI3Kδ	Activated phosphoinositide 3-kinase delta syndrome
	Momelotinib	JAK2	Myelofibrosis
	Pirtobrutinib	BTK	MCL, CLL, SLL

Quizatinib	Flt3	AML in combination with cytarabine and daunorubicin
Repotrectinib	ROS1	ROS1-positive NSCLC
Ritlecitinib	JAK3	Alopecia areata

ALCL, anaplastic large cell lymphoma; ALL, acute lymphoblastic leukemia; AML, acute myeloid leukemia; ASM, aggressive systemic mastocytosis; ATC, anaplastic thyroid cancers; CEL, chronic eosinophilic leukemia; CLL, chronic lymphocytic leukemia; CML, chronic myeloid leukemia; DTC, differentiated thyroid cancer; FL, follicular lymphoma; GIST, gastrointestinal stromal tumors; GvHD, graft versus host disease; HCC, hepatocellular carcinoma; MCL, mantle cell lymphoma; MDS, myelodysplastic syndrome; MPD, myeloproliferative disease; MTC, medullary thyroid cancer; MZL, marginal zone lymphoma; NSCLC, non-small-cell lung cancer; PNET, pancreatic neuroendocrine tumors; RCC, renal cell carcinoma; SLL, small lymphocytic lymphoma

* FDA approval

** Approval withdrawn

7.3. List of dried matrix microsampling devices

Microsampling device	Collected matrix	Technique (volume)	Description and application
DBS cards Manufacturer: several Manufacturers	Dried capillary blood	Non-volumetric (~ 70-80 µL)	DBS cards consist of different untreated or pretreated filter paper. Application of one or more blood drops onto the filter paper card. Blood samples can be punched out afterwards for extraction.
HemaSpot HD Manufacturer: Spot On Sciences; San Francisco, CA, USA	Dried capillary blood	Non-volumetric (~ 160 µL)	The device consists of a cartridge and a large filter membrane inside. Five drops of capillary blood are placed at the center of the membrane for high volume DBS collection.
HemaSpot HF Manufacturer: Spot On Sciences; San Francisco, CA, USA	Dried capillary blood	Non-volumetric (~ 9.2 µL)	The device consists of a cartridge and a fan-shaped filter membrane inside. Two-three drops of capillary blood are dropped onto the middle of the pre-cut membrane with eight blades of absorbent paper. The capillary blood is equally distributed among the blades. Samples can be extracted separately.
VAMS Mitra Manufacturer: Neoteryx by Trajan; Torrance, CA, USA	Dried capillary blood	Volumetric (10, 20, or 30 µL)	A polymeric tip is attached on a plastic holder for sampling and placed in a cartridge. A defined volume of capillary blood is absorbed at the polymeric tip. The polymeric tip can be detached from its plastic holder for sample extraction. Different sizes and cartridges are available.
hemaPEN Manufacturer: Neoteryx by Trajan; Torrance, CA, USA	Dried capillary blood	Volumetric (2.74 µL)	The device can be described as a pen with four integrated capillaries. The different capillaries are filled simultaneously with a defined volume of capillary blood. The blood is transferred from the capillaries onto four integrated pre-punched filter paper discs. Afterwards, each sample can be extracted separately.

HemaXis DB 10 Manufacturer: DBS System SA; Gland, Switzerland	Dried capillary blood	Volumetric (10 µL)	The device consists of a microfluidic chip, a standard filter card and a protective case. Four micro-channels are separately filled with a defined volume of capillary blood. The blood is transferred subsequently onto the filter paper. Afterwards, the samples can be punched out and extracted.
Capitainer B (formerly Capitainer qDBS) Manufacturer: Capitainer AB; Solna, Sweden	Dried capillary blood	Volumetric (10 µL)	The device incorporates an excess membrane via a volumetric channel with a sampling membrane at the outlet of the channel. Two samples are included in one device. Capillary blood is applied onto the channel that meters a defined volume. The collected specimen is then transferred from the channel onto a filter disc which can be extracted afterwards. Additional Capitainer products are available with enzyme inhibitor for phosphatidylethanol testing (B Vanadate) or larger collection volumes (B 50).
TASSO-M20 Manufacturer: Tasso, Inc.; Seattle, WA, USA	Dried capillary blood	Volumetric (17.5 µL)	The device consists of a lancet covered by a plastic housing with a big button and a sample pod below. The device is sticked to the shoulder. After pressing the button, capillary blood will flow into the sample pod in which four capillary blood samples are generated.
HemaSpot SE Manufacturer: Spot On Sciences; San Francisco, CA, USA	Dried blood cells and/ or serum	Non-volumetric	The device consists of a cartridge and a blood separation membrane inside. Multiple drops of capillary blood are placed at the center of the membrane. The device prevents blood cells from flowing through the spiral-shaped membrane, while small molecules and proteins can migrate further, resulting in different matrix compositions in the membrane. Extraction samples can be punched from different positions.
HemaSep plasma separation cards Manufacturer:	Dried plasma/ serum	Non-volumetric	A filter paper card is used as device. Application of a blood drop onto a filter membrane that allows for separation of

Ahlstrom-Munksjö; Helsinki, Finland			cellular components (inner circle) and plasma/ serum surrounding the distinct cellular area. Samples can be cut afterwards for extraction. Different variants are available.
Telimmune Plasma Separation Card (formerly Noviplex) Manufacturer: Telimmune; North Webster, IN, USA	Dried plasma	Volumetric (~ 3 µL)	A multilayer sampling card is used as device. Capillary blood drops are placed onto a sample port. The combination of three different layers, a spreading layer, a separation membrane, and a collection disc, allows for plasma sampling. The upper layers are removed after sampling and the collection disc can be extracted afterwards. Two versions are available, in which either one or two samples are generated.
Autonomous Microfluidic DPS Device Manufacturer: Capitainer AB; Solna, Sweden	Dried plasma	Volumetric (11.6 µL)	The device is currently under development. Dried plasma is collected by the combination of a filtration membrane, a capillary metering channel and a filter paper. Capillary blood is applied onto the filtration membrane retaining the blood cells. The capillary behind is filled with a defined volume of plasma, which is transferred subsequently onto the filter paper.
HemaXis DX Manufacturer: DBS System SA; Gland, Switzerland	Plasma or serum	Volumetric (2 µL)	The device is currently under development. Capillary blood is applied onto the microfluidic device which allows passive separation of plasma or serum from whole blood by sedimentation. The samples can be collected either in dried or liquid form.

7.4. List of publications

Research papers

Kroiss, M.; Megerle, F.; Kurlbaum, M.; Zimmermann, S.; Wendler, J.; Jimenez, C.; Lapa, C.; Qunkler, M.; Scherf-Clavel, O.; Habra, M.A.; Fassnacht, M. *Objective Response and Prolonged Disease Control of Advanced Adrenocortical Carcinoma with Cabozantinib,* J Clin Endocrinol Metab **2020**, 105(5), 1-8.

Aghai, F.; Zimmermann, S.; Kurlbaum, M.; Jung, P.; Pelzer, T.; Klinker, H.; Isberner, N.; Scherf-Clavel, O. *Development and validation of a sensitive liquid chromatography tandemmass spectrometry assay for the simultaneous determination of ten kinase inhibitors in human serum and plasma*, Anal Bioanal Chem **2021**, 413(2), 599-612.

Isberner, N.; Kraus, S.; Grigoleit, G.U.; Aghai, F.; Kurlbaum, M.; Zimmermann, S.; Klinker, H.; Scherf-Clavel, O. *Ruxolitinib exposure in patients with acute and chronic graft versus host disease in routine clinical practice – a prospective single-center trial*, Cancer Chemother Pharmacol **2021**, 88(6), 973-983.

Zimmermann, S.; Kurlbaum, M.; Mayer, S.; Fassnacht, M.; Kroiss, M.; Scherf-Clavel, O. *Simulation-Based Interpretation of Therapeutically Monitored Cabozantinib Plasma Concentration in Advanced Adrenocortical Carcinoma with Hemodialysis,* Ther Drug Monit **2021**, 43(5), 706-711.

Mc Laughlin, A.M.; Schmulenson, E.; Teplytska, O.; Zimmermann, S.; Opitz, P.; Groenland, S.L.; Huitema, A.D.R.; Steeghs, N.; Müller, L.; Fuxius, S.; Illerhaus, G.; Joerger, M.; Mayer, F.; Fuhr, U.; Holdenrieder, S.; Hempel, G.; Scherf-Clavel, O.; Jaehde, U.; Kloft, C. and for the ON-TARGET Study Consortium *Developing a Nationwide Infrastructure for Therapeutic Drug Monitoring of Targeted Oral Anticancer Drugs: The ON-TARGET Study Protocol*, Cancers (Basel) **2021**, 13(24), 6281.

Zimmermann, S.; Aghai, F.; Schilling, B.; Kraus, S.; Grigoleit, G.U.; Kalogirou, C.; Goebeler, M.E.; Jung, P.; Pelzer, T.; Klinker, H.; Isberner, N.; Scherf-Clavel, O. *Volumetric absorptive microsampling (VAMS) for the quantification of ten kinase inhibitors and determination of their in vitro VAMS-to-plasma ratio,* J Pharm Biomed Anal **2022**, 211, 114623.

Aghai-Trommeschlaeger, F.; Zimmermann, S.; Gesierich, A.; Kalogirou, C.; Goebeler, M.E.; Jung, P.; Pelzer, T.; Kurlbaum, M.; Klinker, H.; Isberner, N.; Scherf-Clavel, O. *Comparison of a newly developed high performance liquid chromatography method with diode array detection to a liquid chromatography tandem mass spectrometry method for the quantification of cabozantinib, dabrafenib, nilotinib and osimertinib in human serum - Application to therapeutic drug monitoring,* Clin Biochem **2022**, 105-106, 35-43.

Opitz, P.; Zimmermann, S.; Mc Laughlin, A.M.; Müller, L.; Fuxius, S.; Illerhaus, G.; Scherf-Clavel, O.; Kloft, C.; Hempel, G.; for the On-Target study consortium *Development and validation of a bioanalytical method for the quantification of axitinib from plasma and capillary blood using volumetric absorptive microsampling (VAMS) and on-line solid phase extraction (SPE) LC-MS,* J Pharm Biomed Anal **2022**, 221, 115033.

Isberner, N.; Gesierich, A.; Balakirouchenane, D.; Schilling, B.; Aghai-Trommeschlaeger, F.; Zimmermann, S.; Kurlbaum, M.; Puszkiel, A.; Blanchet, B.; Klinker, H.; Scherf-Clavel, O. *Monitoring of Dabrafenib and Trametinib in Serum and Self-Sampled Capillary Blood in Patients with BRAFV600-Mutant Melanoma,* Cancers (Basel) **2022**, 14(19), 4566.

Gerner, B.; Aghai-Trommeschlaeger, F.; Kraus, S.; Grigoleit, G.U.; Zimmermann, S.; Kurlbaum, M.; Klinker, H.; Isberner, N.; Scherf-Clavel, O. *A Physiologically-Based Pharmacokinetic Model of Ruxolitinib and Posaconazole to Predict CYP3A4-Mediated Drug – Drug Interaction Frequently Observed in Graft versus Host Disease Patients,* Pharmaceutics **2022**, 14(12), 2556.

Zimmermann, S.; Aghai-Trommeschlaeger, F.; Kraus, S.; Grigoleit, G.U.; Gesierich, A.; Schilling, B.; Kalogirou, C.; Goebeler, M.E.; Kurlbaum, M.; Klinker, H.; Isberner, N.; Scherf-Clavel, O. *Clinical validation and assessment of feasibility of volumetric absorptive microsampling (VAMS) for monitoring of nilotinib, cabozantinib, dabrafenib, trametinib, and ruxolitinib,* J Pharm Biomed Anal **2023**, 228, 115311

Conference contributions – Abstracts and posters

Zimmermann, S.; Wahl, O. *Minimally invasive, model informed drug monitoring of tyrosine kinase inhibitors,* Annual Meeting of the Deutsche Pharmazeutische Gesellschaft (DPhG), **2018**, Hamburg, Germany

Isberner, N.; Aghai, F.; Zimmermann, S.; Bolz, M.; Kraus, S.; Grigoleit, G.U.; Kurlbaum, M.; Scherf-Clavel, O.; Klinker, H. *Bestimmung von Ruxolitinib-Serumspiegeln bei Patienten mit steroidrefraktärer Graft-versus-Host Erkrankung in der klinischen Routine mit einer neuen Flüssigchromatographie-Tandem-Massenspektrometrie-Method,* Annual Meeting of the Deutsche Gesellschaft für Hämatologie und Medizinische Onkologie (DGHO), **2020**, Virtual Meeting

Zimmermann, S.; Kurlbaum, M.; Lopau, K.; Fassnacht, M.; Kroiss, M.; Scherf-Clavel, O. *Case report of cabozantinib therapeutic drug monitoring and pharmacokinetic modelling in advanced adrenocortical carcinoma with hemodialysis,* 64th German Congress of Endocrinology, **2021**, Virtual Meeting

Aghai, F.; Isberner, N.; Zimmermann, S.; Kraus, S.; Grigoleit, G.U.; Kurlbaum, M.; Scherf-Clavel, O.; Klinker, H. *Ruxolitinib exposure in patients with acute and chronic graft versus host disease – a prospective single-center trial,* European Society of Clinical Pharmacy International Workshop, **2021**, Virtual Meeting

Mc Laughlin, A.M.; Schmulenson, E.; Teplytska, O.; Zimmermann, S.; Opitz, P.; Groenland, S.L.; Huitema, A.D.R.; Steeghs, N.; Müller, L.; Fuxius, S.; Joerger, M.; Mayer, F.; Fuhr, U.; Holdenrieder, S.; Hempel, G.; Scherf-Clavel, O.; Mikus, G.; Jaehde, U.; Kloft, C. for the ON-TARGET Study Consortium *Developing a nationwide infrastructure for Therapeutic Drug Monitoring of targeted oral anticancer drugs: The ON-TARGET study,* Annual Meeting of the Deutsche Pharmazeutische Gesellschaft (DPhG), **2021**, Virtual Meeting

Mc Laughlin, A.M.; Schmulenson, E.; Teplytska, O.; Zimmermann, S.; Opitz, P.; Groenland, S.L.; Huitema, A.D.R.; Steeghs, N.; Müller, L.; Fuxius, S.; Joerger, M.; Mayer, F.; Fuhr, U.; Holdenrieder, S.; Hempel, G.; Scherf-Clavel, O.; Mikus, G.; Jaehde, U.; Kloft, C. for the ON-TARGET Study Consortium *Therapeutic Drug Monitoring for oral anticancer drugs in clinical routine: The ON-TARGET Study,* Annual

Meeting of the Deutsche Gesellschaft für Hämatologie und Medizinische Onkologie (DGHO), **2021**, Berlin / Hybrid Meeting

Mc Laughlin, A.M.; Schmulenson, E.; Teplytska, O.; Zimmermann, S.; Opitz, P.; Groenland, S.L.; Huitema, A.D.R.; Steeghs, N.; Müller, L.; Fuxius, S.; Joerger, M.; Mayer, F.; Fuhr, U.; Holdenrieder, S.; Hempel, G.; Scherf-Clavel, O.; Mikus, G.; Jaehde, U.; Kloft, C. *Therapeutisches Drug Monitoring bei oralen Tumortherapeutika: Die ON-TARGET Studie,* Annual Meeting of the Deutsche Gesellschaft für Klinische Pharmazie (DGKPha), **2021**, Virtual Meeting

Aghai, F.; Zimmermann, S.; Schilling, B.; Kalogirou, C.; Goebeler, M.E.; Jung, P.; Pelzer, T.; Kurlbaum, M.; Isberner, N.; Scherf-Clavel, O.; Klinker, H. *Quantification Of Cabozantinib, Dabrafenib, Nilotinib And Osimertinib In Human Serum With A Newly Developed High Performance Liquid Chromatography Method With Diode Array Detection And Its Comparison To A Liquid Chromatography Mass Spectrometry Method For The Application To Therapeutic Drug Monitoring,* EUREKA! Symposium, **2021**, Würzburg / Virtual Meeting

Aghai, F.; Gerner, B.; Isberner, N.; Kraus, S.; Grigoleit, G.U.; Zimmermann, S.; Kurlbaum, M.; Klinker, H.; Scherf-Clavel, O. *Physiologically-based pharmacokinetic model of Ruxolitinib and Posaconazole to predict clinically relevant CYP3A4 mediated Drug-Drug Interaction*, 12th American Conference on Pharmacometrics (ACoP), **2021**, Virtual Meeting

Aghai, F.; Zimmermann, S.; Gesierich, A.; Schilling, B.; Kalogirou, C.; Goebeler, M.E.; Jung, P.; Pelzer, T.; Kurlbaum, M.; Isberner, N.; Scherf-Clavel, O.; Klinker, H. *Comparison of a newly developed high performance liquid chromatography method with diode array detection to a liquid chromatography tandem mass spectrometry method for the quantification of cabozantinib, dabrafenib, nilotinib and osimertinib in human serum - Application to therapeutic drug monitoring,* Annual PhD Student & Postdoc Meeting of the Deutsche Pharmazeutische Gesellschaft (DPhG), **2022**, Virtual Meeting

Conference contributions – Oral presentations

Zimmermann, S. *Minimally invasive, model informed drug monitoring of tyrosine kinase inhibitors,* Annual Meeting of the Deutsche Pharmazeutische Gesellschaft (DPhG) – poster short talk (invited), **2018**, Hamburg, Germany

Other references

Kroiss, M.; Goebeler, M.E.; Röser, C.; Zimmermann, S.; Landwehr, L.; Scherf-Clavel, O.; Malzahn, U.; Kurlbaum, M.; Fassnacht, M. *CaboACC: Cabozantinib beim fortgeschrittenen Nebennierenkarzinom nach Versagen der Standardtherapie,* Forum **2019**, 34, 376-378.

7.5. Documentation of authorship

In this section, the individual contribution for each author to the publications reprinted in this thesis is specified. Unpublished manuscripts are handled, accordingly.

Erklärung zur Autorenschaft

Simulation-Based Interpretation of Therapeutically Monitored Cabozantinib Plasma Concentration in Advanced Adrenocortical Carcinoma with Hemodialysis

Zimmermann, S.; Kurlbaum, M.; Mayer, S.; Fassnacht, M.; Kroiss, M.; Scherf-Clavel, O.

Therapeutic Drug Monitoring 2021, 43(5), 706-711.

Sebastian Zimmermann (SZ), Max Kurlbaum (MK), Stefanie Mayer (SM), Martin Fassnacht (MF), Matthias Kroiss (MKr), Oliver Scherf-Clavel (OSC)

Autor	SZ	MK	SM	MF	MKr	OSC							∑ in Prozent
Studiendesign	1.5	1.5			1	1.5							5.5
Klinischer Teil und Datenbeschaffung		1		1	1								3
Experimentelle Arbeit	22.5	2.5	1										26
Datenanalyse und Interpretation	10	2.5				10							22.5
Verfassen der Veröffentlichung	15	10											25
Korrektur der Veröffentlichung		5		1.5	2.5	5							14
Koordination der Veröffentlichung	1.5				1	1.5							4
Summe	50.5	22.5	1	2.5	5.5	18							100

Erklärung zur Autorenschaft

Volumetric absorptive microsampling (VAMS) for the quantification of ten kinase inhibitors and determination of their in vitro VAMS-to-plasma ratio

Zimmermann, S.; Aghai, F.; Schilling, B.; Kraus, S.; Grigoleit, G.U.; Kalogirou, C.; Goebeler, M.E.; Jung, P.; Pelzer, T.; Klinker, H.; Isberner, N.; Scherf-Clavel, O.

Journal of Pharmaceutical and Biomedical Analysis 2022, 211, 114623.

Sebastian Zimmermann (SZ), Fatemeh Aghai (FA), Bastian Schilling (BS), Sabrina Kraus (SK), Götz Ulrich Grigoleit (GUG), Charis Kalogirou (CK), Maria-Elisabeth Goebeler (MEG), Pius Jung (PJ), Theo Pelzer (TP), Hartwig Klinker (HK), Nora Isberner (NI), Oliver Scherf-Clavel (OSC)

Autor	SZ	FA	BS	SK	GUG	CK	MEG	PJ	TP	HK	NI	OSC	∑ in Prozent
Studiendesign	1.5									1	1	1.5	5
Klinischer Teil und Datenbeschaffung			1	1	1	1	1	1	1	1.5	1.5		10
Experimentelle Arbeit	23.5	2.5											26
Datenanalyse und Interpretation	14	2.5										6	22.5
Verfassen der Veröffentlichung	15											5	20
Korrektur der Veröffentlichung		1		1						1	3.5	7	13.5
Koordination der Veröffentlichung	1.5											1.5	3
Summe	55.5	6	1	2	1	1	1	1	1	3.5	6	21	100

Erklärung zur Autorenschaft

Clinical validation and assessment of feasibility of volumetric absorptive microsampling (VAMS) for monitoring of nilotinib, cabozantinib, dabrafenib, trametinib, and ruxolitinib

Zimmermann, S.; Aghai-Trommeschlaeger, F.; Kraus, S.; Grigoleit, G.U.; Gesierich, A.; Schilling, B.; Kalogirou, C.; Goebeler, M.E.; Kurlbaum, M.; Klinker, H.; Isberner, N.; Scherf-Clavel, O.

Journal of Pharmaceutical and Biomedical Analysis 2023, 228, 115311.

Sebastian Zimmermann (SZ), Fatemeh Aghai-Trommeschlaeger (FAT), Sabrina Kraus (SK), Götz Ulrich Grigoleit (GUG), Anja Gesierich (AG), Bastian Schilling (BS), Charis Kalogirou (CK), Maria-Elisabeth Goebeler (MEG), Max Kurlbaum (MK), Hartwig Klinker (HK), Nora Isberner (NI), Oliver Scherf-Clavel (OSC)

Autor	SZ	FAT	SK	GUG	AG	BS	CK	MEG	MK	HK	NI	OSC	∑ in Prozent
Studiendesign	1.5									1	1	1.5	5
Klinischer Teil und Datenbeschaffung			1	1	1	1	1	1	1	2.5	2.5		12
Experimentelle Arbeit	15	5											20
Datenanalyse und Interpretation	20	2.5										2.5	25
Verfassen der Veröffentlichung	15												15
Korrektur der Veröffentlichung		1	1			1			1	1	5	10	20
Koordination der Veröffentlichung	1.5											1.5	3
Summe	53	8.5	2	1	1	2	1	1	2	4.5	8.5	15.5	100